KU LEUVEN

FACULTEIT BIO-INGENIEURSWETENSCHAPPEN

Insight into methanolysis as a chemical recycling method for bisguaiacol-based polycarbonates

Methanolyse als een chemische recyclagemethode voor bisguaiacol gebaseerde polycarbonaten

Promotor:
Prof. Bert Sels
Departement Microbiële en Moleculaire Systemen
Centrum voor Oppervlaktechemie en Katalyse

Masterproef voorgedragen
tot het behalen van het diploma van
Master of Science in de bio-ingenieurswetenschappen:
katalytische technologie

Benjamin Vermeeren

juni 2019

"Dit proefschrift is een examendocument dat na de verdediging niet meer werd gecorrigeerd voor eventueel vastgestelde fouten. In publicaties mag naar dit proefwerk verwezen worden mits schriftelijke toelating van de promotor, vermeld op de titelpagina."

KU LEUVEN

FACULTEIT BIO-INGENIEURSWETENSCHAPPEN

Insight into methanolysis as a chemical recycling method for bisguaiacol-based polycarbonates

Methanolyse als een chemische recyclagemethode voor bisguaiacol gebaseerde polycarbonaten

Promotor:
Prof. Bert Sels
Departement Microbiële en Moleculaire Systemen
Centrum voor Oppervlaktechemie en Katalyse

Masterproef voorgedragen
tot het behalen van het diploma van
Master of Science in de bio-ingenieurswetenschappen:
katalytische technologie

Benjamin Vermeeren

juni 2019

Dankwoord

Hoewel dit voor (vele) moedige lezers het prille begin is van deze masterthesis, is dit dankwoord voor mij het prangende einde. Het thesisjaar een uitdaging noemen is een understatement. Het is behalve uitdagend hoofdzakelijk zwoegen, zweten en blijven doorgaan, maar op het einde, het toch allemaal waard.

Eerst wil ik Steven-Friso Koelewijn enorm bedanken. Zowel in als buiten het labo was Stef voor mij van goudwaarde. Steeds als het onderzoek één stap achteruit leek te gaan, zorgde hij ervoor dat we er nadien twee vooruitvlogen; reculer pour mieux sauter. Hij gaf me vrijheid en vertrouwen om steeds mijn ding te doen, maar stond meteen klaar met raad en daad indien het nodig was. Ook tijdens het verwerken en schrijven van deze thesis bleef hij me verbazen met zijn vindingrijke tips, ideeën en suggesties.

Zonder Stef geen Laura en zonder Laura geen Stef. Laura Trullemans, als haar energieke, kordate zelve, heeft me enorm geholpen doorheen heel het jaar. Ze leerde me niet alleen alle kneepjes van het vak, maar ze deed mij ook onmiddellijk op mijn gemak voelen.

Ook wil mijn promotor, Prof. Bert Sels bedanken voor het leiden van, in mijn ogen, erg interessant en belangrijk onderzoek.

Mijn familie wil ik bedanken voor de steun en kansen die ze me dit jaar hebben geboden. S.O.A. voor alle leeghoofdige gesprekken, luchtige debatten en levensvragen, de Parkstraat voor alle lasten verlichtende “half uurtjes” uit en in het bijzonder Gaëlle, mijn steun en toeverlaat op alle mogelijke momenten.

De afgelopen dagen is het nog eens duidelijk geworden dat alles wat we essentieel en vanzelfsprekend achten in ons leven eigenlijk helemaal niet vanzelfsprekend is. Het is belangrijk om deze mensen en zaken te blijven koesteren en van elk waardevol moment met volle teugen te genieten. Het was niet alleen een verhelderend jaar op wetenschappelijk vlak, maar ook op menselijk vlak.

Benjamin Vermeeren

7 mei 2019

Wetenschappelijke samenvatting

De transitie van een lineaire ‘neem-maak-gebruik-stort naar een circulaire ‘hergebruik-recyclage’ plastic economie vermindert de input van nieuwe grondstoffen. Deze transitie laat ook toe dat plastic ontkoppeld wordt van fossiele grondstoffen en verschuift naar bio-gebaseerde grondstoffen. Om deze ontkoppeling mogelijk te maken is er nood aan afvalbeheer methoden, zoals chemische recyclage, die geschikt zijn voor deze bio-gebaseerde polymeren. In deze context onderzoekt dit proefschrift de chemische recyclage van hernieuwbare bisguaiacol gebaseerde polycarbonaten (PC) door middel van solvolyse. In de literatuur worden *o*-methoxy bisfenolen – zogenaamde ‘bisguaiacolen’ – voorgesteld als hernieuwbare en veilige alternatieven voor petroleum-gebaseerde, hormoonverstorende bisfenolen, zoals bisfenol A (BPA). Het draagvlak van bisguaiacol gebaseerde PCs zal, onder andere, afhankelijk zijn van de mogelijk tot recyclage. Nochtans, voor zover wij weten, is er momenteel geen informatie beschikbaar over de (chemische) recyclage van zulke bisguaiacol gebaseerde PCs.

In Hoofdstuk 2 leidt een uitgebreide literatuurstudie omtrent chemische recyclage technieken tot het concept van base gekatalyseerde methanolyse. Het voornaamste doelwit van PC methanolyse is de carbonaat(ester)brug – de verbinding tussen twee monomeren. Momenteel zijn bisguaiacol gebaseerde PCs niet commercieel verkrijgbaar, om dit probleem te omzeilen start deze masterthesis vanuit carbonaat bevattende structuren met een gelijkaardige chemische omgeving als PCs. Het gekozen modelsubstraat is een *o*-gemethoxyleerd diaryl carbonaat (DAC), *viz.* Diguaiacyl carbonaat (DGC) dewelke bisguaiacol gebaseerde PCs vertegenwoordigt.

Aangezien solvolyse een reversibele transesterificatie is, worden thermodynamische berekeningen uitgevoerd in Hoofdstuk 5. Ter vergelijking wordt naast methanolyse ook ethanolyse en hydrolyse gemodelleerd. Dit verstrekt een duidelijk inzicht in de ligging van het chemische evenwicht (K_{eq}), en bijgevolg in de haalbaarheid van de beoogde reactie. Inzicht inzake de invloed van de additionele *o*-methoxy substituent, wordt verkregen door DGC steeds te vergelijken met difenyl carbonaat (DPC). In Hoofdstuk 6 wordt de reactiekinetiek (k, E_a) experimenteel geverifieerd. Een vergelijkende studie tussen verschillende metaal hydroxides (*e.g.* NaOH) en organokatalysatoren (*e.g.* TBD) toont het belang van de nucleofiliciteit/alkaliniteit van de katalysator aan. Hoewel DGC over het algemeen minder reactief is dan DPC voor methanolyse, wordt er toch succesvol een volledige conversie bereikt bij milde condities.

Scientific abstract

A transition from a linear ‘take-make-use-dispose’ to a circular ‘remake-reuse-recycle’ plastic economy lowers the input of virgin feedstock, and allows to shift towards bio-based feedstock, while decoupling plastics from fossil feedstock. To do so, adequate end-of-life processes, such as chemical recycling, should be adapted to or developed for bio-based polymers. As a perfect example, this dissertation studies the chemical recycling of renewable bisguaiacol-based polycarbonates (PCs) by solvolysis.

In literature, *o*-methoxy bisphenols – so-called ‘bisguaiacols’ – are proposed as renewable and safer alternatives to petroleum-based, endocrine-disruptive bisphenols such as, for instance, bisphenol A (BPA). Among others, the feasibility of bisguaiacol-based PCs will dependent on its potential for recycling. However, to the best of our knowledge, no information is currently available on the (chemical) recycling of such bisguaiacol-based PCs.

In Chapter 2, a profound study of literature on chemical recycling techniques leads to the concept of base-catalysed methanolysis. The main target for methanolysis of PCs is the carbonate (ester) linkage – the connection between two monomers. To circumvent the current commercial unavailability of bisguaiacol-based PCs, this MSc thesis starts from a carbonate-containing model with a chemical environment identical to its corresponding PCs. The model substrate of choice is an *o*-methoxylated diaryl carbonate (DAC), *viz*. diguaiacyl carbonate (DGC), which represents bisguaiacol-based PCs.

As solvolysis entails a reversible transesterification, initially, theoretical thermodynamic calculations are performed in Chapter 5. For comparison, not only methanolysis, but also ethanolysis and hydrolysis are modelled. Overall, this gives a good understanding about the position of the chemical equilibrium (K_{eq}), and therefore the feasibility of the targeted reaction. By benchmarking against diphenyl carbonate (DPC), insight is gained about the effect of the additional *o*-methoxy moiety.

Supported by the favourable thermodynamics, Chapter 6 experimentally verifies the reaction kinetics (k, E_a). A comparative study with different metal hydroxides (*e.g.* NaOH) and organocatalysts (*e.g.* TBD) illustrates the importance of catalyst nucleophilicity/basicity. Although DGC is in general less reactive towards methanolysis than DPC, full conversion is successfully achieved at relative mild conditions.

List of Abbreviations

ΔH_{fus}°	Standard enthalpy of fusion
ΔH_{v}°	Standard enthalpy of vaporization
ΔG_{f}°	Standard Gibbs free energy of formation
ΔG_{r}°	Change in standard Gibbs free reaction energy
ΔH_{f}°	Standard enthalpy of formation
ΔH_{r}°	Standard reaction enthalpy
ΔS_{f}°	Standard entropy of formation
ΔS_{r}°	Standard reaction entropy
2-MeTHF	2-methyltetrahydrofuran
ACN	Acetonitrile
BADGE	Bisphenol A diglycidyl ether
BGF	Bisguaiacol F
BPA	Bisphenol A
DABCO	1,4-diazabicyclo[2.2.2]octane
DAC	Diaryl carbonate
DBC	Dibutyl carbonate
DBU	diazabicyclo[5.4.0]undec-7-ene
DEC	Diethyl carbonate
DGC	Diguaiacyl carbonate
DMA	*N*,*N*-dimethylaniline
DMAP	4-dimethylaminopyridine
DMC	Dimethyl carbonate
DPC	Diphenyl carbonate
EGC	Ethyl guaiacyl carbonate
EPC	Ethyl phenyl carbonate
ER	Oestrogen receptor
EtOH	Ethanol
GC-FID	Gas chromatography – Flame ionization detection
GC-MS	Gas chromatography mass spectrometry
HGC	Hydrogen guaiacyl carbonate
HPC	Hydrogen phenol carbonate
k	Reaction rate constant
K_{eq}	Chemical equilibrium constant
MAC	Methyl aryl carbonate
MeOH	Methanol
MGC	Methyl guaiacyl carbonate
MPC	Methyl phenyl carbonate
NMDRC	Non-monotonic dose response curve
NMI	1-methylimidazole
PC	Polycarbonate
RDS	Rate determining step
STP	Standard temperature and pressure
TBD	1,5,7-triazabicyclo[4.4.0]-dec-5-ene
X	Conversion
Y	Yield

List of Figures

Figure 1.1 The three-step Hock process; (**A**) alkylation of benzene with propene to cumene, (**B**) undesired alkylation of cumene to DIPB and TIPB, (**C**) autoxidation of cumene to cumene hydroperoxide and (**D**) acidic cleavage of cumene hydroperoxide to phenol and acetone.[4,12] 4

Figure 1.2 BPA synthesis mechanism in detail; (**A**) acetone protonation, (**B**) nucleophilic attack of phenol on protonated acetone molecule, (**C**) dehydration of the tertiary alcohol leading to isopropenylphenol, (**D**) nucleophilic attack of the second phenol molecule leading to BPA.[15,16] 5

Figure 1.3 The three possible BPA isomers formed by acid-catalysed condensation of acetone with two equivalents of phenol: (**a**) *p,p'*-BPA, (**b**) *o,p'*-BPA and (**c**) *o,o'*-BPA. 6

Figure 1.4 Common BPA-free analogues, (**a**) BPF, (**b**) BPS and (**c**) BPAF. 8

Figure 1.5 Different pathways for the production of BPA-PC. (**A**) Phosgene pathway and non-phosgene pathway; (**B**) Bayer process, (**C**) SABIC process, (**D**) Asahi Kasei process and (**E**) MGC process. 11

Figure 1.6 Production of BADGE oligomers by the condensation of BPA and epichlorohydrin. 13

Figure 2.1 Plastic waste management distribution between recycling, incineration and landfilling worldwide, in the United States, Europe and China.[57–60] 16

Figure 2.2 Relationship between the integral waste production [ton waste production/ton C in polymer] and the enthalpy of depolymerisation [kJ/mole monomer] of selected polymers. This relationship leads to four quadrants, representing the theoretically most suitable waste management technique: (**1**) reuse, (**2**) reuse or chemical recycling, (**3**) reuse, thermal recycling or incineration and (**4**) reuse, chemical or thermal recycling, incineration or landfill. Adapted from: Lange *et al* (2002).[75] 21

Figure 2.3 The three main constituents of lignin: *p*-coumaryl alcohol, coniferyl alcohol and sinapyl alcohol are generally abbreviated as H (*p*-hydroxyphenyl), G (guaiacyl) and S (syringyl), respectively.[99] 28

Figure 2.4 General reaction of the acid-catalysed condensation of two *p*-substituted *o*-methoxyphenol molecules leading to bisphenols (or bissyringols). (**A**) hydroxyalkylation/alkylation condensation reaction with methoxyalkylphenols, (**B**) alkylation condensation reaction with vanillyl (or syringyl) alcohol. 29

Figure 4.1 Investigation of carbonate bond cleavage *via* solvolysis (*i.e.* hydrolysis or alcoholysis) starting from (**A**) (*o*-methoxylated) BPA-PCs or (**B**) (*o*-methoxylated) diaryl carbonates, with indication of corresponding products. The carbonate bond is highlighted in bold. X = –H (bisphenols) or –OCH_3 (bisguaiacols) and R = –H (water), –alkyl (alcohol). 36

Figure 5.1 Transesterification of an ester and an alcohol resulting in a new ester and new alcohol. 37

Figure 5.2 Alcoholysis of DAC consists of two consecutive transesterification reactions: (**1**) transesterification into an alkyl aryl carbonate (and phenol), and (**2**) transesterification into a dialkyl carbonate (and phenol). Methanolysis (R' = –CH_3) converts DPC (or DGC) to DMC and phenol (or guaiacol) with intermediate formation of MPC (or MGC), respectively. Ethanolysis (R' = –CH_2CH_3) converts DPC (or DGC) to DEC and phenol (or guaiacol) with intermediate formation of EPC (or EGC), respectively. 38

Figure 6.1 Typical GC-FID chromatogram for (**A**) DPC and (**B**) DGC methanolysis. 49

Figure 6.2 Mass spectra of the intermediates (**A**) MPC and (**B**) MGC with annotation and molecular structure of the most abundant fragments. 50

Figure 6.3 Organocatalysts used in the methanolysis of DPC and DGC arranged according to decreasing acidity. Data and figure adapted from Jehanno *et al.* (2019).[94] N/A stands for "Not Available". 54

Figure 6.4 General mechanism of base-catalysed methanolysis of DPC (R = –H) and DGC (R = –OCH_3) with B as a base. (1) and (2) indicate the first and second transesterification reaction, respectively. 56

Figure 6.5 3D visualisation of (left) DPC and (right) DGC. The central, tetrahedral carbon of DGC can be sterically hindered due to the additional *o*-methoxy functionalities, hampering the nucleophilic attack of the methoxide anion. 56

Figure 6.6 DPC (grey) and DGC (black) methanolysis as function of time. Yield in mol% is indicated as Y, conversion in mol% is indicates as X. Reaction conditions: 40 °C, 450 rpm, DPC:NaOH:MeOH = 1:0.027:10 molar ratio, DGC:NaOH:MeOH = 1:0.021:10 molar ratio.60

Figure 6.7 DPC methanolysis against time at different temperatures: 30 °C (dark blue), 40 °C (dark grey) and 50 °C (dark orange). Reaction conditions: 8 h, 450 rpm, DPC:MeOH = 1:10 molar ratio, catalyst concentration; 1.1 mol% NaOH (30 °C), 1.1 mol% NaOH (40°C), 1.2 mol% NaOH (50 °C). 61

Figure 6.8 DGC methanolysis against time at different temperatures: 40 °C (black), 50 °C (green), 60 °C (blue grey). Reaction conditions: 8 h, 450 rpm, DGC:MeOH = 1:10 molar ratio, catalyst concentration; 2.1 mol% NaOH (40 °C), 2.2 mol% NaOH (50 °C), 2.1 mol% NaOH (60 °C). 61

Figure 6.9 Arrhenius plot based on the experimentally determined reaction rate constants of DAC methanolysis. (**A**): Arrhenius plot of $k1, DPC$, DPC methanolysis to form MPC, (**B**): Arrhenius plot of $k2, MPC$, MPC methanolysis to form DMC, (**C**) Arrhenius plot of $k1, DGC$, DGC methanolysis to form MGC, (**D**): Arrhenius plot of $k2, MGC$, MGC methanolysis to form DMC. 63

Figure 6.10 DGC methanolysis catalysed by TBD against time at different temperatures: 40 °C (red), 50 °C (blue), 60 °C (gold). Reaction conditions: 8 h, 450 rpm, DGC:MeOH = 1:10 molar ratio, catalyst concentration; 2.0 mol% TBD (40 °C), 2.0 mol% TBD (50 °C), 2.1 mol% TBD (60 °C). 65

Figure 6.11 Arrhenius plot based on the experimentally determined reaction rate constants of DGC methanolysis catalysed by TBD and NaOH. (A): Arrhenius plot of $k1, TBD$, DGC methanolysis to form MGC, (B): Arrhenius plot of $k2, TBD$, MGC methanolysis to form DMC, (C) Arrhenius plot of $k1, NaOH$, DGC methanolysis to form MGC, (D): Arrhenius plot of $k2, NaOH$, MGC methanolysis to form DMC. 67

Figure 6.12 Two possible mechanisms of DAC methanolysis catalysed by TBD; R = –H (DPC), R = $-CH_3$ (DGC). Adapted from Do *et al.* (2018).[96] 69

Figure 6.13 TBD-catalysed DGC methanolysis against time. Reaction conditions: 8 h, 60 °C, 450 rpm, DPC: MeOH = 1:10 molar ratio, catalyst concentration; 2.1 mol% TBD (gold) and 5.0 mol% TBD (light blue). 71

Figure 6.14 NaOH-catalysed DGC methanolysis as function of time. Reaction conditions: 8 h, 60 °C, 450 rpm, DPC: MeOH = 1:10 molar ratio, catalyst concentration; 2.2 mol% NaOH (blue grey) and 5.0 mol% NaOH (dark green). 71

Figure 8.1 General overview of the envisioned bio-based circular PC economy with indication of current and future research stages; (**A**) Transesterification of DMC) with guaiacol into DGC and MeOH; (**B**) Methanolysis of DGC into DMC and guaiacol; (**C**) Melt-transesterification of DGC and bisguaiacol towards bisguaiacol-PC; (**D**) Methanolysis of bisguaiacol-PC into DMC and bisguaiacol. Full arrows: reactions research of current MSc thesis. Dashed arrows: possible future research. 78

List of Tables

Table 1.1: Summary of the main physicochemical properties of BPA at 25 °C [20–22] 6

Table 2.1: Literature overview of the methanolysis of BPA-PC pellets [89–93,95,97] 25

Table 2.2: Typical *p*-substituted *o*-methoxyphenols produced by lignin-first processes [99] 28

Table 3.1: Group contribution values of selected functional groups for the enthalpy of formation, Gibbs free energy of formation, enthalpy of vaporization and enthalpy of fusion 32

Table 5.1: Overview of the standard thermodynamic quantities of formation of all species participating in methanolysis, ethanolysis and hydrolysis reaction of DPC and DGC 42

Table 5.2: Overview of the calculated $\Delta Hr°$, $\Delta Gr°$, and Keq values for methanolysis (DPC: reaction 1-2, DGC reaction: 3-4), ethanolysis (DPC: reaction 5-6, DGC: reaction 7-8) and hydrolysis (DPC: reaction 9-10, DGC: reaction 11-12) at STP 44

Table 5.3: Transformed literature-based and theoretical calculated thermodynamic data of the transesterification of DPC to MPC (reaction 1) and the subsequent transesterification of MPC to DMC (reaction 2) [117–119] 45

Table 6.1 Catalyst screening of the DPC and DGC methanolysis reaction. Reaction conditions: DAC:catalyst:MeOH = 1:0.02:10 mol%, 40 °C, 2 h, 450 rpm 53

Table 6.2: Experimentally derived first-order reaction rate constants for the consecutive DAC methanolysis reaction at different temperatures 62

Table 6.3: Experimentally determined activation energies of the consecutive DAC methanolysis 63

Table 6.4: Experimentally derived reaction rate constants for the consecutive DGC methanolysis reaction catalysed by TBD and NaOH at different temperatures 66

Table 6.5: Experimentally determined activation energies of the consecutive methanolysis of DGC catalysed by TBD and NaOH 67

Contents

Dankwoord i

Wetenschappelijke samenvatting ii

Scientific abstract iii

List of Abbreviations iv

List of Figures v

List of Tables ix

Contents xi

Research situation 1

I. Literature study 2

1. Bisphenol A as a key player in the plastic world 3

1.1 Bisphenol A (BPA) 3

1.1.1 BPA in numbers 3

1.1.2 Industrial production of BPA 3

1.1.3 Physicochemical of BPA 6

1.1.4 Toxicity of BPA 7

1.1.5 BPA-free analogues 8

1.2 BPA plastics 9

1.2.1 Polycarbonate (PC) 9

1.2.1.1 Industrial production 9

1.2.1.2 Physicochemical properties 10

1.2.1.3 Applications 10

1.2.2 Epoxy resins 12

1.2.2.1 Industrial production 12

1.2.2.2 Physicochemical properties 12

1.2.2.3 Applications 12

1.3 BPA exposure 13

1.3.1 Environmental exposure 13

1.3.2 Human exposure 14

1.3.2.1 Dietary routes 14

1.3.2.2 Non-dietary routes 14

2. Plastic waste management and the circular economy 15

2.1 The linear (plastic) economy 15

2.2 The circular (plastic) economy 16

2.2.1 Drawbacks associated with the linear economy 16

2.2.2 Towards a circular plastic economy 17

2.2.2.1 Waste management techniques in the circular plastic economy 17

2.2.2.2 Bioplastics 22

2.2.3 Towards a circular PC economy 23

2.2.3.1 BPA PC recycling; current situation and perspectives 23

2.2.3.2 Bio-based BPA-PC alternatives 26

II. Materials and methods 30

3. Materials and methods 31

3.1 Joback-Reid method 31

3.2 Solvolysis reactions 32

3.2.1 Methanolysis 32

3.2.2 Product analysis 33

III. Results and Discussion 34

4. Setting the scene 35

4.1 Introduction 35

4.2 DPC and DGC as model compounds 35

5. Thermodynamics of solvolysis 37

5.1 Transesterification 37

5.2 Concept of thermodynamic chemical equilibrium 38

5.3 Thermodynamic equilibrium of solvolysis 40

5.3.1 Standard thermodynamic quantities 40

5.3.2 Calculating K_{eq} 43

6. Kinetics of DGC methanolysis 48

6.1 Introduction 48

6.2 Product identification 48

6.3 Reactivity of (*o*-methoxy) DAC for methanolysis 51

6.4 Catalyst screening 52

6.5 Difference in methanolysis reactivity of DPC and DGC 55

6.5.1 Hypothesis 55

6.5.2 Methanolysis reaction kinetics 57

6.5.3 DAC methanolysis catalysed by NaOH 58

6.5.3.1 Initial experiment 58

6.5.3.2 Rate constants and activation energy of DAC methanolysis catalysed by NaOH 60

6.6 DGC methanolysis catalysed by NaOH and TBD 64

6.6.1 Reactivity difference of DGC for methanolysis catalysed by NaOH and TBD 64

6.6.2 Optimisation of NaOH- and TBD-catalysed DGC methanolysis 69

7. General conclusions 73

8. Future perspectives 77

References 79

Appendix A: List of chemicals 89

Appendix B: Risk Assessment 90

Summary in layman’s terms 100

Research situation

In the 21st century, a world without plastic is almost unthinkable. Metal, wood, ceramics and other materials are often replaced by cost-, resource- and energy-efficient plastics.[1] In recent years however, public concern has arisen about the negative effects of plastic consumption on people, planet and environment. Firstly, plastic production has a profound impact on greenhouse gas emission due to its petroleum-based origin. For example, in 2017 6% of the total global oil and gas consumption was used in the plastic industry.[2] At the current demand for plastic, estimates project that this percentage will reach 20% in 2050.[3] Secondly, the inert and non-biodegradable nature of plastic has led to a worldwide accumulation of plastic waste due to insufficiently developed waste management systems. Consequently, by 2050 the oceans are expected to contain more plastic than fish by weight, in a business-as-usual scenario.[3] Plastic has become a victim of its own success.

A root cause for this plastic pollution is associated with our current linear economy. In this linear model, feedstock is harvested, transformed into materials, sold as products and discarded as waste after use. A possible solution lies in the transition from a linear towards a more sustainable circular economy. In a circular model, material and energy losses are minimized by the implementation of waste management methods such as reuse and recycling rather than landfilling and disposal.

This MSc thesis focusses on the poly(bisphenol A carbonate) (BPA-PC) industry. In Chapter 1, the role of BPA as a monomer and its implementation into polymers, such as PCs and epoxy resins, is described. BPA is a highly controversial chemical. Namely, in addition to its petroleum-based nature and underdeveloped waste management systems, BPA is scrutinized for its endocrine disruptive properties. Therefore, Chapter 2 addresses the current problems, challenges and developments faced by the BPA-PC industry regarding (i) the replacement of fossil feedstock with bio-based, renewable feedstock and (ii) the end-of-life processing. Based on recent literature, bisguaiacol monomers serve as both renewable and safer BPA alternatives. Furthermore, solvolysis is put forward as the most promising chemical recycling method for BPA-PCs. The combination of these two findings serves as the starting point of the experimental section. In short, this MSc thesis studies the potential of solvolysis in the chemical recycling of bisguaiacol-based PCs based on both theory and practice (Chapter 5 and 6).

I. Literature study

1. Bisphenol A as a key player in the plastic world

1.1 Bisphenol A (BPA)

1.1.1 BPA in numbers

Bisphenol A (BPA) (4,4'-(propane-2,2-diyl)diphenol, CAS 80-05-7) is a synthetic, abundant monomer, an elementary building unit, in the plastic industry. At the beginning of the 21st century, BPA became the biggest consumer of phenol, accounting for roughly 35% of the global phenol consumption in 2001.[4] The global demand of BPA was estimated at 8 million tons in 2016 of which about 1.15 million tons were demanded by Europe.[5,6] The biggest player in the worldwide BPA market is China, who roughly accounted for 20% of the global demand of BPA in 2018.[7]

The main uses of BPA are in the production of polycarbonate (PC) followed by the production of epoxy resins which respectively account for 64% and 34% of the global BPA demand in 2018. The remaining, rather small, amount of BPA is used for different applications such as flame retardants, polysulfones, polyarylates and unsaturated esters.[4,7] The demand of BPA is estimated to increase annually by nearly 5%,[8] because BPA-based plastics are being promoted by the BPA industry as durable materials with long life cycles contributing to resource and energy efficiency.[9]

1.1.2 Industrial production of BPA

BPA is made from phenol and acetone (Fig 1.1). Both reagents originate from the Hock process. This process interconverts fossil-derived benzene and propylene to phenol and acetone.[10]

The Hock process is a three-step reaction (Fig. 1.1). First, cumene is generated out of benzene and propylene by a Friedel-Crafts alkylation reaction at elevated temperature (200 – 350 ˚C) and pressure (10 – 15 bar) (Fig. 1.1A). This reaction is catalysed by both Lewis and Brønsted acidic catalysts, such as $AlCl_3$ and acidic zeolites.[11] Undesired consecutive reactions of cumene with propylene to di- and tri-isopropyl benzene (DIPB and TIPB) (Fig. 1.1B) are especially suppressed when using zeolites, making them effective catalysts.[12] Secondly, the autoxidation of cumene *via* a radical chain mechanism in aqueous alkali gives cumene hydroperoxide (Fig. 1.1C). Finally, the cleavage of cumene hydroperoxide with H_2SO_4 generates phenol and acetone in a 1:1 ratio (Fig. 1.1D).[13]

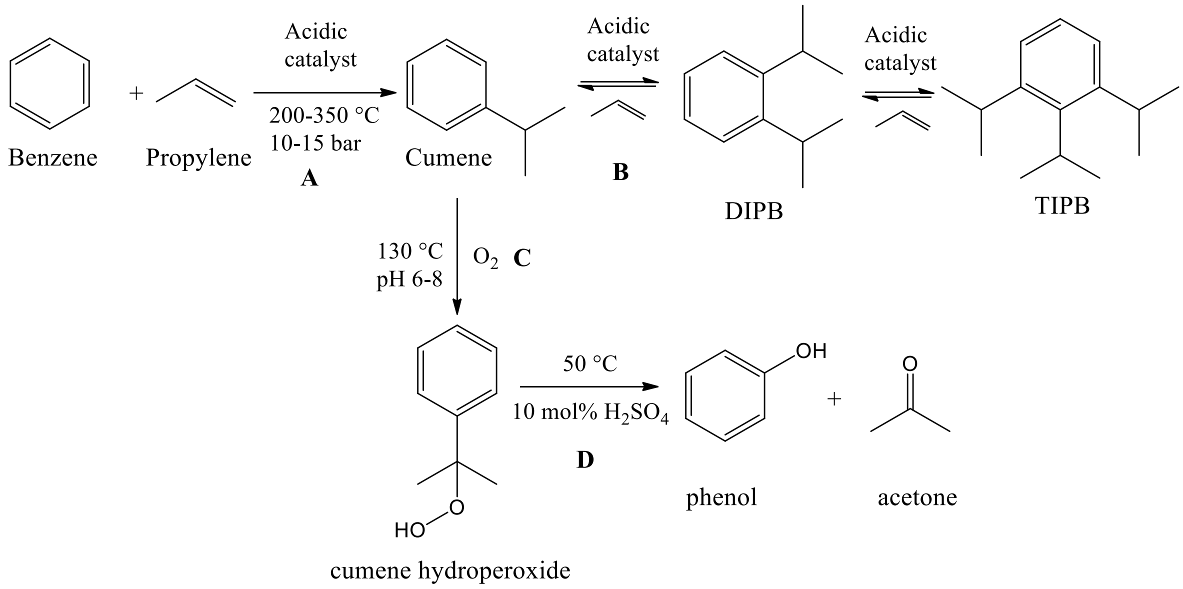

Figure 1.1 The three-step Hock process; (**A**) alkylation of benzene with propene to cumene, (**B**) undesired alkylation of cumene to DIPB and TIPB, (**C**) autoxidation of cumene to cumene hydroperoxide and (**D**) acidic cleavage of cumene hydroperoxide to phenol and acetone.[4,12]

On an industrial scale, BPA is typically produced by acid-catalysed condensation of acetone and two equivalents of phenol. This electrophilic aromatic substitution reaction is conducted at elevated temperatures (50 – 90 °C) in the presence of either strongly acidic homogeneous (*e.g.* HCl, H_2SO_4)[13] or heterogeneous catalysts (*e.g.* Amberlyst®-15, Nafion® NR-50).[14] Heterogeneous catalysts are preferred to homogenous catalysts because (i) a continuous reaction is possible, (ii) minimal waste water is produced, (iii) the set-up is cheaper and easier to handle, and (iv) product purification is simpler.[4]

The general reaction pathway of the electrophilic aromatic substitution comprises four steps (Fig. 1.2). Firstly, acetone is protonated by the strongly acidic catalyst increasing its electrophilic character (Fig. 1.2A). Secondly, phenol will perform a nucleophilic attack on the carbonium ion of acetone resulting in a tertiary alcohol (Fig. 1.2B). The *para*- and *ortho*-position are electronically favoured over the *meta*-position of phenol. Next, this tertiary alcohol is dehydrated to form the protonated *para*- or *ortho*-isopropenylphenol (Fig. 1.3C) which immediately adds a second phenol molecule (Fig. 1.2D). This leads to two isomers of BPA, namely *p,p'*-BPA and *o,p'*-BPA. Furthermore, BPA is prone to acid-catalysed isomerisation under strongly acidic conditions. Herein, BPA is reversely cleaved to phenol and *p*-isopropenylphenol, and immediately recoupled with the *o*- or *p*-position of phenol, leading to an equilibrium mixture of *p,p'*-BPA and *o,p'*-BPA, with traces of *o,o'*-BPA.[15,16]

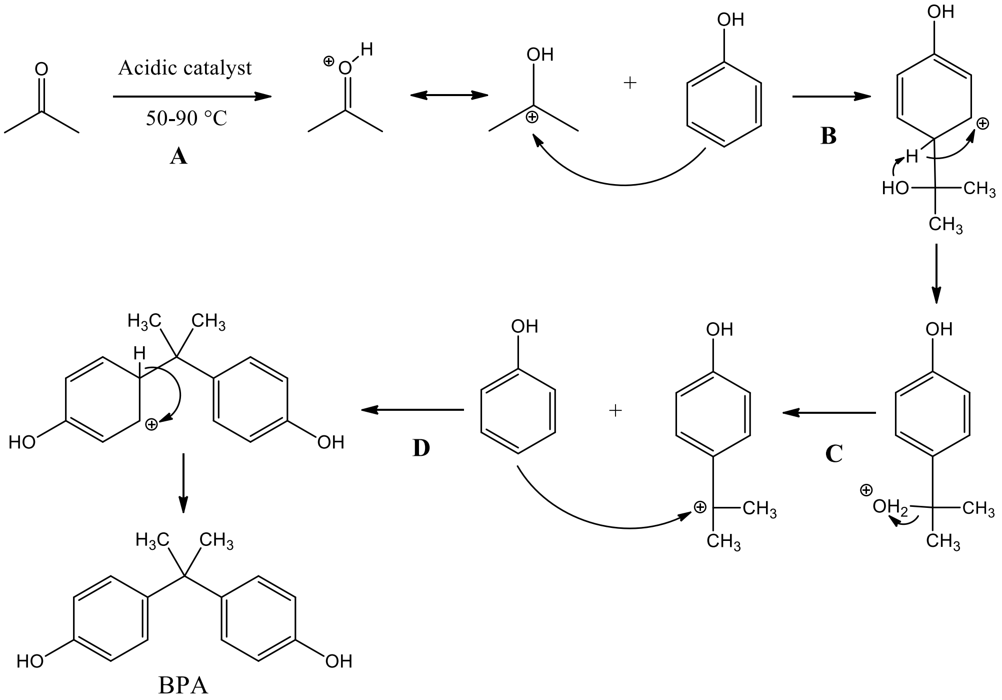

Figure 1.2 BPA synthesis mechanism in detail; (**A**) acetone protonation, (**B**) nucleophilic attack of phenol on protonated acetone molecule, (**C**) dehydration of the tertiary alcohol leading to isopropenylphenol, (**D**) nucleophilic attack of the second phenol molecule leading to BPA.[15,16]

For the polymeric applications of BPA, only *p,p'*-BPA isomers are desired in a high purity. BPA production leads to a mixture of desired *p,p'*-BPA and undesired *o,p'*-BPA isomers, so there is need for a co-catalyst which steers the selectivity towards *p,p'*-BPA. The most used co-catalysts are sulphur-containing molecules, such as thiols. Thiol (*e.g.* an alkylthiol) will perform a nucleophilic attack on the activated acetone leading to a hemithioacetal that is subsequently dehydrated to a positive charged thioketone.[17] Zeidan *et al.* (2006) attributed the increased regioselectivity to steric hinder of the bulky thioketone, which favours the nucleophilic attack of phenol on the less sterically hindered *p*-position.[15,18] A different hypothesis, described by Van de Vyver *et al.* (2012), states that the regioselectivity results from kinetic effects of the thiol co-catalyst.[17]

The molecular structure of BPA is shown in Figure 1.3. It consists of a tetrahedral carbon atom with two methyl and two phenol groups.[19]

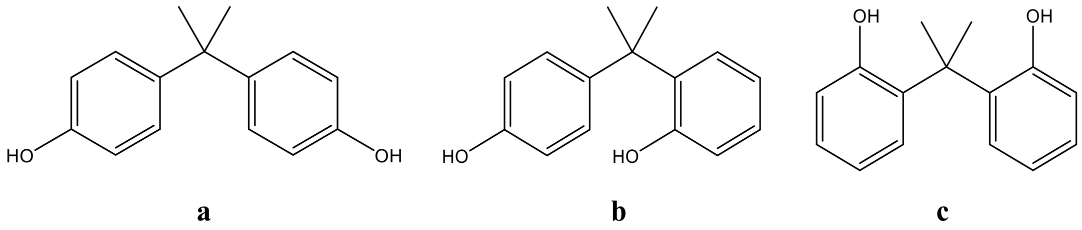

Figure 1.3 The three possible BPA isomers formed by acid-catalysed condensation of acetone with two equivalents of phenol: (**a**) *p,p'*-BPA, (**b**) *o,p'*-BPA and (**c**) *o,o'*-BPA.

1.1.3 Physicochemical of BPA

The main physicochemical properties of BPA are summarised in Table 1.1. Under ambient conditions, BPA is a white crystalline material with a moderate water-solubility (120 – 300 mg. L^{-1} at 25 °C). In aqueous alkaline solutions its solubility increases due to the deprotonation of BPA towards the corresponding (di)phenolate anion(s). According to its octanol-water partition coefficient (log (K_{ow})), BPA is moderately hydrophobic (3.46 ± 0.32) and is therefore soluble in organic solvents (*e.g.* acetone, methanol, THF, benzene). BPA has a low volatility due to its low vapor pressure, moderate water-solubility and high melting temperature. This low volatility can be expressed in terms of a small Henry constant (K_H) meaning that BPA is unlikely to evaporate from aqueous solution. BPA has a half-life time in water, soil and air of 38, 75 and 0.2 days, respectively. The half-life time in air is small compared to the other compartments due to rapid photo-oxidation of BPA in the atmosphere. The half-life time in soil is the largest, indicating that BPA is not readily biodegradable.[20,21]

Table 1.1 Summary of the main physicochemical properties of BPA at 25 °C [20–22]

Physicochemical properties	**Value**
Water solubility [mg.L^{-1}]	120-300
pK_a [-]	10.29 ± 0.69
log(K_{ow}) [-]	3.64 ± 0.32
K_H [Pa.m^3. mol^{-1}]	4.03 x 10^{-6}
Vapor pressure [Pa]	5.3 x 10^{-6}
Melting temperature [°C]	155
Half-life time water [days]	38
Half-life time soil [days]	75
Half-life time air [days]	0.2

1.1.4 Toxicity of BPA

The use of BPA in the polymer industry has resulted in controversy. Despite its excellent properties, leading to high value plastics (as will be discussed in section 1.2), BPA also has a concerning disadvantage. BPA can be classified as an endocrine disruptor.[23] The endocrine system uses hormones to (i) direct development and reproduction, (ii) regulate body function and metabolism, and (iii) influence behaviour and immunity. Endocrine disrupters alter hormone signalling or the response to hormone signalling by interfering with the signalling process.[24]

The endocrine activity of BPA is known since the 1930s when scientists searched for synthetic oestrogens. BPA was not used as a pharmaceutical because other, more powerful, synthetic oestrogens were discovered.[25] It was only in 1991 that a group of scientists came with the statement that “A large number of man-made chemicals that have been released into the environment have the potential to disrupt the endocrine system of animals, including humans”.[26] Since then, a lot of international research and attention went to these endocrine disruptors, including BPA.

The hormonal activity of endocrine disrupters originates from their molecular structure because they need to fit the binding pocket of endocrine receptors. The 4-hydroxyl substituent on both phenyl rings makes it possible for BPA to bind these receptors.[27] BPA can bind several endocrine receptors such as the oestrogen receptor (ER) and the thyroid hormone receptor. ER is normally activated by the natural hormone oestradiol but when BPA binds, it will lead to an altered ability of ER to recruit co-activators important for differences in tissue-dependent responses.[28] Because the endocrine system is essential in a lot of different physiological pathways, modifications in these pathways lead to severe health effects. Animal (and human) exposure to BPA is linked with a wide range of potential negative health effects such as a reduced fertility and sperm quality, ovarian disease, miscarriage, breast cancer, male genital abnormalities, abnormal neurodevelopment, type 2 diabetes, cardiovascular disease, etc.[29]

Despite this long list of potential negative health effects, many scientists and organisations believe that BPA is currently not a threat to human health. National and international bodies such as the American Chemistry Council (ACC), the US National Toxicological Program (NTP), the World Health Organization (WHO) and the US Food and Drug Administration (FDA) all stated that BPA plastics are safe and pose no threat to human health.[30–33] Their main arguments are that BPA is exposed at very low, unharmful concentrations and, in addition, the affinity of BPA to bind ER is 10 000 times less than oestradiol, which makes BPA a weak oestrogen.[34] Other international bodies such as the European Chemical Agency (ECHA) believe in its potential harmful effects and have BPA classified as a "substance of very high concern".[35]

Scientists who are convinced of the potential harmful effects of BPA support their opinion saying that BPA has (i) a non-monotonic dose response curve (NMDRC) and (ii) low dose effects.[36] A dose response curve gives the relationship between the dose of a certain compound and the response, the effect, it causes. When the dose increases in a traditional monotonic dose response curve, the response increases, and the biological effects become more severe. A monotonic dose response curve usually has a linear-like shape. On the other hand, in a NMDRC, two or more contradictory effects compete. The toxic effect of a compound can be more harmful at a lower dose than at a higher dose, where different effects could cancel each other out. NMDRC usually has an inverted U shape. Furthermore, BPA also has a low dose effect. Low dose effects are biological changes occurring in the range of typical human exposures or in doses below those used in toxicology studies. The combination of the low dose effect and NMDRC makes it possible that BPA has significant, harmful effects at low, environmentally relevant, doses, which may not be expressed at higher doses used in toxicological studies.[29,37]

1.1.5 BPA-free analogues

As the scientific world cannot give a unanimous statement about the endocrine disrupting effect of BPA, some countries have decided for themselves and banned certain BPA plastics. In 2010, Canada banned BPA from all food packaging applications for infants and babies.[38] The EU followed in 2011, when the use of BPA in baby bottles was forbidden in all EU-countries. In 2016, the EU strengthened its rules concerning BPA in food packaging applications.[39]

These regulations and the public concern on BPA plastics have led to BPA-free products. These products contain BPA analogues such as BPF, BPS and BPAF (Fig 1.4).[40]

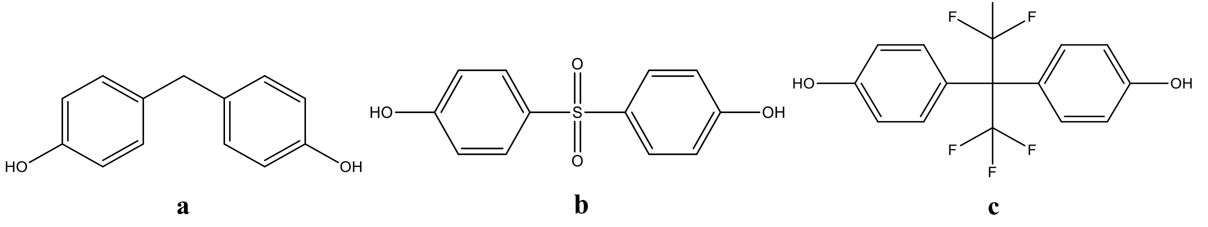

Figure 1.4 Common BPA-free analogues, (**a**) BPF, (**b**) BPS and (**c**) BPAF.

These compounds are structural analogues to BPA which implies that they also fit the binding pocket of some endocrine receptors. Unfortunately, their endocrine disrupting activities have proven to be in the same order of magnitude as BPA's endocrine disruptive activity making them undesirable BPA alternatives.[41]

1.2 BPA plastics

Despite the controversy concerning BPA, BPA-based plastics are still produced in high volumes due to their excellent performance in PC and epoxy resins.

1.2.1 Polycarbonate (PC)

1.2.1.1 Industrial production

Aromatic PCs are conventionally produced *via* interfacial polycondensation of BPA and phosgene. Phosgene is dissolved in an organic solvent, (*e.g.* DCM), and sodium salts of BPA are dissolved in an aqueous solution. Polymerisation takes place at the interface of these two immiscible liquids. The reaction is carried out at 20 – 40 °C. Quaternary ammonium salts (*e.g.* $Bu_4N^+ Cl^-$) are often added as phase transfer catalyst to accelerate the reaction.[42,43] This reaction has some major disadvantages; (i) phosgene, a highly toxic and corrosive molecule, is used in large amounts, (ii) the process uses large amounts of harmful solvent, DCM is classified as possible carcinogenic to humans and (iii) a huge amount of waste water containing organic components must be treated.[44] Because of these drawbacks, more sustainable and less toxic alternatives are developed by industry. Bayer, SABIC, Asahi Kasei and Mitsubishi Gas Chemical (MGC) all developed a non-phosgene, melt-phase transesterification production method (Fig. 1.5).[45] In this process, diphenyl carbonate (DPC) reacts with BPA (Fig. 1.5A), in absence of solvent at a high temperature (200 – 300 °C) under reduced pressure (0.01 bar), resulting in a growing PC chain. This transesterification process varies between the different companies in the way they generate their reactant, *e.g.* DPC and/or dimethyl carbonate (DMC). Bayer (Fig. 1.5B) produces DMC by carbonylation of methyl nitrite. Next, DMC undergoes transesterification with phenol leading to DPC. SABIC (Fig 1.5C) produces DMC *via* oxidative carbonylation of methanol. The pathway of Asahi Kasei (Fig. 1.5D) starts from ethylene oxide and CO_2 leading to ethylene carbonate (EC). On its turn, EC reacts with methanol to DMC and ethylene glycol. In the process of Mitsubishi Gas Chemical (Fig. 1.5E), urea reacts with *n*-butanol leading to dibutyl carbonate (DBC). DBC undergoes transesterification with phenol leading to DPC.[42,44–46] Drawbacks of these non-phosgene pathways are (i) the energy-consuming reaction conditions because of unfavourable reaction equilibria and (ii) the lower reactivity of DPC compared to phosgene. Due to these drawbacks, still approximately 90% of all BPA-PC is industrially produced by interfacial polycondensation with phosgene.[47]

1.2.1.2 Physicochemical properties

BPA-PC is an engineering polymer, *i.e.* it has better mechanical properties than the commodity, bulk polymers. BPA-PC materials have a great impact strength, high toughness and rigidity up to 145 °C, the glass-transition temperature of BPA-PC. They also display an excellent optical transparency and are good electrical insulators. Disadvantages of BPA-PCs are their limited resistance to organophilic hydrolysing chemicals (*e.g.* ammonia and amines) and UV light. In order to produce BPA-PC with such excellent properties, it is necessary to use *p,p'*-BPA isomers with a purity of 99.9% as monomers. Traces of *o,p'*-BPA will lead to more brittle, small chain polymers with inferior properties.[43,48]

1.2.1.3 Applications

Due to its high impact strength and toughness BPA-PC are well-suited for safety applications, such as safety goggles, helmets and laminated sheets for bulletproof glazing. Moreover, its optical transparency makes it suitable in for example the housing for car lights, glazing panels and lenses. Furthermore, microwave resistant cookware, baby bottles and packaging films for medical devices are made of BPA-PC because the plastic can withstand temperatures up to 145 °C and is not easily hydrolysed. Finally, BPA-PC plastic is used as an insulator in multiple applications such as the housing for electronic devices.[43,48]

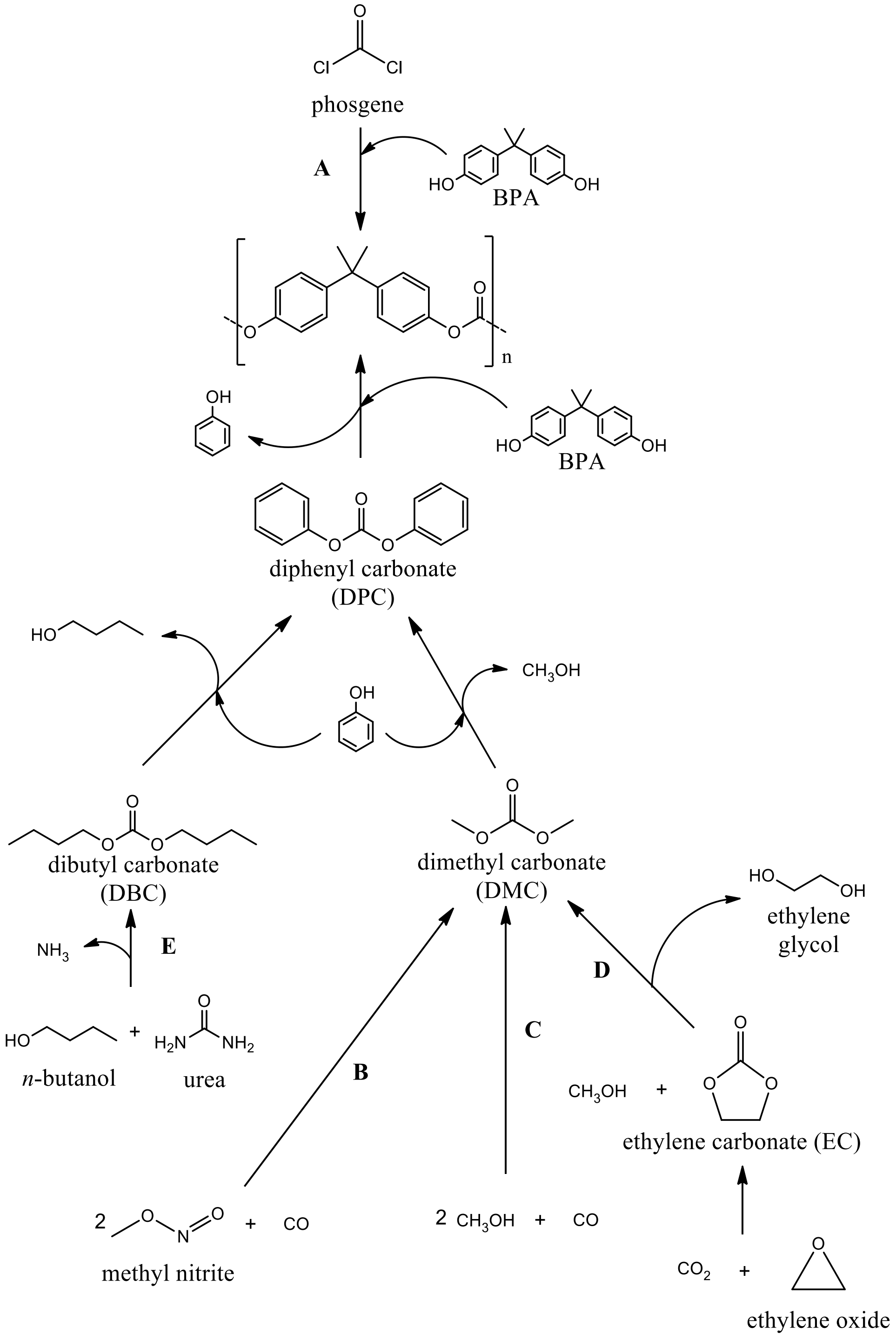

Figure 1.5 Different pathways for the production of BPA-PC. (**A**) Phosgene pathway and non-phosgene pathway; (**B**) Bayer process, (**C**) SABIC process, (**D**) Asahi Kasei process and (**E**) MGC process.

1.2.2 Epoxy resins

Epoxy resins based on diglycidyl ether of BPA (DGEBA or BADGE) were the first commercial epoxy resins produced in the 1940s. After the commercial success of BADGE, other precursors such as phenolphthalein were used to produce a variety of epoxy resins. Until today, BADGE-based epoxy resins are one of the most important epoxy resins (>75% of epoxy resin sales volume in 2012).[49]

1.2.2.1 Industrial production

BADGE oligomers are produced by the condensation of BPA and epichlorohydrin in an aqueous solution at 110 °C with NaOH as the catalyst (Fig. 1.6). The chain length (*n*) of these BADGE oligomers is dependent on the reagents ratio and can range from values of 0.03 to 10. An excess of epichlorohydrin will generally result in a low chain length. Oligomers with a lower chain length have a higher density of functional ends which ultimately leads to a more crosslinked resin. The epoxy resin is formed by adding a hardener or crosslinking agent to the BADGE oligomers which will react with the reactive epoxide end-groups. Polyfunctional amines such as a diamine are typically used as the crosslinking agent.[49,50]

1.2.2.2 Physicochemical properties

BADGE-based polymers derive their profitable properties from their cross-linking ability. This leads to chemically and thermally resistant polymers which have superb adhesive and electrical properties.[42]

1.2.2.3 Applications

The primary use of BADGE-based polymers is as a protective coating for metal containers, ships and appliances where resistance to severe corrosion is required. BADGE-based polymers are also used, in combination with glass or carbon fibres, in aerospace components, circuit boards and sporting equipment. Furthermore, it is used as an adhesive, sealant, casting material and flooring compound.[42,49]

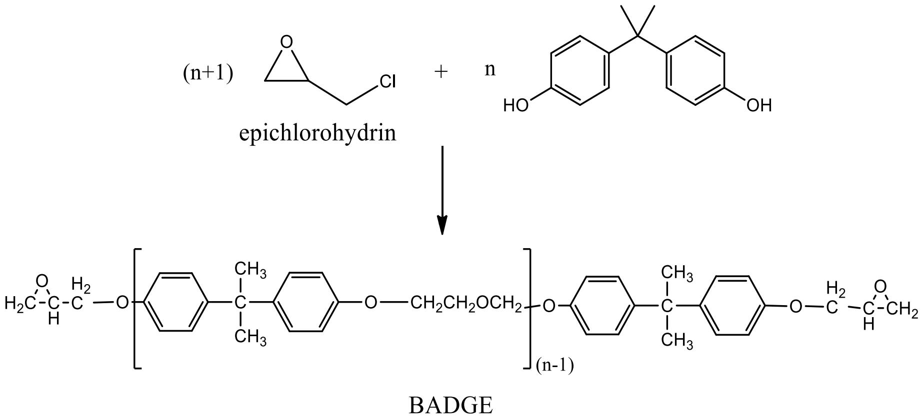

Figure 1.6 Production of BADGE oligomers by the condensation of BPA and epichlorohydrin.

1.3 BPA exposure

1.3.1 Environmental exposure

Although BPA does not occur naturally in the environment, its presence in different environmental compartments is ubiquitous as a result of its high production and consumption. BPA can be found in surface water, seawater, sediments, soils and air all around the world with concentrations ranging from ng.L^{-1} to µg.L^{-1}.[51] BPA, present in the environment, results from different emission routes and sources. First, BPA can leach into the environment from pre-consumer sources such as the effluent discharge of manufacturing plants or transportation and processing of BPA and BPA-containing products. Secondly, post-consumer sources are those associated with disposal of waste, leaching from landfills and combustion of domestic waste. When BPA plastics enters the environment, they are exposed to environmental conditions and stress which may result in the natural degradation of the polymer into monomeric BPA.[21] Natural degradation includes processes such as photodegradation by solar UV radiation, biodegradation and hydrolysis. Sajiki *et al.* (2003) studied the difference in leaching of BPA-PC in seawater, river water and control water. BPA exposure in seawater was three and six times higher than in river and control water, respectively. They concluded that the leaching in seawater was the highest due to the higher pH and mineral concentration of seawater compared to river and control water.[52] Due to the presence of BPA in the aquatic environment, it also has been detected in several different aquatic species. However, BPA shows little ability to bio-accumulate considerably from water in tissues of organisms. It is relatively fast eliminated by the metabolism of these aquatic species.[21]

1.3.2 Human exposure

Despite BPA's limited ability to bio-accumulate, humans also are exposed to BPA. BPA has been detected in almost all human fluids (*e.g.* blood plasma, urine, breast milk and semen) with a concentration in the range of ng.mL^{-1}.[34]

1.3.2.1 Dietary routes

For humans, the diet is the main exposure route of BPA. BPA-containing polymers can come into direct contact with food, leading to the migration of BPA into food. This BPA can be residual BPA, BPA that was not polymerised and is available to freely diffuse into food. In addition, BPA containing polymers can be hydrolysed, catalysed by the food itself, and thus leach BPA into food.[53] The two main BPA containing polymers, PC and epoxy resins, both contribute to the leaching of BPA into food. BPA can leach from PC food containers and bottles. Baby bottles for infant formula milk used to contain BPA-PC but the risk of BPA exposure and accumulation in infants was too high. Infants have a limited capacity to metabolise xenobiotics and they take up a lot of liquid food compared with their body weight.[21] BPA is nowadays banned from baby bottles in many countries.[54] BADGE-based epoxy resins are often used as an internal coating of metal food and beverage cans to prevent direct contact between the metal can walls and the food or beverage and to prevent the cans from rusting and corrosion.[53] The main parameters affecting leaching of BPA are contact time, temperature and pH of the food. These parameters all have a positive correlation, when the parameter increases, also the leaching of BPA will increase.[54]

1.3.2.2 Non-dietary routes

Besides dietary routes, also non-dietary routes contribute to human BPA exposure. Monomeric, 'free' BPA is used as a colour developer in thermal paper (*e.g.* cash receipts). BPA on thermal paper is not covalently bound and can be easily transferred from thermal paper to human skin leading to dermal exposure of BPA. BPA is more easily transferred to wet and greasy fingers.[53] Furthermore, the methacrylated version of BADGE (bis-GMA) is frequently used as a co-monomer in dental composite resins. BPA might still be present as an impurity in the composite resin.[55]

2. Plastic waste management and the circular economy

2.1 The linear (plastic) economy

The current industrial economy can be described as a linear economy. In a linear economy, natural resources are harvested, transformed into base materials, sold as products and, discarded as waste after use. The plastic industry is no exception.[56]

The global plastic production was estimated at 335 million tons in 2016 and at 348 million tons in 2017.[57] During the 21st century, the plastic production annually increased between 3 and 8%.[58] With the industrial rise of (former) developing countries such as China and India, plastic production has gotten and still gets a powerful boost. The industrialization of these countries has increased their standards of living, resulting in the replacement of metal, wood, ceramics, etc. for cost, resource and energy efficient plastics.[1] China currently is the world leader in terms of plastic production, it produces 29% of the global plastics. The rest of Asia, together with China, produces 50% of the plastic materials. Europe, at present, produces 18.5% of the global plastics and its position has shifted from a producing to a trading agent.[57]

There are three different strategies for handling plastic waste. The first is recycling, which aim is to reuse plastic waste or certain parts of it. The second is incineration, where the waste is burned with the aim of energy recovery. And finally landfilling, where the waste is stored in a controlled and/or closed space. The percentage distribution between these three waste management methods varies between different regions in the world and is dependent on the region’s economic situation and political view on environmental care. An overview of this distribution worldwide, in the USA, Europe and China is given in Figure 2.1. Worldwide, landfilling is the most applied method, followed by incineration and recycling as a third option.[57–60] Landfilling is easy and has a low cost while the energy recovery in incineration is high due to the high efficiency of the incinerators.[61]

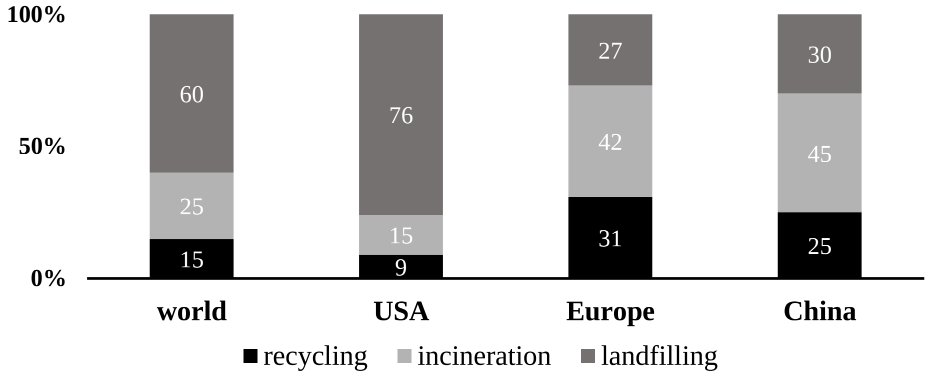

Figure 2.1 Plastic waste management distribution between recycling, incineration and landfilling worldwide, in the United States, Europe and China.[57–60]

Not all plastic waste is collected and treated by one of these three waste management methods. Approximately 60% of all plastic ever produced is mismanaged plastic waste, plastic that is either littered or inadequately disposed.[58] Inadequately disposed waste is waste where there initially was the intention of being managed through waste collection or storage sites, but was ultimately not sufficiently managed. It usually ends up in dumps or open, uncontrolled landfills. Littered plastic waste represents the plastic that is dumped or disposed illegally and uncontrolled at inappropriate locations.[62] Mismanaged plastic waste will easily find its way to the environment. It can be found in soil, sediment, landfills and the aquatic environments making it a global and environmental problem.[63,64]

2.2 The circular (plastic) economy

2.2.1 Drawbacks associated with the linear economy

The linear plastic economy both has environmental and economic drawbacks. The environmental drawbacks are associated with both the feedstock and the end-of-life options of the product while the main economic drawback is the loss of value.[65]

The plastic industry is fossil fuel-based, over 90% of all plastics produced are derived from virgin fossil feedstock.[66] Of all oil and gas used worldwide, roughly 85% is used as a fuel for transport, electricity and heating while the remaining 15% is used to produce chemicals. Of this 15%, 40% is used by the plastic industry, corresponding to 6% of all oil and gas used worldwide.[2] If the current plastic demands continues as expected, the plastic industry will account for 20% of the total gas and oil consumption by 2050.[3] Fossil fuel consumption is heavily linked with greenhouse gas emission. Even though plastics can bring resource efficiency benefits during their use, plastic production has an unneglectable greenhouse gas impact.[3]

The inert and non-biodegradable nature of plastic are advantageous when these materials are in use but cause significant environmental problems without proper end-of-life processing. These properties has led to the accumulation of plastic waste.[64] Landfilling, globally the most used plastic waste management method (Fig. 2.1), occupies a lot of valuable land that could be used for other applications such as agriculture. On top of that, this land can be polluted due to leaching of the landfilled waste. Incineration, globally the second most used method, can result in the release of air pollutants such as CO_2, volatile organic compounds (VOCs), polycyclic aromatic hydrocarbons (PAHs) and dioxins which have a negative impact on the environment and human health.[67]

Plastics have a wide range of application times. Plastics used in the construction sector last many decades, but contrary, materials used in the packaging sector are mainly single-use plastics. These single-use plastics are lost in a linear economy due to landfilling, incineration or mismanaging. Annually, 95% of plastic packaging material is lost after its first-use cycle, corresponding to 70-110 billion euros of material value lost to the economy.[66]

To counter these environmental and economic problems, there is need for a new economic model where these losses are minimized, and the environmental stress is reduced.

2.2.2 Towards a circular plastic economy

2.2.2.1 Waste management techniques in the circular plastic economy

The plastic circular economy attempts to minimize material, energy and value losses by using different recycling techniques and incineration for energy recovery rather than landfilling. Recycling can be subdivided into three main processes; mechanical, chemical and thermal recycling.[68]

Mechanical recycling

In mechanical recycling, the chemical structure of the polymer is maintained throughout the recycling process. In general, it consists of four steps; (i) sorting, (ii) shredding, followed by (iii) washing and drying and (iv) the reprocessing and product formation. Sorting is a crucial first step in the recycling process because of the incompatibility of different polymer types. A small amount of certain polymer types in a waste stream of another polymer type can downgrade the mechanical properties and quality of the final polymer product.[69] Next in the process is the shredding step where the material is reduced in size and improved in density. The third step is the washing and drying step to remove all remaining residues, impurities and moisture.[69] The final step in the mechanical recycling process consists of the reprocessing and formation of the product. The raw, recycled material melts upon heating while pushed through an extruder, is moulded and afterwards cooled into a certain shape depending on the mould (*e.g.* extrusion, injection moulding or blow moulding).[68,70]

Nowadays, mechanical recycling is the main industrial recycling technique but also has some economic drawbacks which temper its use; (i) mechanical recycling can only be executed on a pure feed of certain thermoplastics and (ii) mechanical recycling is hampered by the sorting step which is very time, money and energy consuming.[67]

Chemical recycling

Chemical recycling refers to depolymerisation techniques that either completely break down polymers into monomeric constituents or partially convert polymers into secondary valuable materials.[61] The controlled chain scission is induced by varying chemical agents, all solvolysis reactions. Depending on the type of solvolysis reaction either, the original monomer (*e.g. via* hydrolysis) or a closely related derivate thereof (*e.g. via* alcoholysis, glycolysis or aminolysis) is obtained.[71,72] Chemical recycling is mainly applicable to thermoplastics. The presence of a dense, 3D crosslinked network in thermosets makes it difficult to reprocess them by chemical or thermal means. Contrary, thermoplastics are built from long 2D chains interconnected only by weak Van der Waals interactions. Therefore, (i) the chain linkages in thermoplastics are more easily reached and (ii) chain scission in thermoplastics will result more frequently in monomeric units. Furthermore, chemical recycling is particularly suited for polymers formed by polycondensation reactions (*e.g.* PET, PC, nylon) as the depolymerisation process is fundamentally the reverse of the polymerisation process.[68]

Chemical recycling is still not economically viable on an industrial scale due to the high energy cost. For the moment, it is studied at lab-scale as a future alternative.[69]

Thermal recycling

Thermal recycling methods are based on the combustion of plastic waste to generate useful gases and liquids. The methods are usually categorized based upon their oxygen requirements. **Pyrolysis** is a thermal recycling process in the absence of oxygen. When it is carried out at temperatures between 450 – 600 °C, it is a depolymerisation technique and can be referred to as cracking. The main products are monomers, potentially useful for polymerisation, pyrolysis oil, gases and solid residues, mainly char.[68] Another process is hydrogenation, or **hydrocracking**. The process is similar to pyrolysis with the main difference that the plastic waste is heated in the presence of hydrogen. The cracked molecules are saturated with hydrogen resulting in the formation of saturated liquids and gaseous hydrocarbons. The last thermal recycling process is **gasification**. This process is based on partial combustion, *i.e.* the oxygen input is less than needed for complete combustion. The products of this process are mainly syngas and solid ash residues.[73]

In general, thermal recycling can handle high molar mass organic molecules, but exhibits a low selectivity in terms of the monomer. Thermal recycling produces a wide range of by-products due to random thermal decomposition compared with chemical recycling.[74]

Incineration

Incineration and thermal recycling are both methods based on thermal degradation of polymers, but with different aims. The first is focused on energy recovery while the latter is focused on material recovery. In incineration, plastic waste is used as a fuel source for energy generation.[61] The process focusses on the complete combustion of the waste to generate energy, in the form of heat, which can be converted into more useful forms of energy such as electricity. Incineration is carried out with an excess of oxygen to maximize the combustion and consequently the energy recovery.[71]

Suitable waste management methods

Of all waste management methods, recycling is the most promising in terms of sustainability and should be the most important in the circular economy. Nevertheless, landfilling and incineration are globally applied on a larger scale due to their economic advantages. An economic drawback of recycling is that the recycled products need to compete with virgin materials. The price of the virgin materials is determined by the price of its feedstock, mainly crude oil, and is, for the moment, lower than the production cost of recycled materials. In order to compete with virgin materials, recycled materials also need to be of high quality. Current recycling processes usually lead to products with a lower quality than the virgin materials due to for example contamination of the recycling feed.[67,69]

A polymer’s ability to be mechanically recycled differs between thermoplastics and thermosets. The former polymers melt before they decompose upon heating and can undergo mechanical recycling. The latter polymers decompose before they melt upon heating and cannot undergo mechanical recycling.[71] In theory, every polymer type is chemically and thermally recyclable although thermoplastics are more suited for these methods. The most suitable and sustainable waste management method for a certain polymer depends on many technical, economic and societal factors. In order to theoretically predict the most suitable technique, Lange *et al* (2002) introduced two parameters.[75] The first parameter, the integral waste production, contributes for the total waste generated during the production process. The second parameter is the enthalpy of depolymerisation. The lower the enthalpy requirement, the easier the depolymerisation process. The enthalpy of depolymerisation does not contain the chemistry of depolymerisation, *i.e.* it does not contain any information about the selectivity of depolymerisation. These two parameters are shown in Figure 2.2 for some selected polymers.

Different relationships can be observed between these two parameters leading to four quadrants. Each quadrant has certain preferred waste management techniques. **Quadrant 1** groups the polymers which have a high waste production and a difficult depolymerisation. Polymers such as PUR, PVC and PMMA are least attractive from environmental point of view and they should be reused as much as possible. The development of more efficient production pathways is necessary to make recycling beneficial. **Quadrant 2** contains polymers with a high waste production, but which are more easily depolymerised. PC and polyamides such as nylon-6 and nylon-66 have two preferable disposal techniques, reuse and chemical recycling. Their amide and carbonate linkages are prone to undergo controlled polymerisation. **Quadrant 3** groups polymers with a low waste production and which are difficult to depolymerise. Polymers such as PP, PS and PE can be viewed as crude oil analogues. They could undergo thermal recycling or be incinerated as an energy source. **Quadrant 4** contains polymers that combine low waste production with easy depolymerisation. Polyesters such as PET can be treated by all waste management techniques; reuse, recycling, incineration and even landfilling if the polymer is biodegradable under applicable conditions. Biodegradation cannot be seen as a recycling method but rather as a disposal method. No molecules or energy are recovered from biodegradation and it requires very specific conditions. Biodegradation can be useful for polymers that easily leach into and threaten the natural environment. [75,76,77]

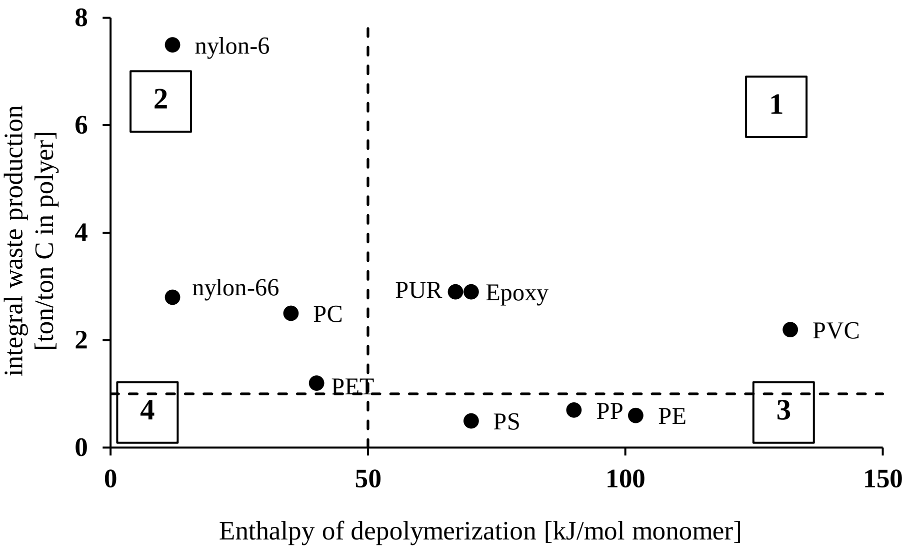

Figure 2.2 Relationship between the integral waste production [ton waste production/ton C in polymer] and the enthalpy of depolymerisation [kJ/mole monomer] of selected polymers. This relationship leads to four quadrants, representing the theoretically most suitable waste management technique: (**1**) reuse, (**2**) reuse or chemical recycling, (**3**) reuse, thermal recycling or incineration and (**4**) reuse, chemical or thermal recycling, incineration or landfill. Adapted from: Lange *et al* (2002).[75]

In order to transit towards a circular economy, plastic recycling rates should strongly increase. Currently, PET is the most recycled plastic, with a recycled fraction of approximately 20% of the global supply. The recycled fraction in the global current supply of PE, PP and PS are about 8%, 5% and 5%, respectively. These four polymers are thermoplastics and can therefore undergo mechanical and chemical recycling. All other polymer types, including some thermoplastics and all thermosets, have a recycled fraction lower than 5% in the current supply.[48] PET is recycled in the highest rates because of its well-established collection and separation processes. PET-bottles have been recycled since the 1990s while other polymer types are still developing their own recycling market and efficient processing steps which results in today's lower recycling rates. For the moment, most of the recycled PET is used in the textile and fibre industry and a fraction is used in the production of new bottles. Newly produced PET bottles contain between 25% and 50% recycled PET.[78]

For the moment, almost every recycling plant uses mechanical recycling to recycle plastic, but this could change in the near future. The market demand for high-quality recycled polymers is growing strongly, due to (i) significantly higher targets for recycled plastics in consumer products and (ii) an increased sense of producer and consumer responsibility. The need for a pure recycling feed makes mechanical recycling an unreliable method to sustain a steady supply of quality feedstock. Chemical recycling can be a promising alternative.[79] Companies in different sectors (*e.g.* Coca-Cola, BASF, Indaver) are currently developing chemical recycling methods. For example, Coca-Cola is planning to have an industrial-scale reactor working in 2021 for the recycling of their PET-bottles.[80–82]

2.2.2.2 Bioplastics

To reduce the environmental impact of fossil fuels and to evolve towards a circular economy, it is necessary to decouple plastics from fossil feedstocks and switch to bio-based feedstock. Bioplastics are plastics that are bio-based, biodegradable or both. Bio-based bioplastics are derived from renewable resources, mostly agro-based feedstock, carbohydrate-rich food crops such as corn or sugar cane (first generation feedstock). These crops are carbon sinks because they absorb CO_2 and transform it into biomass by photosynthesis. This carbon fixation can be extended for a longer period if the material is recycled. When recycling is no longer applicable, energy recovery is still possible by incinerating the bioplastics, making them a source of renewable energy. Besides this first generation feedstock, also a second generation (*i.e.* lignocellulosic feedstock) and third generation feedstock (*i.e.* organic waste) exist, but mainly in a researchers phase. Second and third generation feedstock are not eligible for food or feed production and therefore do not interfere with potential food or feed applications. Furthermore, there is no competition for agricultural area between biomass used for food or feed and for material use. Food, feed and pasture use applications account for about 97% of the global agricultural area, while only 0.02% is attributable to bioplastics.[83,84]

Biomass contains oil, fatty acids, sugar derivatives, terpenes, lignin and other components which can be chemically converted into useful monomers. The resulting polymers can be subdivided in two categories; (i) drop-in polymers and (ii) new polymers. Drop-in polymers are the renewable variant of already existing polymers, examples are bio-PET, bio-PP and bio-PE. These polymers have the same properties as their fossil fuel versions but are made from renewable resources such as bio-ethanol. Furthermore, it is also possible to design completely new polymers with new and unique properties. Polylactic acid (PLA) and polyhydroxylalkanoate (PHA) are new bio-based polymers made of starch.[65,85] Bioplastics currently account for less than one percent of the total plastic produced annually for various reasons. Today, bio-based drop-ins are not very economically attractive. The conversion of renewable feedstock to monomers is more expensive than the price of crude oil, but this equilibrium could shift in the future. The production of new bio-based polymers requires the creation and development of new markets, often starting with niche applications and is therefore very time consuming.[76,86]

2.2.3 Towards a circular PC economy

To make the PC industry compatible with the circular economy, two measures are required. These two measures are inseparable and key in decoupling plastics from fossil feedstocks; (i) developing an effective recycling economy will reduce the need for fossil feedstock and (ii) the development of renewable virgin feedstock that still will be required to compensate for the remaining, inevitable cycle losses. Not only is it necessary to improve recycling rates by exploring effective PC recycling methods, but also the impact of bio-based and safer BPA alternatives on recycling should be investigated.[66]

2.2.3.1 BPA PC recycling; current situation and perspectives

BPA-PC is only recycled in small quantities, 0.5% of the PC in the supply chain originated from the recycled fraction in 2013.[48] Compared to the virgin material, unfortunately, mechanical recycling of BPA-PC produces an inferior-material with decreased impact resistance. Chemical recycling circumvents this disadvantage by reproducing the monomeric building units and is therefore an important, extensively studied, recycling technique for BPA-PC. Currently, hydrolysis and alcoholysis, especially methanolysis, are the most studied chemical recycling techniques.[74]

Most hydrolysis reactions use subcritical (*i.e.* liquid water under pressure at $T_b < T < T_c = 374$ °C) or supercritical conditions ($T > T_c, P > P_c = 22$ MPa) to decompose BPA-PC into BPA and CO_2. Tagaya *et al.* (1999) used subcritical water in the temperature range of 230 – 300 °C. They obtained a maximum BPA yield of 38 wt.% at 300 °C after 2 h without a catalyst. When using the same conditions but adding Na_2CO_3 as a catalyst, BPA was not detected and would undesirably decompose into phenol and *p*-isopropenylphenol. This study concluded that subcritical water is an inexpensive, non-toxic and excellent medium for the decomposition of BPA-PC, but they could not reach desired BPA yields due to the instability of BPA at these conditions.[87] The research performed by Watanabe *et al*. (2009) used high pressure high temperature steam (*i.e.* steam at elevated temperature and $P_{atm} < P < P_{sat}$). A BPA yield of 80 wt.% was reached after 50 min at 200 °C and 7.9 MPa. They concluded that the decomposition of PC is rapid, and the formation of undesired by-products is minimal.[88]

Methanolysis can be performed with many different catalysts and co-solvents. Methanolysis decomposes PC into BPA and DMC. DMC can be used to produce BPA in a non-phosgene pathway (see section 1.2.1.1), and therefore minimize the carbonate loss, as for example in the form of CO_2. An overview of some promising BPA-PC methanolysis reactions is given in Table 2.1. All these researches are focused on BPA yield maximization. Entry 2 obtained high BPA yields in subcritical conditions and high catalyst loading.[89] Entry 4 and entry 7 used imidazole-anion-derived-ionic liquids (ILs) as a catalyst, [Bmim][Cl] and [HDBU][Im], respectively.[90,91] These conditions and catalysts can be used in lab-scale experiments, but the implementation of it on an industrial scale is much more difficult. To be industrially viable, it is necessary to use standard reaction conditions and common solvents and catalysts.[74] A promising chemical recycling method was performed by both Hu *et al.* (entry 1) and Liu *et al.* (entry 3) in similar studies. In these studies, NaOH was used as a catalyst and high BPA yield was obtained at mild reaction conditions (40 – 100 °C) and short decomposition times (35 – 70 min). The use of a co-solvent such as tetrahydrofuran (THF), toluene or 1,4-dioxane was necessary to achieve desirable yields. When the reaction was solely performed in methanol, no BPA and DMC were detected.[92,93]

Besides inorganic alkali hydroxides (*e.g.* NaOH, KOH), organocatalysts, especially organic bases, are studied intensively as depolymerisation catalysts (entry 5 and 6).[94] Strong organic bases such as TBD (1,8-diazabicyclo[5.4.0]undec-7-ene) and DBU (1,5-diazabicyclo[4.3.0]non-5-ene) show excellent depolymerisation rates and BPA/DMC yields at mild conditions (25 – 100 °C and atmospheric pressure). Both TBD and DBU even maintained their activity and successfully decomposed PC into BPA after five *in situ* recycling cycles. In addition, it was also possible to recuperate the catalyst, which is not possible for alkali metal catalysts. Furthermore, Do *et al* (2018) used DMC as co-solvent, reducing the environmental and economic impact of toxic co-solvent such as THF, toluene and 1,4-dioxane.[95,96]

Table 2.1 Literature overview of the methanolysis of BPA-PC pellets [89–93,95,97]

Entry	**Solvent(s) system**	**Catalyst (loading)** [-]	**Temperature** [˚C]	**Pressure** [MPa]	**Time** [min]	**Yield** [%]	**Pro's** [-]	**Cons** [-]	**Reference** [-]
1	MeOH in toluene (50 vol.% on tol. basis)	NaOH (6 mol% on PC basis)	60	atm	70	BPA (96) DMC (100)	Moderate conditions	Product purification	Hu *et al*. (1998)
2	MeOH	NaOH (1.5 kg/m^3)	120-140	10	120	BPA (90) DMC (30-40)	Continuous process	Subcritical conditions	Pinero *et al*. (2005)
3	MeOH in THF (33 wt% on THF basis)	NaOH (2 wt% on PC basis)	40	atm	35	BPA (95) DMC (95)	Mild conditions	Product purification	F. Liu *et al*. (2009)
4	MeOH (150 wt% on PC basis)	[Bmim][Cl] (100 wt% on PC basis)	105	atm	150	BPA (96) DMC (96)	Reusable ILs (8x)	Exotic catalyst	F. Liu *et al*. (2010)
5	MeOH (470 wt% on PC basis)	DBU (10 mg/mL)	100	atm	30	BPA (93) DMC (99)	No co-solvents	PC solubility	Quaranta *et al*. (2017)
6	MeOH in DMC (10 eq. on carbonate basis)	TBD (2 mol% on carbonate basis)	RT	atm	720	BPA (>98) DMC (>98)	Mild conditions No by-products		Do *et al*. (2018)
7	MeOH	[HDBU][Im] (1.6 mol% on PC basis)	70	atm	120	BPA (96)	No co-solvents	Exotic catalyst	M. Liu *et al*. (2018)

2.2.3.2 Bio-based BPA-PC alternatives

To uncouple PC from fossil feedstock, it is possible to produce BPA-PC alternatives from renewable resources such as lignin. Lignin is a main component of lignocellulosic biomass, together with cellulose and hemicellulose, and gives plants their structural integrity. Lignin is the most abundant source of aromatic moieties in nature. In general, lignin is composed of three types of (*ortho*-methoxylated) phenylpropane structures (*viz.* monolignols); *p*-coumaryl alcohol (with no *o*-methoxy), coniferyl alcohol (with one *o*-methoxy) and sinapyl alcohol (with two *o*-methoxy) (Fig. 2.3). These monomers undergo random polymerisation *via* oxidative radical-radical coupling leading to various types of carbon-carbon (*e.g.* β-5, 5-5, β-1) and carbon-oxygen (ether) bonds (*e.g.* β-O-4, α-O-4). Until recent, lignin valorisation received little attention compared with cellulose valorisation. For example, large lignin side streams are typically burned for energy recovery in the paper industry. Nevertheless, lignin has a significant potential as a feedstock for sustainable chemicals.[98]

Lignin valorisation can be subdivided into three, interconnected biorefinery stages. Firstly, biomass fractionation aims to separate lignin from the (hemi)cellulose. Secondly, lignin depolymerisation will lead to mainly mono aromatic components which thirdly can be upgraded to valuable chemicals.[99]

The β-O-4 ether linkage, the most abundant ether linkage in lignin, is often the main target in lignin depolymerisation reactions due to its lower bond strength (210 kJ/mol) compared to more stable C-C bonds (480 kJ/mol).[100] Consequently, β-O-4 ether bonds are more easily cleaved during depolymerisation than C-C bonds. A high β-O-4 content thus leads to a high monomer yield. However, depending on the reaction conditions during biomass fractionation, lignin is prone to structural degradation. Namely, cleaved ether linkages can reconnect into additional C-C linkages, thereby lowering the theoretical monomer yield. Therefore, it was observed that high β-O-4 content can still lead to low isolated lignin yields. Mild reaction conditions lead to more reactive and uncondensed, lignin albeit in a low isolated yield, while severe conditions give a higher isolated lignin yield of less reactive, highly condensed lignin.[101]

Novel biorefinery schemes, such as so-called ‘lignin-first’ fractionation, are able to combine high monomer yields with high isolated lignin yield due to minimal (re)condensation. Namely, biomass fractionation is conducted under severe reaction conditions while actively stabilising the intermediate lignin depolymerisation products, thereby hampering unwanted (re)condensation. This active lignin stabilisation can be executed in three different ways; (i) reductive, (ii) oxidative or (iii) redox-neutral.[102] Typically, such lignin-first approaches lead to a handful of substituted *o*-methoxyphenols (Table 2.2).[99]

Substituted *o*-methoxyphenols such as eugenol[103], creosol[104], 4-*n*-propylguaiacol[105], 4-*n*-propylsyringol[106], guaiacol, syringol and vanillyl alcohol[107] can all be used to produce bio-based bisphenols. These molecules all have a methoxy functionality in their *o*-position which offers several advantages beyond the scope of renewability. In some cases, due to their electron donating character, methoxy groups can promote regioselective coupling of two aromatic molecules into bisphenols by sterically and electronically facilitating the electrophilic substitution on the aromatic ring.[106,108] The *o*-methoxy functionality not only has a positive effect on the reactivity of the reaction, but also on the toxicity of the bisphenol. The *o*-methoxy group lowers the oestrogen activity of the bio-based bisphenol, by preventing the ability to bind and activate oestrogen receptors, making them less toxic and safer in use than BPA.[106,109]

When coupling two substituted *o*-methoxyphenols, so-called ‘bisguaiacol’ and ‘bissyringol’ compounds are formed. Generally, the coupling reaction can occur in two ways; acid-catalysed condensation with an (i) aldehyde or (ii) intrinsic reactive substituent present on *o*-methoxyphenols as a coupling agent. Depending on the substituent, the latter reactions have different coupling mechanisms. The condensation reaction of methoxyalkylphenols (*e.g.* creosol, 4-*n*-propylguaiacol, 4-*n*-propylsyringol) is a two-step hydroxyalkylation/alkylation condesation reaction (Fig. 2.4A), while vanillyl alcohol and syringyl alcohol perform an alkylation condensation reaction (Fig. 2.4B). Bisphenols made from eugenol use metathesis.[105,106,108,110]

A selected example of a renewable and safer bisphenol is bisguaiacol F (BGF) which is produced out of vanillyl alcohol and guaiacol, both lignin-derived molecules.[107] Its bio-based nature and reduced oestrogen ability make BGF a promising BPA alternative.[107,108]

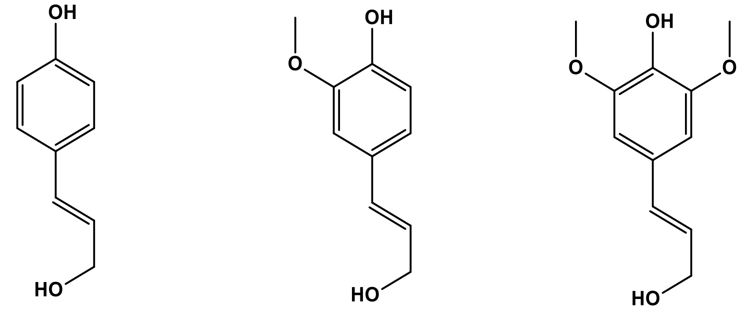

p-coumaryl alcohol coniferyl alcohol sinapyl alcohol

Figure 2.3 The three main constituents of lignin: *p*-coumaryl alcohol, coniferyl alcohol and sinapyl alcohol are generally abbreviated as H (*p*-hydroxyphenyl), G (guaiacyl) and S (syringyl), respectively.[99]

Table 2.2 Typical *p*-substituted *o*-methoxyphenols produced by lignin-first processes [99]

	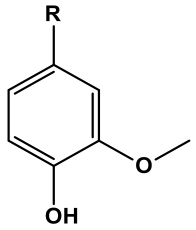	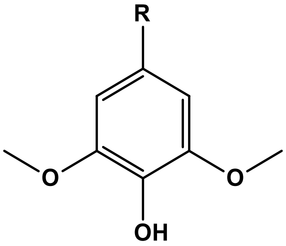
– **R**		
– H	Guaiacol	Syringol
– CH_3	Creosol	4-methylsyringol
– $(CH_2)_2CH_3$	4-*n*-propylguaiacol	4-*n*-propylsyringol
– CH_2OH	Vanillyl alcohol	Syringyl alcohol
– $CH_2CH=CH_2$	Eugenol	4-allylsyringol

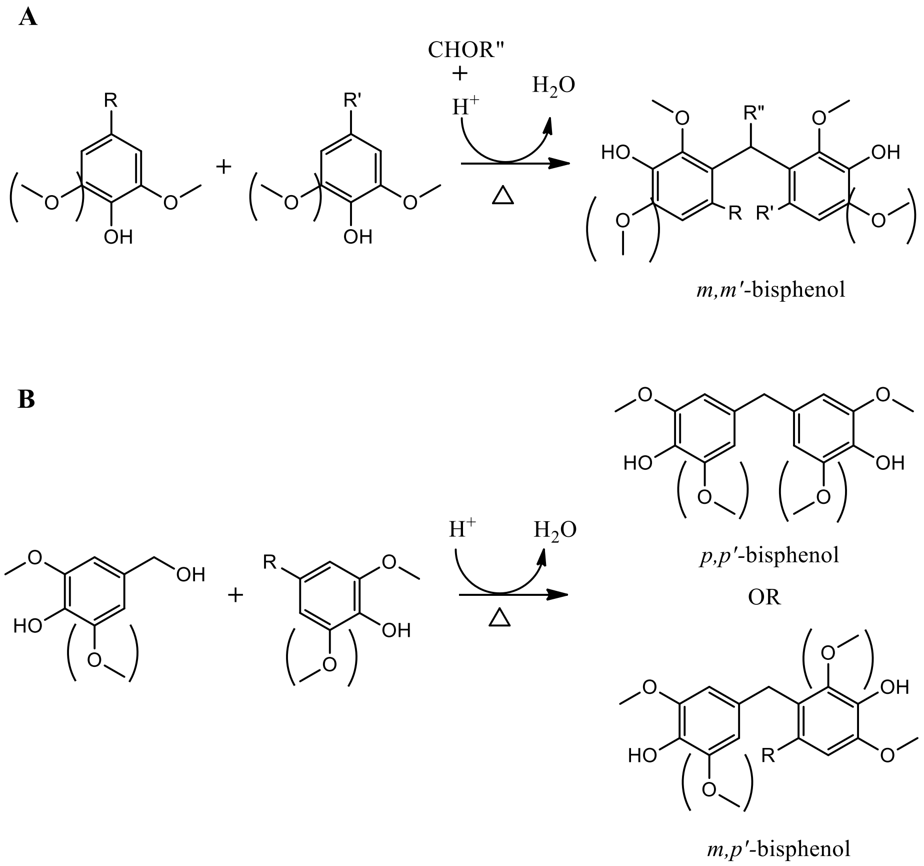

Figure 2.4 General reaction of the acid-catalysed condensation of two *p*-substituted *o*-methoxyphenol molecules leading to bisphenols (or bissyringols). (**A**) hydroxyalkylation/alkylation condensation reaction with methoxyalkylphenols, (**B**) alkylation condensation reaction with vanillyl (or syringyl) alcohol.

II. Materials and methods

3. Materials and methods

A list of all chemical used during this research can be found in Appendix A.

3.1 Joback-Reid method

The Joback-Reid method is a group contribution method that allows the prediction of 11 pure component thermodynamic properties.[111] The Joback-Reid method assigns contributions to common molecular functionalities. The 11 thermodynamic properties are: normal boiling point, melting point, critical temperature, critical pressure, critical volume, heat of formation (ideal gas, 298 K), Gibbs energy of formation (ideal gas, 298 K), heat capacity (ideal gas), heat of vaporization at normal boiling point, heat of fusion and liquid dynamic viscosity. The heat of formation (ΔH_f°), Gibbs energy of formation (ΔG_f°), heat of vaporization (ΔH_v°) and heat of fusion (ΔH_f°) are of interest and used in this research.

The estimation equations of these four thermodynamic properties are,

$$\Delta H_f^{\circ} = 68.29 + \sum H_{f,i} \qquad [kJ.mol^{-1}] \tag{3.1}$$

$$\Delta G_f^{\circ} = 53.88 + \sum G_{f,i} \qquad [kJ.mol^{-1}] \tag{3.2}$$

$$\Delta H_v^{\circ} = 15.30 + \sum H_{v,i} \qquad [kJ.mol^{-1}] \tag{3.3}$$

$$\Delta H_f^{\circ} = -0.88 + \sum H_{f,i} \qquad [kJ.mol^{-1}] \tag{3.4}$$

The group contribution values for the participating functional groups are given in Table 3.1.

Table 3.1 Group contribution values of selected functional groups for the enthalpy of formation, Gibbs free energy of formation, enthalpy of vaporization and enthalpy of fusion

Group	ΔH_f°	ΔG_f°	ΔH_v°	ΔH_f°
Non-ring groups				
–CH2–	-20.640	8.420	2.226	2.590
–CH3	-76.450	-43.960	2.373	0.908
Ring groups				
=CH–	2.090	11.300	2.544	1.101
=C<	46.430	54.050	3.059	2.394
Oxygen groups				
–OH (alcohol)	-208.040	-189.200	16.826	2.406
–OH (phenol)	-221.650	-197.370	12.499	4.490
–O– (non-ring)	-132.160	-105.000	2.410	1.188
–COO– (ester)	-337.920	-301.950	9.633	6.959
–COOH (acid)	-426.720	-387.870	19.537	11.051

The carbonate linkage, the functional group of interest, has no own contribution values. The carbonate linkage can be composed by a combination of the contributions of –O– (non-ring) and –COO– (ester).

3.2 Solvolysis reactions

3.2.1 Methanolysis

The concentrations used in the methanolysis reaction are based on the concentrations used by Do *et al* (2018).[97] A 12 mL glass vial is charged with 2 mmol reagent, respectively 428.4 mg DPC or 548.5 mg DGC, 1-5 mol.% catalyst, 10 mol equivalent methanol (0.8 mL) and 4 mL 2-methyl-THF. The glass vial is heated, during the complete solvolysis, in a copper block at a temperature between 30 and 60°C on a magnetic stir plate (450 rpm) with an 8 mm magnetic stirring bar in the vial. 100µL GC samples are collected at 5, 15, 30, 45, 60, 120, 240, 360 and 480 min with a 1 mL syringe. Before GC analysis, the samples are diluted with 100µL acetonitrile and 7.5 mg toluene is added as internal standard.

3.2.2 Product analysis

Gas chromatography (GC)

The reaction products of the solvolysis reactions are quantitatively analysed with GC. For the GC analysis an Agilent 6890N GC system is used. The GC is equipped with an Agilent 7683B series injector, a Rxi-17, crossbond diphenyl dimethyl polysiloxane, column (30 m x 320 µm and 0.50 µm film thickness), a flame ionization detector (FID) and ChemStation software. An automated injector injects 1 µL of sample with a split ratio of 25.0:1 at a split flow of 12.4 mL min^{-1}. The injection port and initial oven temperatures are 250 and 60 °C, respectively. The oven temperature is instantly increased to 90 °C at 5°C min^{-1}. Secondly, the temperature is increased from 90 °C to 300 °C at 25 °C min^{-1}. The oven temperature is held constant for 6.60 min at 300 °C, leading to a total run time of 21 min. When leaving the column, the products are detected by an FID detector at 300 °C.

High-pressure liquid chromatography (HPLC)

The reaction products of the hydrolysis reactions are quantitatively analysed with HPLC. For the HPLC analysis a Shimadzu LC-2010CHT HPLC system is used. The HPLC is equipped with an automated injector, a serial dual plunger pump, an analytical Prevail C18 column (4.6 m x 250 mm and 5 µm film thickness) and deuterium UV detector with a wavelength range between 190 – 600 nm. As the mobile phase a 50:50 mixture of 95 vol% acetonitrile + 5 vol% MiliQ and 100 vol% MiliQ, both with 0.2 vol% phosphoric acid, is used. The pressure in the column is 80 bar and the flow rate are 1 mL min^{-1}. The samples containing diphenyl carbonate (DPC) and diguaiacyl carbonate (DGC) are analysed respectively at 254 nm and 280 nm.

Gas chromatography mass spectrometer (GC-MS)

For the qualitatively analysis of the reaction products, gas chromatography coupled with a mass spectrometer detector (GC-MS) is used. For the GC-MS analysis an Agilent 5973 Network Mass Selective Detector is used. The GC-MS is equipped with a HP-5MS capillary column (25 m x 0.25 mm and 0.25 µm film thickness) with a maximum temperature of 325 – 350 °C and He as carrier gas. The oven temperature is instantly increased to 90°C at 5°C min^{-1}. Secondly, the temperature is increased from 90 °C to 300 °C at 25°C min^{-1}. The oven temperature is held constant for 6.60 min at 300 °C, leading to a total run time of 21 min.

III. Results and Discussion

4. Setting the scene

4.1 Introduction

As indicated in the literature study, a transition from a linear towards a circular economy will be beneficial for people, planet and environment. In the specific case of the BPA-PC industry, two aspects are of vital importance. Firstly, it is key to develop BPA-PC alternatives which are both (i) renewable/bio-based and (ii) non-toxic as well as (iii) equal, or even better, in terms of material properties. Secondly, it is crucial to develop/safeguard the ability towards efficient recycling for novel aromatic PCs. Whereas the first aspect has been recently tackled through the development of 'so-called' bisguaiacol-based PCs, currently no information is available on the second aspect, *i.e.* the recycling of bisguaiacol-based PCs. Therefore, this MSc thesis will focus on chemical recycling of bisguaiacol-based PCs.

The main difference between bisphenol and bisguaiacol(-based PCs) is the respective absence or presence of *o*-methoxy functionalities. As stated in the literature study, methoxy groups offer several advantages in terms of reactivity and toxicity. It promotes regioselective coupling of two aromatic molecules and significantly lowers the *in vitro* oestrogen activity of bisguaiacols. Consequently, it is interesting to investigate the effect of the methoxy functionality on the chemical recycling (re)activity of both compounds. Throughout this research, a comparison will be made between bisguaiacols and bisphenols.

In Chapter 5, thermodynamic equilibria for various transesterification reactions are calculated to determine the feasibility for chemical recycling. Next, in Chapter 6, experimental methanolysis reactions are performed to determine the optimal chemical recycling conditions.

4.2 DPC and DGC as model compounds

The main target for chemical recycling of PCs by solvolysis is the common carbonate linkage, *i.e.* the interconnection between two monomers (Fig. 4.1A). Although this carbonate cleavage can be studied directly on PCs, here, we decided to start from carbonate-containing model compounds with an identical chemical environment. The model substrates for bisphenol- and bisguaiacol-based PCs are diphenyl carbonate (DPC) and diguaiacyl carbonate (DGC), respectively (Fig. 4.1B).

The use of such diaryl carbonates (DACs) offers several advantages. Unlike the corresponding PCs, these low-M_w models enable to study the isolated influence of the chemical environment on carbonate linkage cleavage without interference due to solubility and mass-transfer limitations. Consequently, all observable differences are directly caused by the additional *o*-methoxy groups. In addition, these model compounds are commercially available which avoids the laborious synthesis of non-commercial bisguaiacol-based PC. Finally, it facilitates both theoretical (Ch. 5) and experimental (Ch. 6) analyses.

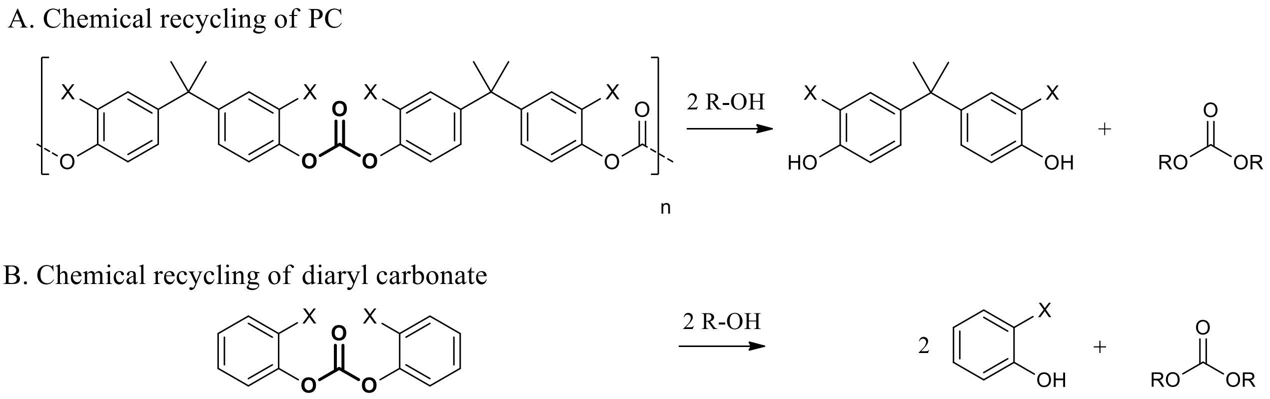
A. Chemical recycling of PC

B. Chemical recycling of diaryl carbonate

Figure 4.1 Investigation of carbonate bond cleavage *via* solvolysis (*i.e.* hydrolysis or alcoholysis) starting from (**A**) (*o*-methoxylated) BPA-PCs or (**B**) (*o*-methoxylated) diaryl carbonates, with indication of corresponding products. The carbonate bond is highlighted in bold. X = –H (bisphenols) or $–OCH_3$ (bisguaiacols) and R = –H (water), –alkyl (alcohol).

5. Thermodynamics of solvolysis

5.1 Transesterification

Solvolysis, as a chemical recycling method, is in fact a transesterification reaction. During transesterification, an ester reacts with an alcohol to form a new ester and a new alcohol through the interchange of the alkoxy moiety (Fig 5.1).[112]

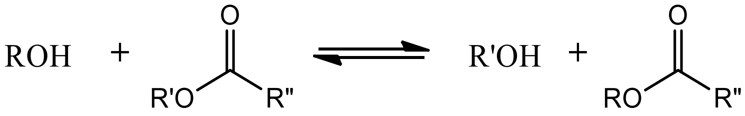

Figure 5.1 Transesterification of an ester and an alcohol resulting in a new ester and new alcohol.

The carbonate linkage can be seen as a di-ester. Therefore, two consecutive transesterification reactions are necessary to depolymerise the PC chain. Applied on DPC and DGC (*i.e.* diaryl carbonates), the first transesterification reaction results in an alkyl aryl carbonate and phenol or guaiacol, respectively. Consecutively, this intermediate alkyl aryl carbonate undergoes a second transesterification reaction resulting in a dialkyl carbonate and a second phenolic compound (Fig. 5.2). If the reaction is carried out with methanol, *i.e.* methanolysis, the dialkyl carbonate will be dimethyl carbonate (DMC). Methyl phenyl carbonate (MPC) and methyl guaiacyl carbonate (MGC) will be the intermediates of DPC and DGC, respectively. Similarly, the first ethanolysis reaction leads to ethyl phenyl carbonate (EPC) and ethyl guaiacyl carbonate (EGC) for DPC and DGC, respectively, followed by the second ethanolysis reaction which forms diethyl carbonate (DEC).

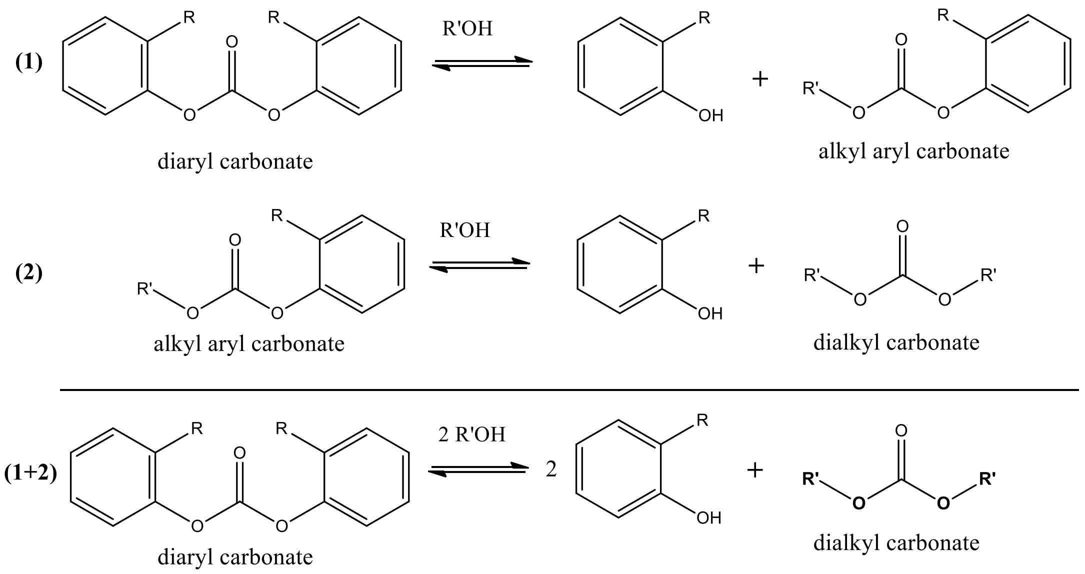

Figure 5.2 Alcoholysis of DAC consists of two consecutive transesterification reactions: (**1**) transesterification into an alkyl aryl carbonate (and phenol), and (**2**) transesterification into a dialkyl carbonate (and phenol). Methanolysis (R' = $–CH_3$) converts DPC (or DGC) to DMC and phenol (or guaiacol) with intermediate formation of MPC (or MGC), respectively. Ethanolysis (R' = $–CH_2CH_3$) converts DPC (or DGC) to DEC and phenol (or guaiacol) with intermediate formation of EPC (or EGC), respectively.

5.2 Concept of thermodynamic chemical equilibrium

As indicated in Figure 5.2, transesterification is a reversible reaction, meaning that both forward and backward reaction are possible, and hence reactants and products are able to interconvert. The various species therefore exist in chemical equilibrium, and the product distribution depends on the relative energies of the reactants and products. The thermodynamically most stable species are favoured, and thus determines the degree of product formation.

If the products are the most stable species, the reaction will proceed spontaneously under mild reaction conditions. On the contrary, if the desired products are thermodynamically less stable, severe reactions conditions and a more complex process set-up are required to obtain desirable yields. Therefore, it is essential to know (the position of) the chemical equilibrium on forehand if high yields are desired in a reversible reaction.

In thermodynamics, the chemical equilibrium of a reaction is expressed as a chemical equilibrium constant (K_{eq}), *i.e.* the molar ratio of products to reagents. To calculate K_{eq}, it is necessary to obtain the value of the change in Gibbs free energy of the reaction (ΔG_r°) at standard conditions (*i.e.* 298.15 K and 1 atm, abbreviated as standard pressure and temperature; STP).

The relation between K_{eq} and ΔG_r° is given in equation 5.1 and 5.2:

$$\Delta G_r^{\circ} = -RT\ln(K_{eq}) \tag{5.1}$$

or

$$K_{eq} = e^{-\Delta G_r^{\circ}/RT} \tag{5.2}$$

with R the universal gas constant (8.314 J mol^{-1} K^{-1}) and T the absolute temperature (in Kelvin).

In its turn, ΔG_r° is defined as:

$$\Delta G_r^{\circ} = \Delta H_r^{\circ} - T\Delta S_r^{\circ} \tag{5.3}$$

with ΔH_r° the standard reaction enthalpy (kJ mol^{-1}) and ΔS_r° the standard reaction entropy (kJ mol^{-1} K^{-1}).

These three thermodynamic quantities can be experimentally determined. In addition, they can also be theoretically derived. According to Hess's Law, the standard reaction enthalpy is equal to the standard enthalpy of formation of the products minus the standard enthalpy of formation of the reactants (equation 5.4). This expression is also valid for the Gibbs free energy and the entropy (equation 5.5 and 5.6):

$$\Delta H_r^{\circ} = \sum n_{products}\,\Delta H_{f\,(products)}^{\circ} - \sum n_{reactants}\,\Delta H_{f\,(reactants)}^{\circ} \tag{5.4}$$

$$\Delta G_r^{\circ} = \sum n_{products}\,\Delta G_{f\,(products)}^{\circ} - \sum n_{reactants}\,\Delta G_{f\,(reactants)}^{\circ} \tag{5.5}$$

$$\Delta S_r^{\circ} = \sum n_{products}\,\Delta S_{f\,(products)}^{\circ} - \sum n_{reactants}\,\Delta S_{f\,(reactants)}^{\circ} \tag{5.6}$$

The standard enthalpy of formation (ΔH_f°) of a compound is defined as: "the change of enthalpy during the formation of one mole of the substance from its constituent elements in their standard states, *i.e.* the most stable form of the element at STP".[113] The definitions for standard Gibbs free energy of formation (ΔG_f°) and standard entropy of formation (ΔS_f°) are analogue.

For common molecules, the values of these thermodynamic formation quantities are known and tabulated. An example of an online free source of thermodynamic data is the National Institute of Standards and Technology (NIST) Chemistry WebBook. It covers a broad scope of molecules, but, unfortunately, is finite.

To estimate standard thermodynamic quantities of substances that are not yet experimentally determined, so-called "group contribution methods" exist. These group contribution methods are techniques to estimate thermodynamic and other properties of pure components based on molecular structures. Relatively simple group contribution methods assign contributions to common molecular functionalities such as $–CH_3$, –O–, –CN, etc. The Joback-Reid method uses this approach to estimate 11 pure component thermodynamic properties.[111] The simplicity of this method is both its strength and weakness. All 11 properties are estimated from a single analysis of the molecular structure, however, sometimes at the expense of high accuracy. In more complicated, and generally more accurate, methods, interactions between neighbouring functionalities are taken into account. The Gani method[114], for example, uses three interactions levels for its estimations. The first level consists of the main molecular functionalities, while the second and third consider proximity effects of these functionalities. Group contribution methods make the main assumption that all species have an ideal gas behaviour. These group contribution methods thus predict temperature dependent thermodynamic properties of ideal gases. Contrary to real gases, ideal gases do not take up volume, display no intermolecular interactions and undergo solely elastic collisions.

5.3 Thermodynamic equilibrium of solvolysis

5.3.1 Standard thermodynamic quantities

Table 5.1 gives an overview of all species and their standard thermodynamic quantities to calculate the chemical equilibria for DPC and DGC in the reversible solvolysis reaction – both alcoholysis and hydrolysis. The NIST database contains values for both ΔS_f° and ΔH_f° for most of the species. The missing values were calculated using group contribution methods.[a]

Group contribution methods lead to thermodynamic quantities for ideal gases. However, in the studied reactions, solely CO_2 occurs in a gaseous state. All other participating components either occur in the liquid or solid state. Yet it is possible to determine the standard enthalpy of formation for each state of matter starting from the gas phase. The Joback-Reid method calculates 11 thermodynamic properties, including the standard enthalpy of vaporization (ΔH_v°)

---

[a] Choosing between the Joback-Reid method and the Gani method, the latter method is the more accurate one. Unfortunately, the carbonate linkage is not described in this method as a distinct functionality. Therefore, the specific interaction contributions cannot be calculated and so it is needless to use the more complex method. In the Joback-Reid method, the carbonate linkage can be composed of an ether and ester functionality.

and the standard enthalpy of fusion (ΔH°_{fus}). ΔH°_{v} and ΔH°_{fus} correspond to the amount of energy needed to transform a part of a liquid or solid substance into the gas or liquid phase, respectively.

ΔH°_{v} and ΔH°_{fus} can be written following Hess's Law:

$$\Delta H^{\circ}_{v} = \Delta H^{\circ}_{f\,(gas)} - \Delta H^{\circ}_{f\,(liquid)} \qquad \textbf{(5.7)}$$

$$\Delta H^{\circ}_{fus} = \Delta H^{\circ}_{f\,(liquid)} - \Delta H^{\circ}_{f\,(solid)} \qquad \textbf{(5.8)}$$

$$\Delta H^{\circ}_{v} + \Delta H^{\circ}_{fus} = \Delta H^{\circ}_{f\,(gas)} - \Delta H^{\circ}_{f\,(solid)} \qquad \textbf{(5.9)}$$

This way, $\Delta H^{\circ}_{f\,(gas)}$ can be transformed into $\Delta H^{\circ}_{f\,(solid)}$ and $\Delta H^{\circ}_{f\,(liquid)}$, and so increasing the accuracy of subsequent calculations. Unfortunately, similar adjustments are not possible in the calculation of ΔG°_{f}.

Comparing the empirical derived data (mainly from NIST) with the theoretically calculated data using the Joback-Reid method, it can be stated that the Joback-Reid method is fairly accurate. All deviations range between 0.1% and 8.1% and the mean deviation amounts to 4.3%.

Table 5.1 Overview of the standard thermodynamic quantities of formation of all species participating in methanolysis, ethanolysis and hydrolysis reaction of DPC and DGC

		ΔG_f° [kJ·mol^{-1}]		ΔH_f° [kJ·mol^{-1}]		ΔS_f° [J·mol^{-1}·K^{-1}]
		Empirical	Theoretical	Empirical	Theoretical	Theoretical
Reagents	DPC(s)	-176.3	-	-401.4	-373.6[e]	-755.5
	DPC(g)	-	-132.0	-311.0	-288.0	-
	DGC(s)	-	-	-	-715.9[e]	-
	DGC(g)	-	-344.4	-	-616.6	-
	MeOH(l)	-166.2	-	-238.4	-250.7[d]	-242.3
	MeOH(g)	-162.7	-179.3	-201.3	-216.2	-129.6
	EtOH(l)	-172.9	-	-276.0	-273.6[d]	-346.0
	EtOH(g)	-	-170.9	-234.0	-236.8	-
	H_2O(l)	-237.2	-	-285.8	-	-163.3
Intermediates	MPC(s)	-	-	-	-482.9[e]	-
	MPC(g)	-	-286.5	-422.8[a]	-421.4	-
	MGC(s)	-	-	-	-655.9[e]	-
	MGC(g)	-	-392.7	-	-585.6	-
	EPC(s)	-	-	-	-508.4[e]	-
	EPC(g)	-	-278.1	-	-442.0	-
	EGC(s)	-	-	-	-681.3[e]	-
	EGC(g)	-	-384.3	-	-606.3	-
	HPC(s)	-	-	-	-494.7[e]	-
	HPC(g)	-	-326.7	-	-420.8	-
	HGC(s)			-	-667.7	
	HGC(g)	-	-432.9	-	-585.1	-
Products	DMC(l)	-	-	-	-586.1[d]	-
	DMC(g)	-	-441.0	-571.0[b]	-554.7	-
	DEC(l)	-	-	-	-632.5[d]	-
	DEC(g)	-	-424.2	-637.9	-596.0	-
	CO_2(g)	-394.4	-	-393.5	-	3.0
	Phenol(s)	-50.5	-	-165.0	-151.6[e]	-384.2
	Phenol(g)	-33.1	-32.9	-96.4	-96.5	-212.6
	Guaiacol(s)	-	-	-	-324.5[e]	-
	Guaiacol(l)	-	-	-308.0[c]	-309.6[d]	-
	Guaiacol(g)	-	-139.2	-245.4	-260.8	-

All empirical and theoretical data originates from NIST and the Joback-Reid method, unless indicated otherwise: [a] Zhu *et al.* (2007)[115], [b] Poling *et al.* (2001)[113], [c] Shen *et al.* (2016)[116], [d] theoretical derived from ΔH_v°, [e] theoretical derived from ΔH_v° and ΔH_{fus}°

5.3.2 Calculating K_{eq}

To perform chemical recycling of PC, a complete conversion into the monomeric units and the dialkyl carbonate is required. Incomplete chemical recycling of PC would result in the formation of large oligomeric compounds which cannot be used in a subsequent (re)polymerisation process. Translating this to DPC (or DGC), a complete conversion into the dialkyl carbonate and phenol (or guaiacol) is required. High yields of the intermediate alkyl aryl carbonate correspond to high yields of undesirable oligomeric compounds.

The chemical equilibrium constant of the two consecutive solvolysis reactions should be known in order to know if full conversion could be achieved. The two consecutive methanolysis and ethanolysis reactions of DPC and DGC are shown in reactions 1-4 and reactions 5-8, respectively,

(1) $\mathrm{DPC_{(s)} + MeOH_{(l)} \xleftrightarrow{K_{eq1}} MPC_{(s)} + phenol_{(s)}}$

(2) $\mathrm{MPC_{(s)} + MeOH_{(l)} \xleftrightarrow{K_{eq2}} DMC_{(l)} + phenol_{(s)}}$

(3) $\mathrm{DGC_{(s)} + MeOH_{(l)} \xleftrightarrow{K_{eq3}} MGC_{(s)} + guaiacol_{(s)}}$[b]

(4) $\mathrm{MGC_{(s)} + MeOH_{(l)} \xleftrightarrow{K_{eq4}} DMC_{(l)} + guaiacol_{(s)}}$

(5) $\mathrm{DPC_{(s)} + EtOH_{(l)} \xleftrightarrow{K_{eq5}} EPC_{(s)} + phenol_{(s)}}$

(6) $\mathrm{EPC_{(s)} + EtOH_{(l)} \xleftrightarrow{K_{eq6}} DEC_{(l)} + phenol_{(s)}}$

(7) $\mathrm{DGC_{(s)} + EtOH_{(l)} \xleftrightarrow{K_{eq7}} EGC_{(s)} + guaiacol_{(s)}}$

(8) $\mathrm{EGC_{(s)} + EtOH_{(l)} \xleftrightarrow{K_{eq6}} DEC_{(l)} + guaiacol_{(s)}}$

Firstly, DAC undergoes alcoholysis leading to an alkyl aryl carbonate and a phenolic compound. The alkyl aryl carbonate undergoes a second alcoholysis into a dialkyl carbonate and a second phenolic compound.

Additionally, the hydrolysis reactions of DAC are shown in reactions 9-12,

(9) $\mathrm{DPC_{(s)} + H_2O_{(l)} \xleftrightarrow{K_{eq9}} HPC_{(s)} + phenol_{(s)}}$

(10) $\mathrm{HPC_{(s)} \xleftrightarrow{K_{eq10}} CO_{2\,(g)} + phenol_{(s)}}$

(11) $\mathrm{DGC_{(s)} + H_2O_{(l)} \xleftrightarrow{K_{eq11}} HGC_{(s)} + guaiacol_{(s)}}$

(12) $\mathrm{HGC_{(s)} \xleftrightarrow{K_{eq12}} CO_{2\,(g)} + guaiacol_{(s)}}$

---

[b] It is assumed that guaiacol is a solid in the transesterification reactions.
However, at STP, guaiacol can both be solid and liquid, the melting temperature of guaiacol amounts to 32 °C.

Firstly, DPC (or DGC) undergoes hydrolysis into hydrogen phenyl carbonate (HPC) (or hydrogen guaiacyl carbonate (HGC)). Secondly, HPC (or HGC) does not undergo a second hydrolysis reaction but will decompose into CO_2 and phenol (or guaiacol).

A first step in determining K_{eq} values, is to calculate ΔH_r° and ΔG_r° for each reaction, using the data from Table 5.1 and equations 5.4 and 5.5. The ΔH_r° and ΔG_r° values are calculated using both empirical and theoretical ΔH_f° values. Empirical data is chosen in preference to the theoretical data. If no empirical data is available, theoretical data corresponding the proper state of matter of the compound is chosen. Secondly, the respective K_{eq} values are calculated from the corresponding ΔG_r° values, using equation 5.2. The ΔH_r°, ΔG_r°, and K_{eq}values of reactions 1 to 12 are displayed in Table 5.2

Table 5.2 Overview of the calculated ΔH_r°, ΔG_r°, and K_{eq} values for methanolysis (DPC: reaction 1-2, DGC reaction: 3-4), ethanolysis (DPC: reaction 5-6, DGC: reaction 7-8) and hydrolysis (DPC: reaction 9-10, DGC: reaction 11-12) at STP

Reaction	ΔH_r° [kJ·mol^{-1}]	ΔG_r° [kJ·mol^{-1}]	K_{eq} [-]
1	-35.9	-38.8	$6.42\ 10^{6}$
2	-30.5	-38.8	$6.42\ 10^{6}$
1+2	**-66.4**	**-77.7**	**$4.12\ 10^{13}$**
3	-26.1	-21.3	$5.35\ 10^{3}$
4	-17.0	-21.3	$5.35\ 10^{3}$
3+4	**-43.1**	**-42.6**	**$2.86\ 10^{7}$**
5	-23.8	-23.7	$1.42\ 10^{4}$
6	-13.1	-23.7	$1.42\ 10^{4}$
5+6	**-36.9**	**-47.4**	**$2.02\ 10^{8}$**
7	-14.0	-6.1	11.8
8	0.4	-6.1	11.8
7+8	**-13.6**	**-12.2**	**$1.40\ 10^{2}$**
9	-0.3	-8.1	26.2
10	-63.8	-118.2	$5.26\ 10^{20}$
9+10	**-64.1**	**-126.3**	**$1.38\ 10^{22}$**
11	9.5	9.5	$2.18\ 10^{-2}$
12	-50.4	-100.6	$4.39\ 10^{17}$
11+12	**-40.8**	**-91.2**	**$9.57\ 10^{15}$**

Literature allows to validate the thermodynamic quantities for DPC methanolysis (reaction 1 and 2). Namely, the thermodynamics of the reverse reaction, *i.e.* the formation of DPC from DMC and phenol, have been studied by different researchers. As stated in section 1.2.1, DMC can be used as a starting material in the non-phosgene PC production. Rivetti *et al.* (2000), Haubrock *et al.* (2008) and Sun *et al.* (2017) experimentally studied the thermodynamic equilibrium of the transesterification of DMC towards DPC.[117–119] Due to the reversibility of the reaction, literature-based ΔH_r° and ΔG_r° values for the DMC to DPC reaction can be transformed into values for DPC methanolysis by simply changing their sign. These transformed literature-based results are shown in Table 5.3.

Table 5.3 Transformed literature-based and theoretical calculated thermodynamic data of the transesterification of DPC to MPC (reaction 1) and the subsequent transesterification of MPC to DMC (reaction 2) [117–119]

Reaction	$\boldsymbol{\Delta H_r^\circ}$ [kJ·mol^{-1}]	$\boldsymbol{\Delta G_r^\circ}$ [kJ·mol^{-1}]	$\boldsymbol{K_{eq}}$ [-]	**Reference** [-]
1	-	-32.3	$4.59\ 10^5$	Rivetti *et al.* (2000)
2	-	-23.8	$1.49\ 10^4$	
1+2	-	**-56.1**	$\mathbf{6.82\ 10^9}$	
1	-25.2	-28.0	$8.04\ 10^4$	Haubrock *et al.* (2007)
2	-23.8	-23.9	$1.55\ 10^4$	
1+2	**-49.0**	**-51.9**	$\mathbf{1.25\ 10^9}$	
1	-40.9	-34.2	$9.88\ 10^5$	Sun *et al.* (2017)
2	-32.9	-27.9	$7.77\ 10^4$	
1+2	**-73.8**	**-62.1**	$\mathbf{7.68\ 10^{10}}$	
1	-35.9	-38.8	$6.42\ 10^6$	Theoretically calculated
2	-30.5	-38.8	$6.42\ 10^6$	
1+2	**-66.4**	**-77.7**	$\mathbf{4.12\ 10^{13}}$	

First and foremost, the chemical equilibrium constants in Table 5.2 indicate that DPC methanolysis is a thermodynamic favourable, exothermic reaction. The overall equilibrium constants are in the range of 10^{10}, meaning that the reaction strongly favours the product formation and is spontaneously driven towards the product side at STP. The theoretically calculated ΔH_r° values correspond relatively well with the literature-based experimental values. The ability to use ΔH_f° of the resembling state of matter of the species positively increases the accuracy of the calculation. Such accuracy is not achieved in the calculation of ΔG_r°, because the calculations are made with ideal gas ΔG_f° values. This inaccuracy leads to a deviation between $K_{eq,overall}$ (*i.e.* equilibrium constant of the total reaction) derived from the theoretical data and the literature-based experimental data. Experimental $K_{eq,overall}$ values range between 10^9 – 10^{10}, while the theoretically calculated $K_{eq,overall}$ value amounts to 10^{13}. Despite this deviation, both theoretical and experimental values describe similar general thermodynamic behaviour, *i.e.* the spontaneous reaction of DPC to DMC and phenol at STP.

Now knowing that the theoretical derived data approaches the experimental values, it is possible to compare the results from Table 5.2, which have no experimental validation, with each other, bearing in mind the deviations caused by the ideal gas approximation. Furthermore, because both consecutive alcoholysis transesterification reactions have the same ΔG_r° and K_{eq}value, it is more clear to use $K_{eq,overall}$ when comparing the alcoholysis reaction.

Both the methanolysis of DPC (reaction 1+2) and DGC (reaction 3+4) have favourable thermodynamics, the equilibrium spontaneously favours the product side. The respective $K_{eq,overall}$ values for DPC and DGC are 4.12 10^{13} and 2.86 10^7. Even though both $K_{eq,overall}$ values are very large, there is a significant difference. $K_{eq,overall}$ for the methanolysis reaction of DPC is roughly two times bigger than $K_{eq,overall}$ for DGC methanolysis. Therefore, the undesirable backward reaction of DGC methanolysis (*i.e.* the transesterification of DMC and guaiacol to form DGC) will occur more frequently compared with the backward reaction of DPC methanolysis, yet at very low and negligible rates compared with the forward methanolysis reaction.

$K_{eq,overall}$ of DPC methanolysis (reaction 1+2) and ethanolysis (reaction 5+6) amount to 4.2 10^{13} and 2.02 10^8, respectively. The same conclusion made in the comparison of methanolysis between DPC and DGC is valid. Both reactions are spontaneous and thermodynamically driven towards the product formation while, due to the smaller equilibrium constant, the backward reaction will occur relatively more often in ethanolysis than in methanolysis. The same reasoning is valid for DGC methanolysis (reaction 3+4) and ethanolysis (reaction 7+8). The equilibrium constant of DGC ethanolysis amounts to 1.40 10^2. Thermodynamics still favour the product formation, but the backward reaction takes places and DGC is formed in non-negligible quantities.

DPC (reaction 9+10) and DGC (reaction 11+12) hydrolysis are exceptions. The actual hydrolytic cleavage of the carbonate linkage is in thermodynamic equilibrium or even slightly unfavourable (DPC: $K_{eq,9}$ = 26.1, DGC: $K_{eq,11}$ = 0.0218). On the other hand, the hydrogen aryl carbonate is very unstable and its decomposition into CO_2 and a phenolic compound is thermodynamically favoured, leading to an overall spontaneous reaction (DPC: $K_{eq,overall}$ = 5.26 10^{20}, DGC: $K_{eq,overall}$ = 4.39 10^{17}).

To conclude, DPC and DGC alcoholysis are thermodynamic spontaneous, exothermic processes. The frequency of the undesired backward reaction from dialkyl carbonate to DPC/DGC is very small but increases when using EtOH instead of MeOH as a recycling agent. The comparison of DPC and DGC shows that the backward reaction is more frequent when using DGC as reagent. On the other hand, the process to produce DGC from DMC and guaiacol is thermodynamically less unfavourable and therefore more attractive than DPC formation. Presumably, the methoxy functionality, as an *ortho-para* directing group, facilitates the backward reaction by stabilising and promoting the transesterification reaction of guaiacol with DMC.

6. Kinetics of DGC methanolysis

6.1 Introduction

In Chapter 5 it was proven that the alcoholysis of DGC is an exothermic, spontaneous, and reversible reaction, which favours alcoholysis as a means of recycling. Therefore, in theory, high yields of the dialkyl carbonate should be achievable at mild reaction conditions.

In this part, the reactivity of DGC towards methanolysis – benchmarked against DPC – will be experimentally verified. Methanolysis is preferred over ethanolysis as most promising alcoholysis method because (i) the chemical equilibrium of methanolysis lies further to the right than in ethanolysis, hence products are more favoured, (ii) the solubility of DPC, DGC and their corresponding PCs is higher in MeOH than in EtOH, and (iii) methanolysis yields DMC, which is industrially important as a non-phosgene alternative in PC production (section 1.2.1).

Due to the poor solubility of PCs in MeOH, methanolysis will be executed in the presence of a co-solvent. The addition of a co-solvent that is compatible with PC facilitates depolymerisation by increasing the solubility of the PC. Even though DPC and DGC are fairly soluble in MeOH, their methanolysis will also be executed with a co-solvent, namely 2-methyl-tetrahydrofuran (2-MeTHF). The use of 2-MeTHF allows to easily translate the optimal reaction conditions determined for methanolysis of the DPC and DGC model compounds on PCs. 2-MeTHF shows similar solvent properties as THF but can be labelled as a green alternative because it can be derived from renewable sources (*e.g.* corn, bagasse, etc.).[120] Furthermore, 2-MeTHF has a higher boiling point compared to THF, 80 °C and 66 °C respectively, resulting in a more accurate product analysis (see section 6.2).

6.2 Product identification

Quantitative analysis of the products after methanolysis was done by GC-FID.

Figure 6.1 shows a typical chromatogram for (A) DPC and (B) DGC methanolysis. The solvents, *i.e.* MeOH (t_r = 6.1 min), ACN (t_r = 6.7 min) and 2-MeTHF (t_r = 7.5 min), elute first. DMC (t_r = 7.3 min) elutes in between these solvents with a low sensitivity due to its high oxygen to carbon ratio. If THF is used as the co-solvent, both peaks undesirably overlap. In contrast, using 2-MeTHF as the co-solvent results in a clear baseline separation. Next, phenol (t_r = 11.7 min) or guaiacol (t_r = 12.7 min) elutes followed by MPC (t_r = 13.1 min) or MGC (t_r = 14.5 min) and finally by DPC (t_r = 16.2 min) or DGC (t_r = 19.6 min).

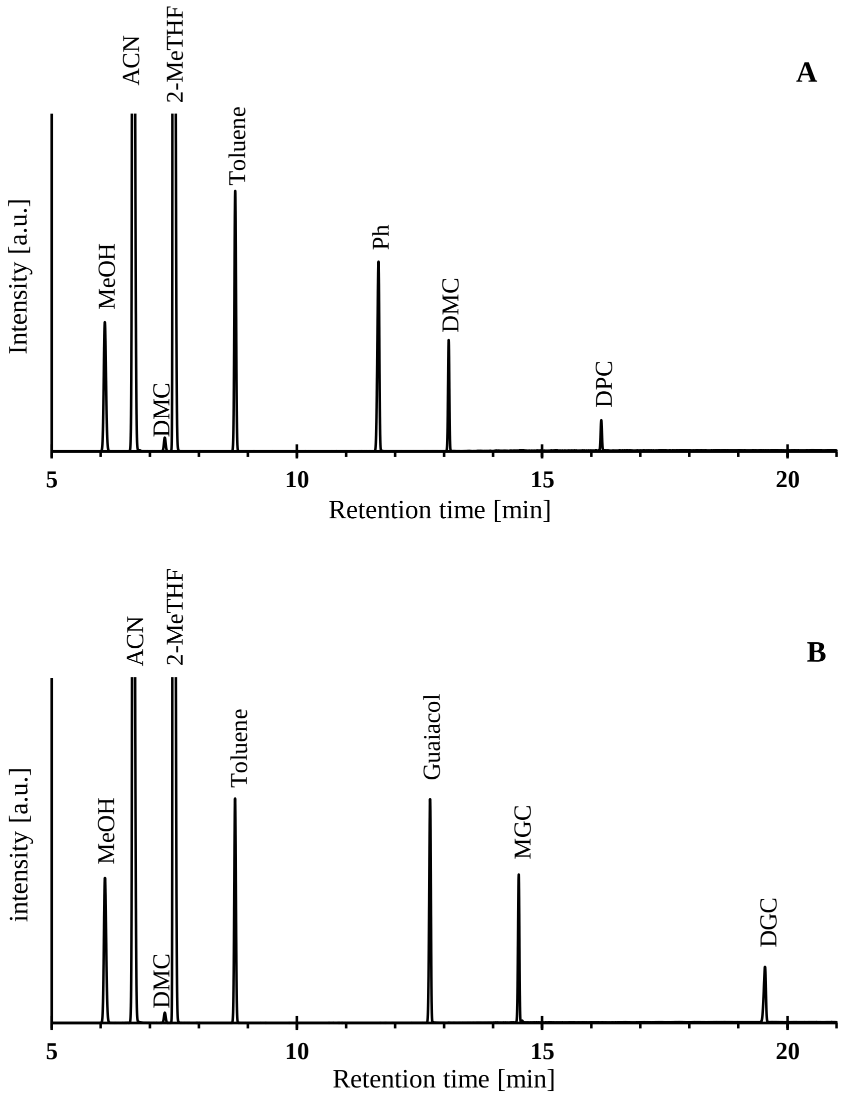

Figure 6.1 Typical GC-FID chromatogram for (**A**) DPC and (**B**) DGC methanolysis.

Because the intermediates MPC and MGC were not available during research, it is necessary to qualitatively validate that they correspond to the appointed retention times in the chromatogram. This qualitative validation of both intermediates is done by GC-MS (Fig. 6.2).

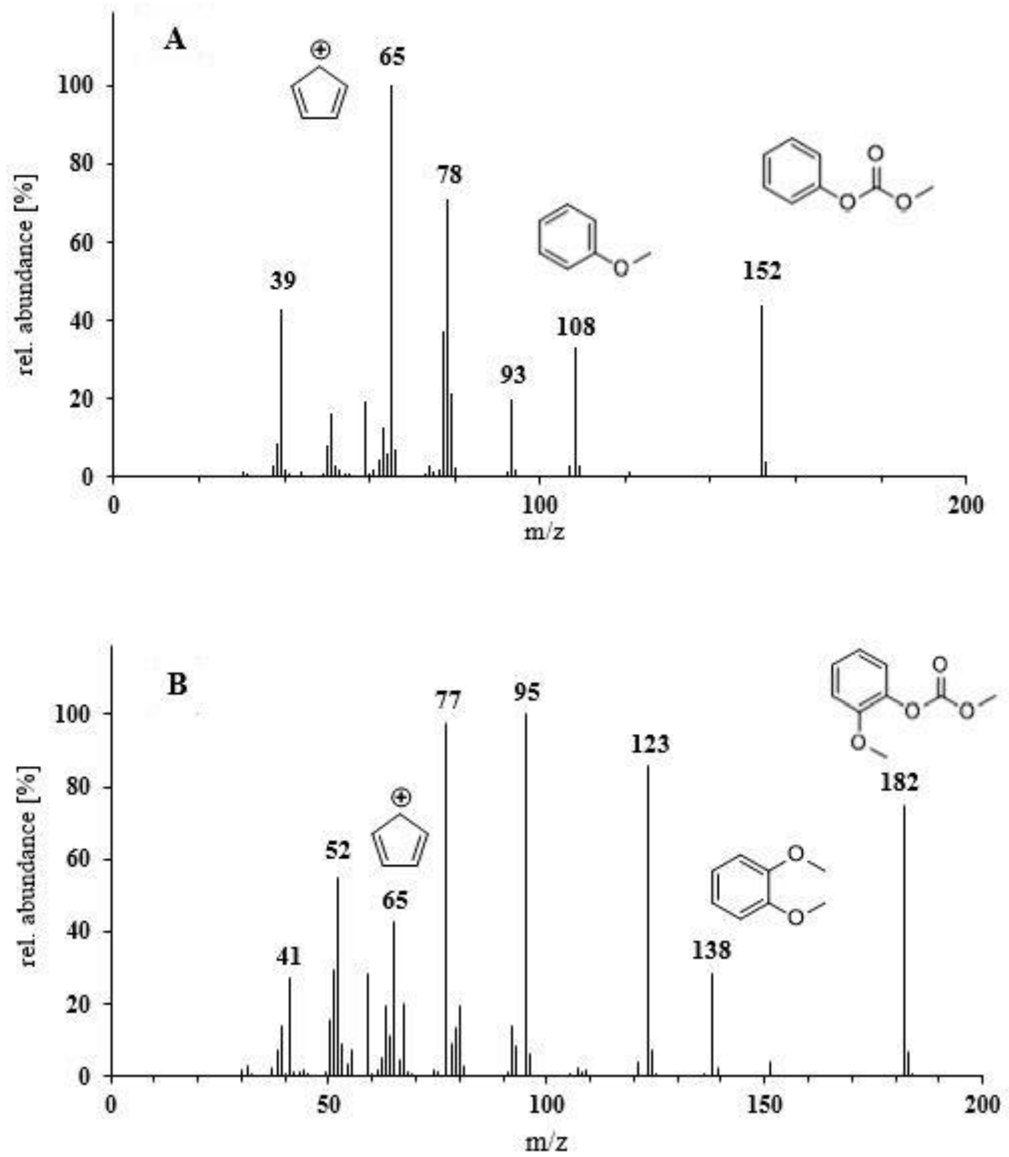

Figure 6.2 Mass spectra of the intermediates (**A**) MPC and (**B**) MGC with annotation and molecular structure of the most abundant fragments.

As seen in Figure 6.2, the molecular ions of the intermediates give a mass to charge ratio (m/z) of 152 and 182 which corresponds to molecular weights of MPC and MGC, respectively ($M_{\mathrm{w,MPC}}$ = 152 g/mol; $M_{\mathrm{w,MGC}}$ = 182 g/mol). Indeed, the difference in m/z ratio (*i.e.* 30) accounts for the additional methoxy moiety in MGC. Consequently, fragments of MPC and MGC which differ 30 m/z are in fact similar fragments, albeit with or without the methoxy group.

The interpretation of the first fragmentation pattern (Fig 6.2A) starts with the loss of a 44 m/z fragment from the molecular ion (152 m/z). This loss corresponds to the loss of a neutral CO_2

molecule and the intramolecular rearrangement to form anisole (108 m/z). Next, the methyl moiety of anisole is cleaved leading to a phenoxy carbocation (93 m/z), followed by the loss of a neutral CO molecule (28 m/z) resulting in the formation of a cyclopentadiene carbocation of 65 m/z. The cyclopentadiene carbocation can be further cleaved into a propadiene carbocation fragment ($C_3H_3^+$) of 39 m/z. The loss of 30 m/z from anisole corresponds to the loss of a neutral formaldehyde molecule resulting in a benzylic carbocation ($C_6H_6^+$) of 78 m/z.

The fragmentation pattern of the second intermediate (Fig. 6.2B) shows similarities with the pattern of the first intermediate. Firstly, veratrole (138 m/z) is formed due to the loss of neutral CO_2 molecule. Secondly the methyl moiety is cleaved leading to a guaiacoxy carbocation (123 m/z). Next, the guaiacoxy carbocation loses a neutral CO molecule resulting in a methoxylated cyclopentadiene carbocation (95 m/z) which results in a cyclopentadiene carbocation (65 m/z) after the loss of the methoxy moiety. Veratrole results in a benzyl carbocation ($C_6H_5^+$) of 77 m/z after the loss of a neutral formaldehyde molecule and the methoxy moiety. The 52 and 41 m/z fragments correspond to $C_4H_4^+$ and $C_3H_5^+$ carbocations, respectively.

Based on (i) the mass of the molecular ions and (ii) their fragmentation pattern, it can be concluded that the observed first and second intermediate correspond to MPC and MGC, respectively.

6.3 Reactivity of (*o*-methoxy) DAC for methanolysis

Up to now, only the thermodynamics have been addressed. However, thermodynamics only give information about the equilibrium conditions of products once the reaction equilibrates, but it does not explain the rate of reaction. Hence, also the kinetics should be evaluated. Kinetics describe the rate of reaction and how fast equilibrium is reached.

As an initial starting point, a blank reaction was performed (without addition of catalyst). This experiment followed the standard procedure for methanolysis as described in Chapter 3. In short, 2 mmol (*o*-methoxy) diaryl carbonate was dissolved in 0.8 mL MeOH (10 equivalents) and 4 mL 2-MeTHF at 40 °C for 4 h.

Despite the previously determined favourable thermodynamics, only 4 and 3 mol% conversion was obtained for DPC and DGC, respectively. Presumably, the reactivity of DAC (*i.e.* both DPC and DGC) for methanolysis is low due to a high reaction activation energy (E_a). This energy barrier prevents the reaction to evolve towards its most stable products. In general, the reactivity of a reaction can be improved by (i) increasing reaction temperature and/or (ii) applying catalysis. However, no improvement could be achieved at higher temperatures, being rather restricted by the boiling point of MeOH (T_b = 65 °C). After 4 h at 60 °C, only 5 and 3 mol% conversion was obtained for DPC and DGC, respectively. Therefore, to perform methanolysis at mild reaction conditions, catalysis was employed to increase reactivity. Catalysis allows to enhance the rate of the reaction by lowering the E_a without altering the thermodynamic chemical equilibrium of the reaction.

6.4 Catalyst screening

Most, if not all, literature-described PC methanolysis reactions are base-catalysed (section 2.2.3.1). In general, acid-catalysed transesterifications proceed slower and require higher reaction temperatures than base-catalysed transesterifications. The two most promising types of alkaline catalysts are alkali hydroxides and organocatalysts. Selected catalyst include two alkali hydroxides, *i.e.*, sodium hydroxide (NaOH) and potassium hydroxide (KOH) and six organocatalysts, *i.e.*, 1,5,7-triazabicyclo[4.4.0]-dec-5-ene (TBD), 1,8-diazabicyclo[5.4.0]undec-7-ene (DBU), 1,4-diazabicyclo[2.2.2]octane (DABCO), 4-dimethylaminopyridine (DMAP), 1-methylimidazole (NMI) and *N*,*N*-dimethylaniline (DMA). The molecular structures of these organocatalysts are illustrated in Figure 6.3. The amount of catalyst used, is expressed in terms of catalytic concentration, *i.e.* the ratio of mole catalyst to mole reagent.

To investigate the most active catalyst(s), DAC methanolysis was initially performed with 2 mol% catalyst at 40 °C for 2 h. The results of DAC methanolysis for the eight catalysts are shown in Table 6.1.

For DPC methanolysis, four catalysts achieved quasi-full conversion, *i.e.*, NaOH, KOH, TBD and DBU. However, only NaOH and TBD also led to high DMC yield of 86 and 96 mol%, respectively. KOH and DBU gave only 20 and 17 mol% yield, respectively. The other catalysts displayed conversions ≤ 10 mol% and no DMC was detected.

Under identical conditions, in contrast to DPC, the base-catalysed methanolysis of DGC gave slightly different results. In general, DGC seems to be less reactive for all tested catalysts leading to lower conversion and yields. Despite its lower reactivity, the overall order of catalyst activity seems to be almost unaltered, expect for KOH and DBU. Unlike as seen for DPC, here, the conversion for KOH and DBU is limited to 20 mol% with practically no yield towards DMC (≤ 1 mol%). The best results are obtained for NaOH and TBD giving 78 and 63 mol% DGC conversion combined with 24 and 54 mol% DMC yield, respectively. As before, the other organocatalysts (DMAP, DABCO, NMI and DMA) showed little ability to catalyse the methanolysis of DGC (*i.e.* DGC conversion ≤ 7 mol%).

Table 6.1 Catalyst screening of the DPC and DGC methanolysis reaction. Reaction conditions: DAC:catalyst:MeOH = 1:0.02:10 molar ratio, 40 °C, 2 h, 450 rpm

Catalyst	DPC			DGC		
	Conversion [mol%]	DMC yield [mol%]	MPC yield [mol%]	Conversion [mol%]	DMC yield [mol%]	MGC yield [mol%]
NaOH	100	86	16	78	24	58
KOH	92	20	60	20	1	22
TBD	99	96	2	63	54	16
DBU	98	17	67	21	0	20
DMAP	10	0	11	7	0	3
DABCO	6	0	5	3	0	1
NMI	3	0	1	2	0	1
DMA	0	0	0	1	0	1

Within DAC methanolysis, the catalytic activity, in terms of DAC conversion and DMC yields, varied between the different catalysts. Firstly, the difference in catalytic activity of the alkali hydroxides will be discussed, followed by the discussion of the organocatalysts.

When comparing NaOH and KOH, NaOH is the more active catalyst in DAC methanolysis. In DPC methanolysis, DPC conversion is very high for both catalysts but there is a significant difference in DMC yield. In DGC methanolysis, there is already a significant difference in DGC conversion between NaOH and KOH. Despite the fact that KOH is a stronger base in water than NaOH ($pK_{b,\,KOH} = -0.7$ versus $pK_{b,\,NaOH} = -0.56$), NaOH is a more active catalyst than KOH for methanolysis. Possibly, the difference in activity of alkali hydroxides can be explained by their difference in polarity and stability in MeOH. The electronegativity difference in KOH is (slightly) larger than in NaOH and thus is KOH more polar than NaOH. Consequently, KOH will dissociate more easily in MeOH, a polar solvent, than NaOH. On top of that, the formed $KOCH_3$ will be more stable than $NaOCH_3$ in MeOH leading to a less reactive transesterification.[121] However, the difference in electronegativity between potassium and sodium is relatively small and cannot be the main reason for the difference in catalyst activity. In a study conducted by Do *et al.* (2018) the catalytic activity of NaOH and KOH in BPA-PC methanolysis was similar. At 25 °C after 12 h, BPA yields amounted to 85 and 88 mol% for NaOH and KOH.[97] Presumably, deactivated or less active KOH was used during the experiment. KOH is hygroscopic and can contain significant amounts of water if it is not stored properly.

In Figure 6.3, the used organocatalysts are arranged according their acidity in water and acetonitrile (ACN). The acidity decreases from left to right, meaning that the basicity increases from left to right. The results of the organocatalysts confirm the earlier postulated rule of thumb that transesterification proceeds slower in acidic than in alkaline conditions. With increasing the pK_a, both consecutive transesterification reactions proceed faster. Firstly, DAC is faster converted to methyl aryl carbonate (MAC) followed by a faster conversion of MAC to DMC. The organocatalyst with the highest basicity (*i.e.* TBD) is the most active methanolysis organocatalyst. DAC methanolysis catalysed by TBD results in a fast first transesterification (*i.e.* high conversion) followed by a fast second transesterification (*i.e.* high DMC yield combined with low MAC yield).

In general, from this catalyst screening it can be concluded that NaOH and TBD prove to be the most active catalysts for both DPC and DGC methanolysis. More specifically, in view of the recycling context, especially the TBD catalyst seems promising as it not only gives high DAC conversions but – more importantly – high DMC yields. Although NaOH ($pK_b = -0.7$) is more alkaline than TBD ($pK_b < 2.1$), the latter is the more active catalyst. Therefore, another effect besides the basicity contributes to the activity of these catalysts. This additional effect will be discussed in more detail in section 6.6.1.

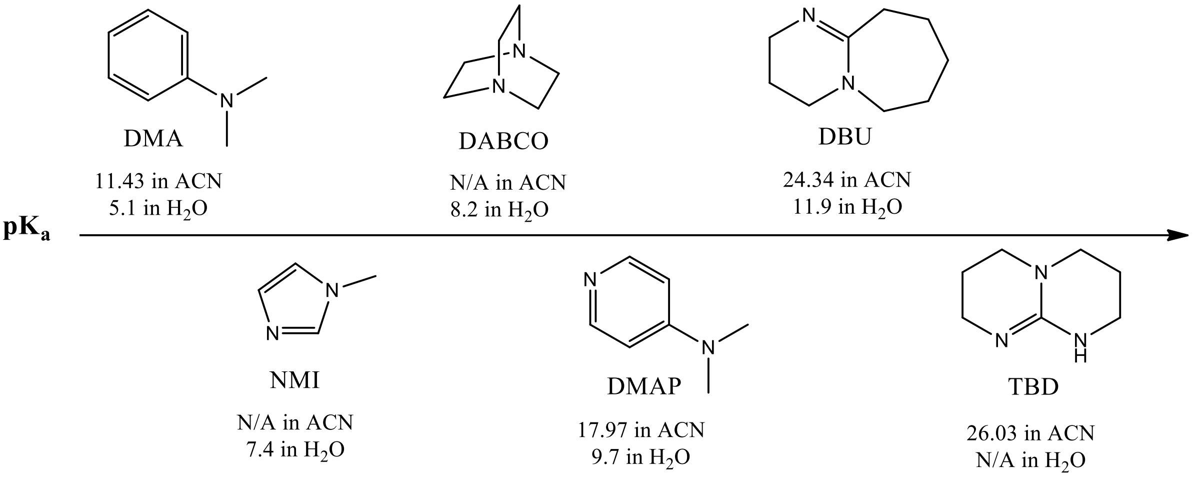

Figure 6.3 Organocatalysts used in the methanolysis of DPC and DGC arranged according to decreasing acidity. Data and figure adapted from Jehanno *et al.* (2019).[94] N/A stands for “Not Available”.

6.5 Difference in methanolysis reactivity of DPC and DGC

Based on the results in Table 6.1, it is noticeable that the methanolysis of DPC gives higher conversion and yield than for DGC under similar conditions. In other words, DPC is more reactive than DGC towards methanolysis.

6.5.1 Hypothesis

Before conducting any further experiment, a hypothesis can be made in order to explain the higher reactivity of DPC for methanolysis. The reactivity is influenced by two effects; (i) an electronic and (ii) a steric effect.

For transesterification, as a rule of thumb, the more nucleophilic alkoxy compound will displace the more electrophilic compound. In this rule, the reactivity is influenced by electronic effects. Nucleophiles have a free electron pair and are able to donate it, they are by definition Lewis bases. On the other hand, electrophiles are electron pair acceptors, *i.e.* Lewis acids. One way to predict the nucleophilic strength of a compound is by looking at its pK_a value. Strong nucleophiles are strong Lewis bases and therefore possess a high pK_a value while strong electrophiles possess a low pK_a value. After the methanolysis reaction, the strongest nucleophile will be bound to the carbonate linkage and the strongest electrophile will form an alcohol. Furthermore, the reactivity of the methanolysis reaction will be influenced by the strength of both nucleophile and electrophile.

During methanolysis (of both DPC and DGC), MeOH ($pK_a = 15.5$) will act as the nucleophile and will be bound to the carbonate linkage resulting in MAC and (subsequently) DMC. The methoxy functionality of MeOH will be interchanged with phenoxy and guaiacoxy of DPC and DGC, respectively. The pK_a value of phenol and guaiacol lies around 9.9 and 10.0, respectively.[122] The difference in pK_a, although very small, originates from the *o*-methoxy functionality of guaiacol. The electron-donating character of a methoxy substituent on an aromatic ring makes the aromatic ring more electron-rich, and hence (slightly) increases the basicity. Based on the pK_a values, a phenolate is the strongest electrophile, meaning that it will be a better leaving group than guaiacolate, due to its lower pK_a value, making DPC more reactive towards methanolysis.

Besides an electronic effect, also a steric effect influences the reactivity for methanolysis. This steric effect can be explained with the general reaction mechanism of base-catalysed methanolysis shown in Figure 6.4. The base catalyses the reaction by deprotonating MeOH and increasing its nucleophilicity. The nucleophilic methoxide anion performs a nucleophilic attack on the tetrahedral carbon atom of the carbonate linkage. Afterwards, the (*o*-methoxy) phenoxy substituent, the more electrophilic substituent, is eliminated. The nucleophilic substitution occurs two times to complete the methanolysis reaction.

A steric effect can influence the reactivity by affecting the nucleophilic attack on the tetrahedral carbon. The two *o*-methoxy functionalities of DGC could sterically hinder the incoming nucleophilic methoxide anion and hence hamper the reactivity of the reaction. A 3D visualisation of DPC and DGC is made in Figure 6.5 to illustrate the steric hindrance.

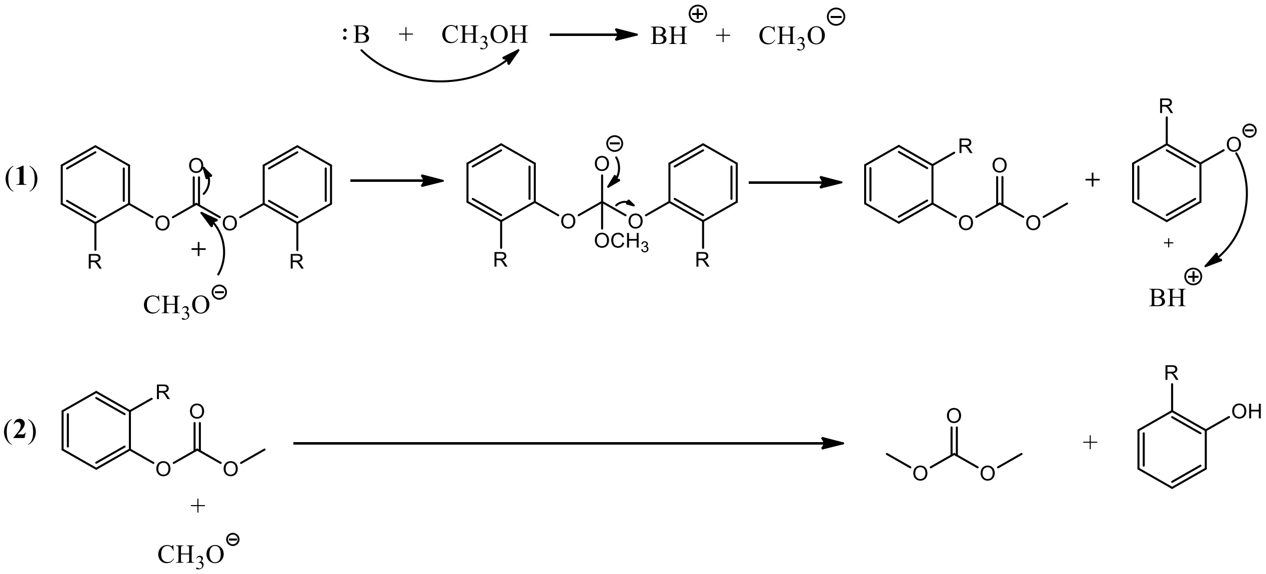

Figure 6.4 General mechanism of base-catalysed methanolysis of DPC (R = –H) and DGC (R = –OCH$_3$) with B as a base. (1) and (2) indicate the first and second transesterification reaction, respectively.

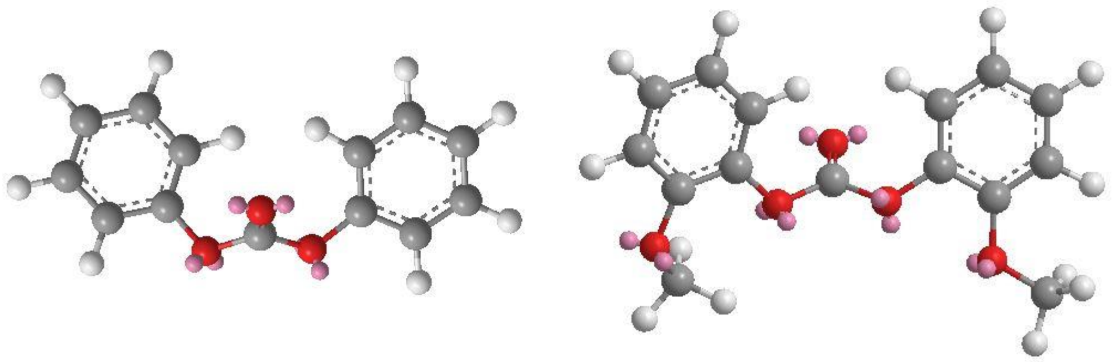

Figure 6.5 3D visualisation of (left) DPC and (right) DGC. The central, tetrahedral carbon of DGC can be sterically hindered due to the additional *o*-methoxy functionalities, hampering the nucleophilic attack of the methoxide anion.

6.5.2 Methanolysis reaction kinetics

In order to quantify the difference in reactivity between DPC and DGC methanolysis, the activation energy of both reactions can be calculated. A relationship between the reaction rate constant (*k*) and E_a is given by the Arrhenius equation (6.1):

$$k = Ae^{-E_a/RT} \tag{6.1}$$

$$\ln(k) = \ln(A) - \frac{E_a}{RT} \tag{6.2}$$

with *A* as a pre-exponential factor, *R* the universal gas constant and *T* the absolute temperature (in Kelvin).

To determine E_a of a reaction, it is necessary to know the reaction rate constant. k can be calculated if the reaction kinetics are known. Because methanolysis is a consecutive reaction, the overall reaction will result in two rate constants. Using reaction equations 1 – 4 described in section 5.3.2, following reaction rates (r) can be formulated:

(1) $r_{1,DPC} = k_{1,DPC} * [DPC]$

(2) $r_{2,MPC} = k_{2,MPC} * [MPC]$

(3) $r_{1,DGC} = k_{1,DGC} * [DGC]$

(4) $r_{2,MGC} = k_{2,MGC} * [MGC]$

In order simplify the model, it is assumed that the reactions are irreversible, forward reactions and that no backward reactions take place. This assumption is based on the chemical equilibrium constants calculated in section 5.3.2. Furthermore, the MeOH concentration is present in excess and therefore considered to be constant. All reactions are therefore first order reactions.

Using the reaction rates, a material balance of all components can be written:

(1) $\frac{d[DPC]}{dt} = -r_{1,DPC}$

(2) $\frac{d[MPC]}{dt} = r_{1,DPC} - r_{2,MPC}$

(3) $\frac{d[DMC]}{dt} = r_{2,MPC}$

(4) $\frac{d[phenol]}{dt} = r_{1,DPC} + r_{2,MPC}$

(5) $\frac{d[DGC]}{dt} = -r_{1,DGG}$

(6) $\frac{d[MGC]}{dt} = r_{1,DGC} - r_{2,MGC}$

(7) $\frac{d[DMC]}{dt} = r_{2,MGC}$

(8) $\frac{d[guaiacol]}{dt} = r_{1,DGC} + r_{2,MGC}$

Solving this material balances for DPC, MPC and DMC, the following equations are obtained (analogue solutions for DGC and MGC):

$$[DPC] = [DPC]_0 * e^{-k_{1,DPC} * t} \tag{6.3}$$

$$[MPC] = [DPC]_0 * \frac{k_{1,DPC}}{k_{2,MPC} - k_{1,DPC}} * (e^{-k_{1,DPC}*t} - e^{-k_{2,MPC}*t}) \tag{6.4}$$

$$[DMC] = [DPC]_0 * \left(1 + \frac{k_{1,DPC} * e^{-k_{2,MPC}*t} - k_{2,MPC} * e^{-k_{1,DPC}*t}}{k_{2,MPC} - k_{1,DPC}}\right) \tag{6.5}$$

These solutions are based on the general solutions for an irreversible, consecutive reaction described by Vallance (2017).[123]

The rate constants can be calculated when rearranging equation 6.3 and 6.5:

$$\ln([DPC]/[DPC]_0) = -k_{1,DPC} * t \tag{6.6}$$

$$\ln\left(1 - \frac{[DMC]}{[DPC]_0}\right) = -k_{2,MPC} * t \tag{6.7}$$

Equation 6.7 is only valid if $k_1 >> k_2$, *i.e.* the second reaction is the rate determining step (RDS). Therefore, the calculated values of k_2 will be simplifications. Nevertheless, these values will give an indication about the reaction's reactivity.

6.5.3 DAC methanolysis catalysed by NaOH

6.5.3.1 Initial experiment

In a kinetic experiment, the aim is to determine reaction rate constants from which the activation energy of the reaction can be obtained. Before such experiment can be executed, the reaction conditions need to be optimised.

In the initial, exploratory DAC methanolysis experiment, the reaction was conducted with 2 mol% NaOH, at 40 °C for 8 h. To visualize the reaction progress, samples were taken after 5, 10, 15, 30 and 45 min and after 1, 2, 4, 6 and 8 h. DAC conversion (X) and MAC and DMC yield (Y) against time are shown in Figure 6.5.

For DPC, already 93 mol% DPC was converted after 5 min, and full conversion was reached after 30 min. Initially, the yield of intermediate MPC strongly increased reaching a maximum of 59 mol% after 15 min. Afterwards, the MPC yield gradually decreased until all MPC was converted into DMC (after 6 h). Because DPC and MPC were converted quickly, high DMC yields were obtained after relative short reaction times. After 5 min, the DMC yield amounted to 22 mol%, after 1 h it amounted to 68 mol% and the yield reached 100 mol% after 6 h. A carbon balance was made for every sample, to monitor the accuracy of the results obtained. The carbon balance varied between 93 and 101 mol% with an average value of 98 mol%, confirming the accuracy of the analysis.

In contrast, DGC, *i.e. o*-methoxylated DPC, did not reach full conversion (93 mol%) after 8 h. Initially, the MGC yield followed the same rate as DGC conversion. After roughly 30 min, the rate of MGC production slowed down, and the MGC yield reached a maximum of 58 mol% after 2 h. After this maximum, the MGC yield decreased slowly to 52 mol% after 8 h. Throughout the whole reaction, the DMC yield increased steadily, almost at a constant rate. The maximum DMC yield, achieved after 8 h, amounted 51 mol%. The carbon balance of this experiment varied between 98 and 105 mol% with an average value of 101 mol%.

Comparing DPC and DGC methanolysis, the same trend as in the catalyst screening (section 6.4) is observed. Both consecutive reactions in DPC methanolysis proceed faster than in DGC methanolysis. DPC is faster converted than DGC and additionally, MPC is faster converted than MGC. Early in the reaction, MPC obtains a high yield due to a fast first methanolysis reaction, but MPC is also converted into DMC immediately after. MGC is formed and converted more slowly than MPC, resulting in a high yield after 8 h.

The purpose of this initial experiment was to verify if the reaction conditions are optimal to conduct a kinetic study. At these conditions, DPC is very reactive for methanolysis and the conversion was already high after the first sampling. In order to slow down the reaction rate and to be able to determine reaction rate constants, DPC methanolysis will be executed at a lower catalytic concentration and moderate temperatures. The kinetic study of DGC methanolysis is carried out at elevated temperatures to increase the reaction rates.

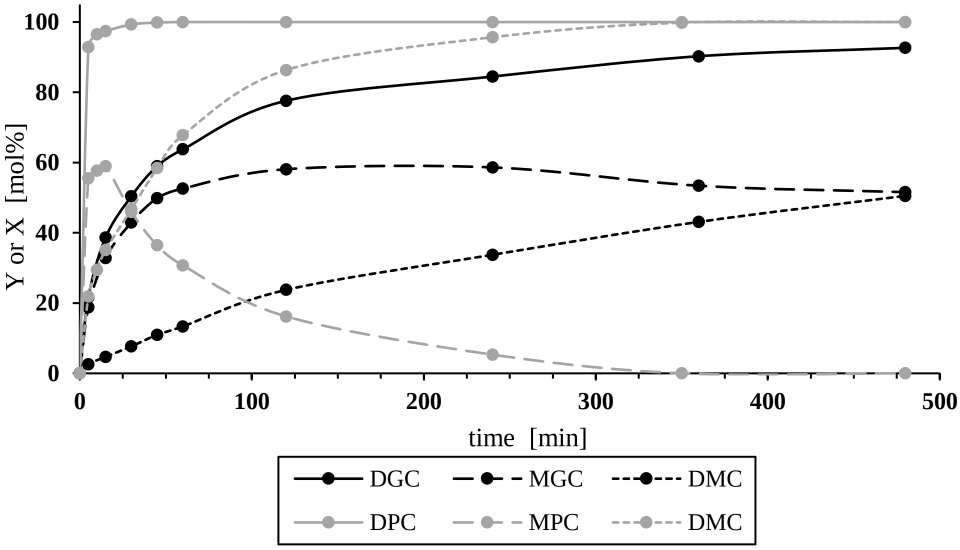

Figure 6.6 DPC (grey) and DGC (black) methanolysis as function of time. Yield in mol% is indicated as Y, conversion in mol% is indicates as X. Reaction conditions: 40 °C, 450 rpm, DPC:NaOH:MeOH = 1:0.027:10 molar ratio, DGC:NaOH:MeOH = 1:0.021:10 molar ratio.

6.5.3.2 Rate constants and activation energy of DAC methanolysis catalysed by NaOH

The activation energy of DAC methanolysis can be calculated using an Arrhenius plot based on equation 6.2. In this plot, the natural logarithm of k is plotted versus $1/T$.

To construct an Arrhenius plot, at least three rate constants at different temperatures are necessary. DPC methanolysis was carried out with 1 mol% NaOH as catalysts for 8 h at 30, 40 and 50 °C. The three DGC methanolysis reactions were carried out with 2 mol% NaOH for 8 h at 40, 50 and 60 °C.

Plots of methanolysis of DPC and DGC against time for different temperatures are shown in Figure 6.7 and 6.8, respectively.

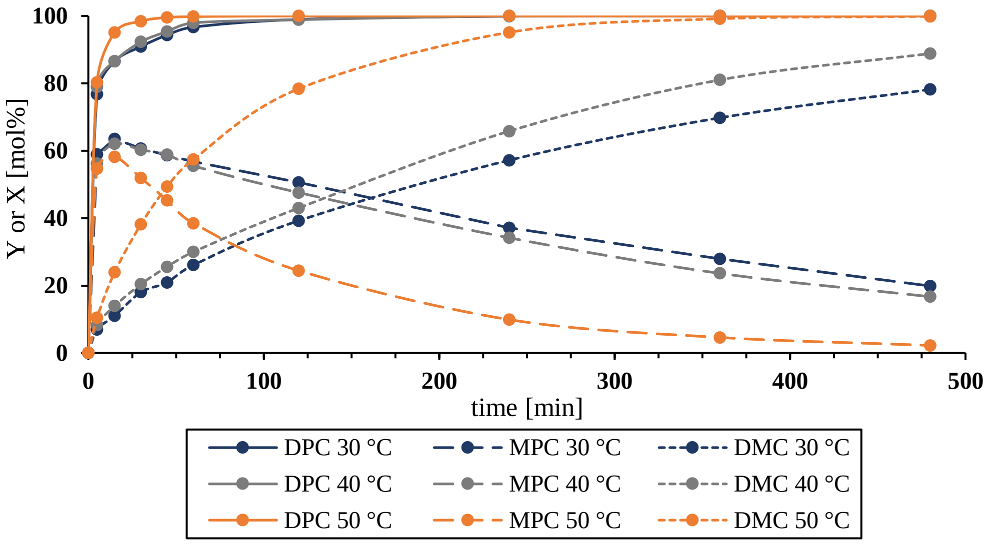

Figure 6.7 DPC methanolysis against time at different temperatures: 30 °C (dark blue), 40 °C (dark grey) and 50 °C (dark orange). Reaction conditions: 8 h, 450 rpm, DPC:MeOH = 1:10 molar ratio, catalyst concentration; 1.1 mol% NaOH (30 °C), 1.1 mol% NaOH (40°C), 1.2 mol% NaOH (50 °C).

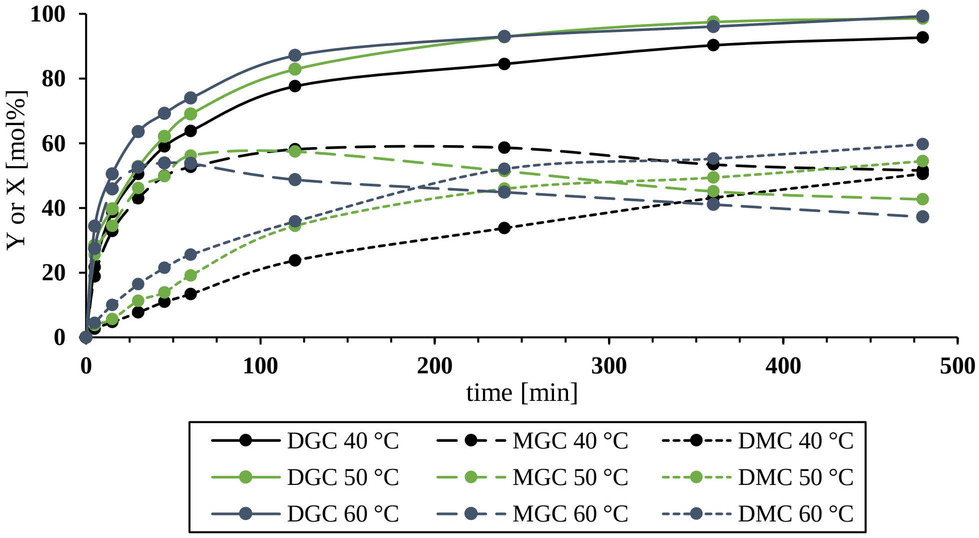

Figure 6.8 DGC methanolysis against time at different temperatures: 40 °C (black), 50 °C (green), 60 °C (blue grey). Reaction conditions: 8 h, 450 rpm, DGC:MeOH = 1:10 molar ratio, catalyst concentration; 2.1 mol% NaOH (40 °C), 2.2 mol% NaOH (50 °C), 2.1 mol% NaOH (60 °C).

The strategy to initially temper DPC methanolysis seems to have worked. Only the reaction at 50 °C (after 6 h) reaches a DMC yield of 100 mol%. The increasing temperature has a positive effect on both consecutive methanolysis reaction rates. Complete DPC conversion is faster achieved when using higher temperatures. Furthermore, the increasing temperature results in a faster conversion of MPC in the desired DMC. The average value of the carbon balance of the reaction at 30, 40 and 50 °C was 95, 97 and 99 mol%, respectively.

The same rationale also applies to DGC methanolysis. Complete DGC conversion is faster achieved at elevated temperatures, only at 40 °C no complete conversion is achieved after 8 h (93 mol%). Higher temperatures result in a desired higher DMC yield and lower MGC yield. The highest DMC yield is achieved at 60 °C and amounts to 60 mol% after 8 h. The corresponding MGC yield amounts to 37 mol%, the lowest MGC yield of all three temperatures. The average value of the carbon balance of the reaction at 40, 50 and 60 °C was 101, 102 and 101 mol%, respectively.

The initial reaction rate constants k_1 and k_2 for both DPC and DGC methanolysis can be calculated using equations 6.6 and 6.7 and are shown in Table 6.2.

Table 6.2 Experimentally derived first-order reaction rate constants for the consecutive DAC methanolysis reaction at different temperatures

Temperature [°C]	**Rate constant** [min $^{-1}$]			
	$k_{1,DPC}$	$k_{1,DGC}$	$k_{2,MPC}$	$k_{2,MGC}$
30	0.292	–	0.014	–
40	0.312	0.049	0.017	0.003
50	0.326	0.067	0.022	0.004
60	–	0.084	–	0.006

In DAC methanolysis, the second transesterification reaction proceeds slower than the first transesterification. The rate constant of the first DPC ($k_{1,DPC}$) or DGC transesterification ($k_{1,DGC}$) is roughly 15 to 20 times bigger than the rate constant of the second DPC ($k_{2,MPC}$) or DGC transesterification ($k_{2,MGC}$) at a certain temperature. $k_{1,DPC}$ and $k_{2,MPC}$ are significantly bigger than $k_{1,DGC}$ and $k_{2,MGC}$, respectively. Based on k_1 and k_2, the total DPC methanolysis reaction proceeds roughly five to six times faster than the total DGC methanolysis reaction.

These reaction rate constants can be used to construct and Arrhenius plot. The Arrhenius plots for DAC methanolysis are shown in Figure 6.9.

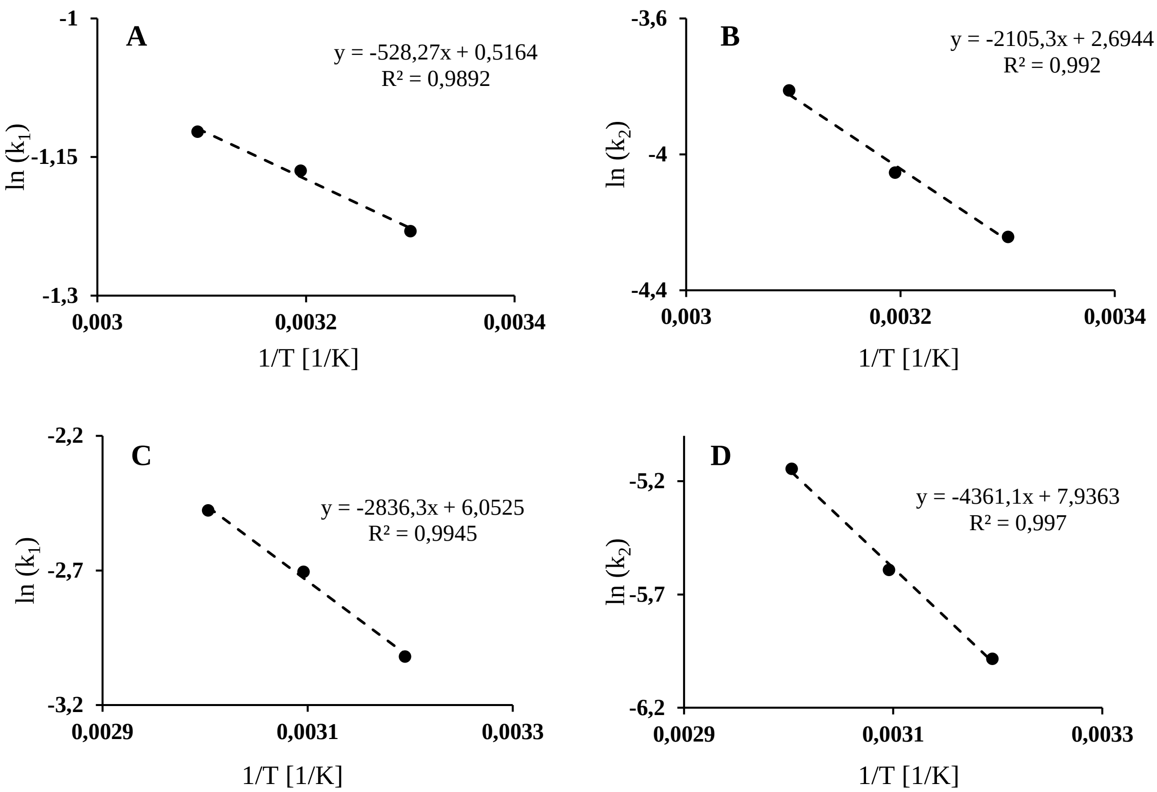

Figure 6.9 Arrhenius plot based on the experimentally determined reaction rate constants of DAC methanolysis. (**A**): Arrhenius plot of $k_{1,DPC}$, DPC methanolysis to form MPC, (**B**): Arrhenius plot of $k_{2,MPC}$, MPC methanolysis to form DMC, (**C**) Arrhenius plot of $k_{1,DGC}$, DGC methanolysis to form MGC, (**D**): Arrhenius plot of $k_{2,MGC}$, MGC methanolysis to form DMC.

The activation energy of each reaction is calculated from the slope of the corresponding Arrhenius plot and shown in Table 6.3.

Table 6.3 Experimentally determined activation energies of the consecutive DAC methanolysis

Reaction	$E_{a,DPC}$ [kJ mol^{-1}]	$E_{a,DGC}$ [kJ mol^{-1}]
DPC + MeOH -> MPC + Ph DGC + MeOH -> MGC + G	4.4	23.6
MPC + MeOH -> DMC + Ph MGC + MeOH -> DMC + G	17.5	36.6

The activation energy for the first and second DPC methanolysis reaction amounts to 4.4 and 17.5 kJ mol^{-1}, respectively. For the two DGC methanolysis reactions, the activation energy amounts 23.6 kJ mol^{-1} and 36.6 kJ mol^{-1}, respectively. For both DPC and DGC methanolysis, the assumption, that the second transesterification reaction is the RDS in equation 6.7, is valid based on both the rate constants and the activation energies. DAC undergoes methanolysis faster compared to MAC due to the lower activation energy of the first step.

The activation energy gives an indication how the reaction rate varies at different temperatures. For DAC methanolysis, the activation energy of the first transesterification is the smallest. Increasing the temperature will enhance the reaction rate of the first transesterification less than it will for the reaction rate of the second transesterification. In DPC methanolysis, higher temperatures will accelerate the full methanolysis reaction mainly by speeding up the second transesterification reaction. In DGC methanolysis, both transesterifications are more temperature sensitive. Higher temperatures will accelerate the full DGC methanolysis by speeding up both transesterification reactions.

The methanolysis experiment of DAC showed that DPC methanolysis is more reactive than DGC methanolysis. DPC methanolysis with 1 mol% NaOH at 50 °C obtained a full conversion of DPC into DMC after 8 h. DGC methanolysis with 2 mol% NaOH at 60 °C obtained only 60 mol% DMC and full conversion after 8 h. This observation was confirmed by a kinetic study which determined reaction rate constants and activation energies of the two methanolysis reactions. For both DPC and DGC methanolysis, the second transesterification reaction is the RDS.

From an environmental point of view, the reduced reactivity of DGC for methanolysis also has an advantage. DGC, and its corresponding bisguaiacol-PC, will degrade more slowly than DPC, and its corresponding BPA-PC, once exposed in the environment. The release of monomers resulting from bisguaiacol-PCs will probably be less abundant than the release of monomers resulting from BPA-PCs.

6.6 DGC methanolysis catalysed by NaOH and TBD

6.6.1 Reactivity difference of DGC for methanolysis catalysed by NaOH and TBD

The previous section (section 6.5) has shown that DPC is more reactive towards methanolysis than DGC. Nonetheless, DGC methanolysis seems to be feasible under more severe reaction conditions, *i.e.* higher catalyst concentration and increased temperature and reaction time. Besides NaOH, another catalyst that showed desirable yields in the catalyst screening (section 6.4) was TBD. In the following experiment, DGC methanolysis will be subjected to the same kinetic experiment as in section 6.5, but now with TBD as catalyst. The data from DGC methanolysis catalysed by NaOH from section 6.5 are used to compare the catalysts.

DGC methanolysis catalysed by TBD and NaOH against time at different temperatures are shown in Figure 6.10 and Figure 6.8, respectively.

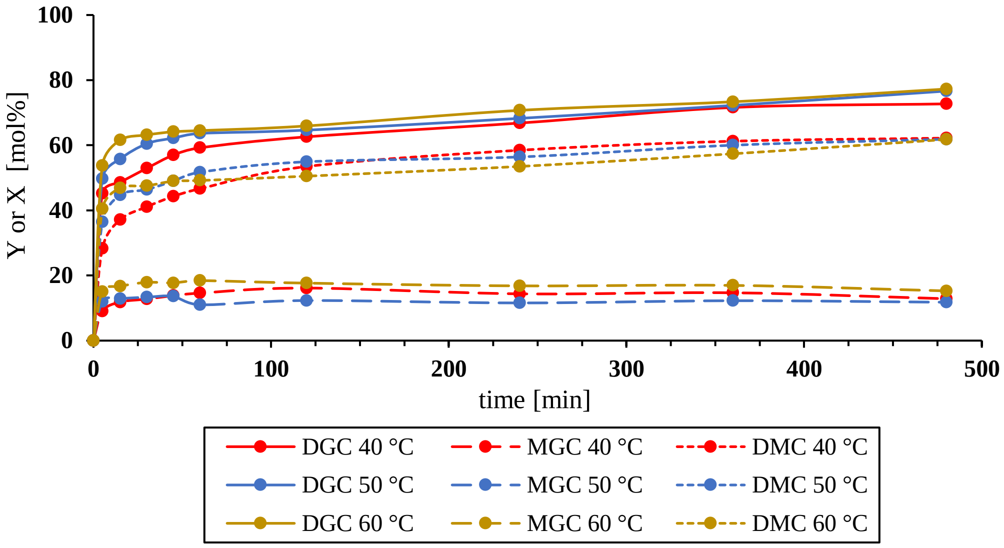

Figure 6.10 DGC methanolysis catalysed by TBD against time at different temperatures: 40 °C (red), 50 °C (blue), 60 °C (gold). Reaction conditions: 8 h, 450 rpm, DGC:MeOH = 1:10 molar ratio, catalyst concentration; 2.0 mol% TBD (40 °C), 2.0 mol% TBD (50 °C), 2.1 mol% TBD (60 °C).

DGC methanolysis catalysed by TBD does not seem very influenced by temperature at the used catalyst concentration, when evaluating the whole reaction progress. DGC conversion, MGC yield and DMC yield all seem to converge towards the same value after a longer reaction period. After 8 h, the DGC conversion, MGC yield and DMC yield at 40, 50 and 60 °C seem to converge approximately toward 75, 15 and 60 mol%, respectively. The average value of the carbon balance of the methanolysis at 40, 50 and 60°C was 100, 100 and 101 mol%, respectively.

Initially, the reaction rates of DGC conversion and MGC and DMC production varies at different temperatures. Therefore, initial reaction rate constants k_1 and k_2 for TBD-catalysed DGC methanolysis can be determined. These rate constants, together with the rate constants for NaOH-catalysed DGC methanolysis, are shown in Table 6.4.

Table 6.4 Experimentally derived reaction rate constants for the consecutive DGC methanolysis reaction catalysed by TBD and NaOH at different temperatures

Temperature [°C]	**Rate constant** [min $^{-1}$]			
	$k_{1,TBD}$	$k_{1,NaOH}$	$k_{2,TBD}$	$k_{2,NaOH}$
40	0.120	0.049	0.067	0.003
50	0.138	0.067	0.091	0.004
60	0.154	0.084	0.104	0.006

For DGC methanolysis at 2 mol% catalyst concentration, TBD is a more active catalyst than NaOH at all tested temperatures. The first transesterification reaction catalysed by TBD is roughly two times faster than the NaOH-catalysed reaction. In terms of rate constants, the main difference between TBD and NaOH can be seen in the second transesterification. k_2 values at 40, 50 and 60 °C for the TBD-catalysed reaction amount to 0.067, 0.091 and 0.104 min^{-1}, respectively, while these k_2 values for the reaction catalysed by NaOH amount to 0.003, 0.004 and 0.006 min^{-1}, respectively. The second transesterification reaction catalysed by TBD proceeds 17 to 23 times faster than the same reaction catalysed by NaOH. This second transesterification reaction is still the RDS, but the difference in activity is far less pronounced. This is also visible when comparing the reaction progress of the reaction catalysed by TBD and NaOH (Fig. 6.10 and 6.8, respectively). In the NaOH-catalysed methanolysis, the maximal MGC yield approximates 55 mol% and slowly decreases afterwards, while the maximal MGC yield of the TBD-catalysed methanolysis only approaches 20 mol% before decreasing.

The obtained reaction rate constants from Table 6.4 can be used to construct an Arrhenius plot. The Arrhenius plots for TBD- and NaOH-catalysed DGC methanolysis are shown in Figure 6.11.

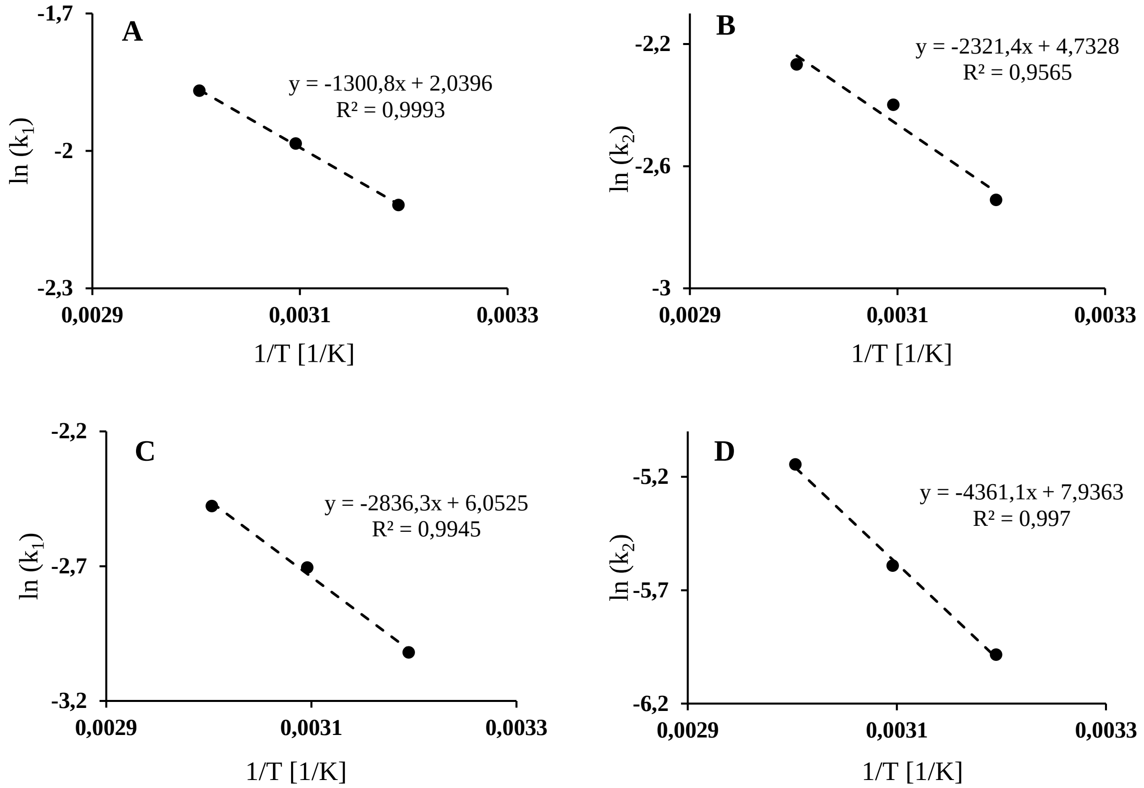

Figure 6.11 Arrhenius plot based on the experimentally determined reaction rate constants of DGC methanolysis catalysed by TBD and NaOH. (A): Arrhenius plot of $k_{1,TBD}$, DGC methanolysis to form MGC, (B): Arrhenius plot of $k_{2,TBD}$, MGC methanolysis to form DMC, (C) Arrhenius plot of $k_{1,NaOH}$, DGC methanolysis to form MGC, (D): Arrhenius plot of $k_{2,NaOH}$, MGC methanolysis to form DMC.

The activation energy of each reaction is calculated from the slope of the corresponding Arrhenius plot and shown in Table 6.5.

Table 6.5 Experimentally determined activation energies of the consecutive methanolysis of DGC catalysed by TBD and NaOH

Reaction	$E_{a,TBD}$ [kJ mol^{-1}]	$E_{a,NaOH}$ [kJ mol^{-1}]
DGC + MeOH -> MGC + G	10.8	23.6
MGC + MeOH -> DMC + G	19.3	36.6

The activation energy for the consecutive reactions of TBD-catalysed methanolysis amount to 10.8 kJ mol^{-1} and 19.3 kJ mol^{-1}, respectively. These activation energies confirm that the second transesterification reaction is still the RDS. However, the difference between the first and second reaction is far less pronounced than in NaOH-catalysed methanolysis. Equation 6.7, used to determine k_2, is only applicable if k_1 >> k_2. In the case of TBD, the difference between the two rate constants is not very significant making this assumption not completely valid. Therefore, the calculated k_2 values will not be highly accurate. This can be seen in Figure 6.11B, R^2 of this Arrhenius plots amounts to 0.9565 which is not as accurate as the other R^2 values. Despite the inaccuracy in the k_2 calculation, a main conclusion can be drawn. The second transesterification reaction proceeds roughly 20 times faster when TBD is used a catalyst instead of NaOH.

Although the TBD-catalysed reaction has the highest rate constants and lowest activation energies, no full DGC conversion or DMC production is obtained after 8 h. The NaOH-catalysed reaction, characterized by lower rate constants and higher activation energies, results in higher DGC conversions and DMC yields after 8 h. A possible explanation can be found in the catalytic reaction mechanism of both catalysts.

NaOH-catalysed DGC methanolysis follows the general base-catalysed reaction mechanism shown in Figure 6.4 (section 6.5.1). NaOH, as the base, will deprotonate MeOH into methoxide anion which acts as a nucleophile. This nucleophile will perform a nucleophilic attack on the carbonate linkage and the electrophile (the guaiacoxy fragment) will be eliminated. NaOH is reformed after the guaiacolate is protonated to guaiacol. On the other hand, research conducted by Do *et al.* (2018) illustrated that TBD has a second possible reaction mechanism besides the general base-catalysed mechanism (Fig 6.12).[97] In this mechanism, TBD itself performs a nucleophilic attack on the carbonate linkage and forms a carbamate intermediate with the elimination of a phenolic compound. Next, the alcohol addition to the carbamate intermediate is facilitated by hydrogen bonding between TBD and the alcohol leading to the elimination of TBD. The other plausible reaction mechanism is similar to the general base-catalysed reaction mechanism. Horn *et al.* (2012) demonstrated that the amine and imine moieties in TBD facilitated the carbonate and alcohol activation, increasing the electrophilic and nucleophilic character, respectively.[124] In both reaction pathways, the electron donor and acceptor property of the guanidine functionality present in TBD plays a crucial role in the activity of the catalyst. The presence and accessibility of this guanidine functionality indicates why TBD is the most active catalyst compared to NaOH or other organocatalysts such as DBU which do not possess this functionality.

These reaction pathways indicate that TBD is associated with the intermediate throughout the complete reaction. However, TBD can also associate with the carbonate linkage of DMC and hence be temporary unavailable. When methanolysis proceeds, the concentration of DMC will increase and so the number of interactions between DMC and TBD. Due to these interactions, no additional DMC is formed, leading to a stagnation of the reaction rate regardless of the reaction conditions. It can be concluded that the catalytic amount of 2 mol% TBD is too low to obtain a complete methanolysis reaction. In comparison, NaOH only plays a role in the activation of MeOH and does not interact with the substrate. Because the reaction is performed with an excess of MeOH, an excess of methoxide anions will be activated by NaOH and no stagnation will take place.

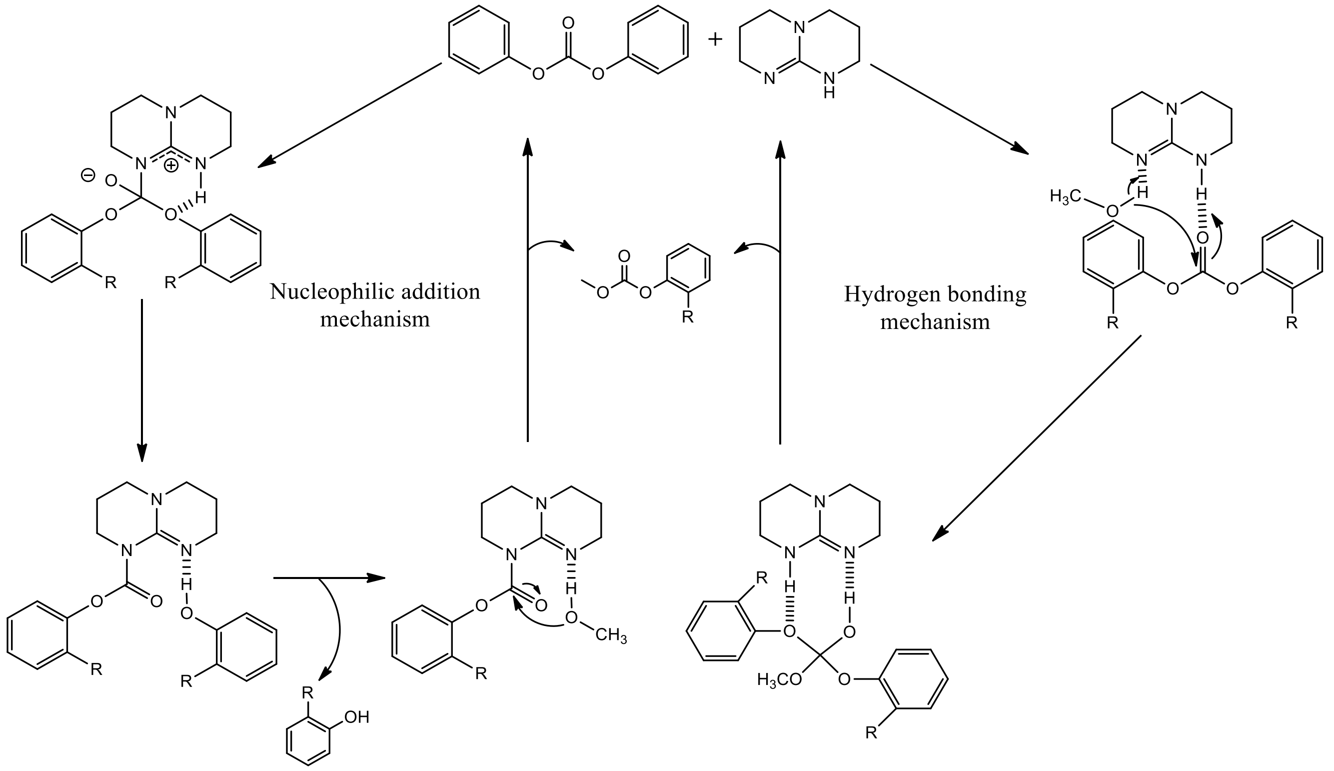

Figure 6.12 Two possible mechanisms of DAC methanolysis catalysed by TBD; R = –H (DPC), R = $–CH_3$ (DGC). Adapted from Do *et al.* (2018).[96]

6.6.2 Optimisation of NaOH- and TBD-catalysed DGC methanolysis

The ultimate goal of DGC methanolysis is to obtain a DMC yield near 100 mol%. In previous experiments, the highest DMC yield obtained was 62 and 60 mol% by TBD- and NaOH-catalysed methanolysis, respectively. In order to evaluate the hypothesis of stagnation due to catalyst deactivation, DGC methanolysis will be performed with a higher catalyst concentration. Instead of the previous 2 mol%, methanolysis will now be conducted with a catalyst concentration of 5 mol% (at 60 °C for 8 h).

A comparison of DGC methanolysis catalysed by TBD and NaOH against time at a catalyst concentration of 2 and 5 mol% are shown in Figure 6.13 and Figure 6.14, respectively. The data from the methanolysis experiments with 2 mol% catalyst originate from the experiments in the previous section (section 6.5.1).

Increasing the TBD concentration from 2 to 5 mol% results in an increased methanolysis rate (Fig. 6.13). After 5 min, the DGC conversion and DMC yield were 83 and 70 mol%, respectively, while DGC conversion and DMC yield with 2 mol% TBD amount to 54 and 40 mol%, respectively. As discussed before, all reaction rates seem to stagnate after the initial increase at 2 mol% TBD. In contrast, no stagnation is observed at a loading of 5 mol% TBD. Full conversion is reached after 30 min, and DMC reaches a yield of 100 mol% after 4 h. The carbon balance of DGC methanolysis catalysed by 5 mol% TBD has an average value of 102 mol%.

Increasing the NaOH concentration from 2 mol% to 5 mol% also results in increased reaction rates (Fig. 6.14). With 5 mol% NaOH, full conversion is reached after 2 h, while it is only reached with 2 mol% NaOH after 8 h. In addition, the increased NaOH concentration has a significant beneficial effect on the reaction rate of the second transesterification reaction of MGC into DMC. At 2 mol% NaOH, MGC reaches a maximal yield of 54 mol% after 45 min and the yield slowly decreases afterwards to 37 mol% after 8 h. At 5 mol% NaOH, MGC reaches a maximal yield of 60 mol% after 15 min and the yield strongly decreases afterwards. MGC is fully converted into DMC after 8 h. The carbon balance of DGC methanolysis catalysed by 5 mol% NaOH has an average value of 103 mol%.

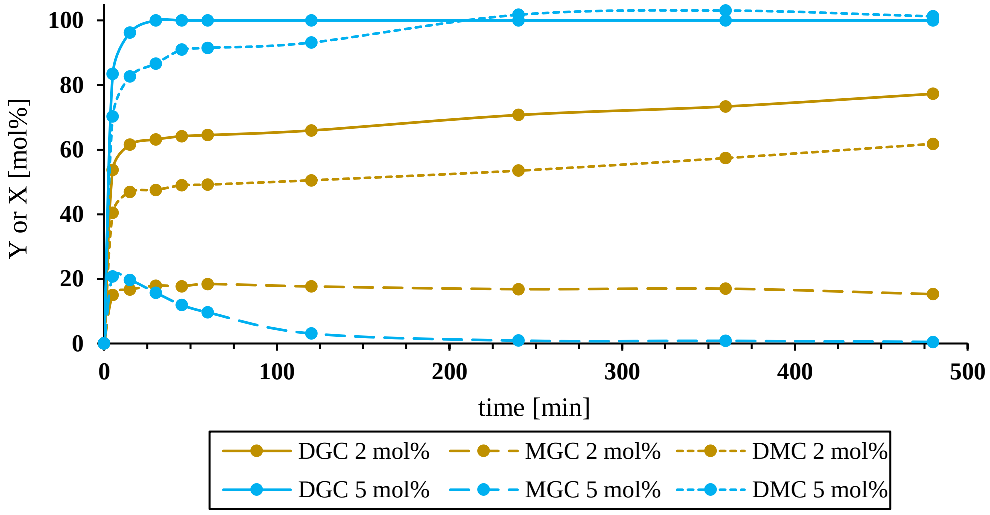

Figure 6.13 TBD-catalysed DGC methanolysis against time. Reaction conditions: 8 h, 60 °C, 450 rpm, DPC: MeOH = 1:10 molar ratio, catalyst concentration; 2.1 mol% TBD (gold) and 5.0 mol% TBD (light blue).

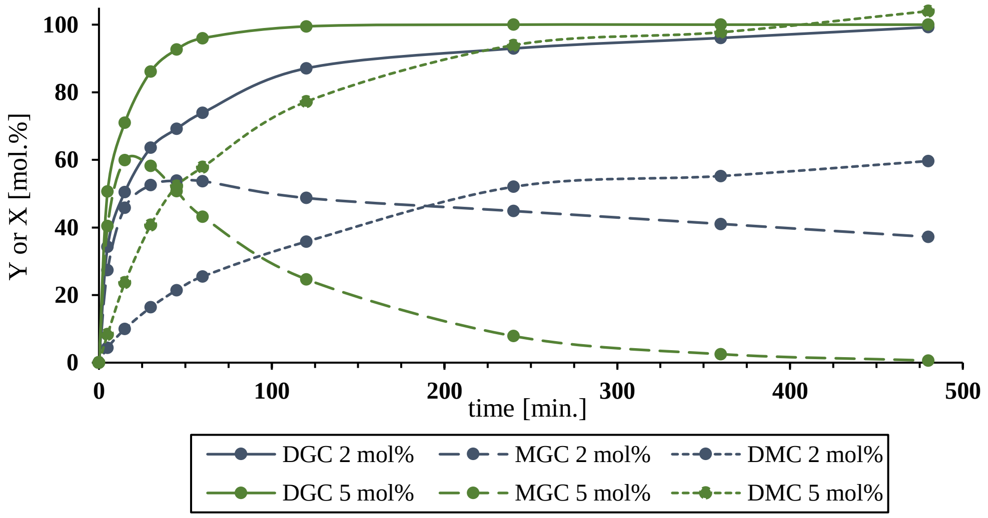

Figure 6.14 NaOH-catalysed DGC methanolysis as function of time. Reaction conditions: 8 h, 60 °C, 450 rpm, DPC: MeOH = 1:10 molar ratio, catalyst concentration; 2.2 mol% NaOH (blue grey) and 5.0 mol% NaOH (dark green).

An increased TBD concentration has a beneficial effect on the reaction rate of both consecutive transesterification reactions. Due to the higher concentration, the initial methanolysis rate is faster than the methanolysis rate at 2 mol% TBD. Methanolysis proceeds until all DGC and MGC are converted into DMC. TBD will likely still bind DMC but, because of the higher concentration, there is always sufficient catalyst present to catalyse the methanolysis reaction. Therefore, no stagnation occurs after the initial increased methanolysis rate.

Although methanolysis catalysed by NaOH did not seem to stagnate at 2 mol%, an increased NaOH concentration of 5 mol% does enhance both transesterification reactions. The increased reaction rate of the first methanolysis reaction results faster in a full conversion. Especially the second methanolysis reaction is positively influenced by the increased catalyst loading. At 2 mol% NaOH, the MGC yield stayed nearly constant after it reached its maximum. At 5 mol% NaOH, the MGC yield decreased gradually after its maximum until it was fully converted.

It can be concluded that the main goal, to find reaction conditions resulting in a maximal DMC yield, is achieved. Both TBD and NaOH at 5 mol% catalyse the full methanolysis of DGC into DMC at 60 °C. For TBD, a full conversion is obtained after 4 h, while for NaOH, it is obtained after 8 h.

7. General conclusions

The current plastics industry is mostly a linear ‘take-make-use-dispose’ economy. Consequently, this linear model is associated with a significant loss of material, value and energy. Upon transition to a circular economy model, these losses are minimized through proper end-of-life processing, such as remaking, repairing, reusing and recycling. Without this significant loss of material, such an effective after-use plastic economy would require substantial lower input of virgin feedstock. This allows to decouple plastics from fossil feedstock by exploring and adopting renewably sourced feedstock.

In recent years, the aromatic polycarbonate (PC) industry has been discredited due to the use of bisphenol A (BPA) as a monomer. BPA, a petroleum-based chemical, is highly controversial due to its endocrine disruptive properties. The search for safer alternatives has led to the development of ‘so-called’ bisguaiacols. Bisguaiacols are safer than BPA and are, in addition, derived from renewable lignocellulosic biomass. Several studies have been dedicated to the production of bisguaiacols and their implementation into polymers. However, these renewable monomers are only viable in a circular economy with an effective waste management system. One such waste management method is chemical recycling based on solvolysis, which has already been successfully applied to BPA-PCs on lab-scale. In contrast, similar research has not yet been conducted for bisguaiacol-based PCs. Therefore, in general, this MSc thesis focused on the chemical recycling of bisguaiacol-based PCs by solvolysis. More specifically, the influence of the extra *o*-methoxy moiety (as present in bisguaiacol-based PC) on solvolysis was examined by direct comparison with bisphenol-based PCs.

The main target for solvolysis of PCs is the carbonate (ester) linkage – the interconnection between two monomers. To circumvent the current commercial unavailability of bisguaiacol-based PCs, this MSc thesis started from carbonate-containing model compounds with chemical environments identical to the corresponding PCs. The model substrates of choice were diphenyl carbonate (DPC) and diguaiacyl carbonate (DGC), representing bisphenol- and bisguaiacol-based PCs, respectively.

Solvolysis entails in fact a reversible transesterification reaction. Because the carbonate (ester) linkage can be regarded as a di-ester functionality, two consecutive transesterifications are needed to reach full conversion, and hence to allow complete chemical recycling of the polymer into its monomeric constituents. For this reason, the intermediate components, formed after only one transesterification, were regarded unsuitable. For both diaryl carbonate (DAC) model compounds, DPC and DGC, the first transesterification resulted in an alkyl aryl carbonate and a phenolic compound. Afterwards, this intermediate underwent a second transesterification giving a dialkyl carbonate and a second phenolic compound.

Due to the reversibility of the transesterification reactions, it was key to know their thermodynamic (chemical) equilibria in advance. At chemical equilibrium, the thermodynamically most stable species are favoured, and hence this determines the degree of product formation. The chemical equilibrium can be expressed by its chemical equilibrium constant (K_{eq}). K_{eq} values were determined for both alcoholysis (using methanol and ethanol) and hydrolysis, *i.e.* different types of solvolysis, of DACs. For the alcoholysis of DACs, the overall chemical equilibrium constants ($K_{eq,overall}$) were theoretically determined and found to favour product formation at STP. For the methanolysis of DPC and DGC, $K_{eq,overall}$ values were $4\ 10^{13}$ and $3\ 10^{7}$, while ethanolysis gave values of $2\ 10^{8}$ and 10^{2}, respectively. Although both types of alcoholysis reactions were exothermic and thermodynamic spontaneous, still, from a thermodynamic point of view, methanolysis is more suitable as a chemical recycling method for DACs than ethanolysis. With regard to the substrate, the respective $K_{eq,overall}$ values for methanolysis of DPC and DGC were higher for DPC than DGC, indicating the thermodynamic equilibrium lay further to the right (*i.e.* in favour of product formation) for DPC than DGC. Despite this significant difference, $K_{eq,overall}$ for methanolysis of DGC was high and strongly favoured product formation. Nevertheless, this also implicated that formation of DGC from dimethyl carbonate (DMC) and guaiacol will be thermodynamically more attractive than DPC formation using DMC and phenol. The thermodynamic difference between DPC and DGC methanolysis was attributed to the presence of the additional *o*-methoxy functionality. The electron-donating properties of the *o*-methoxy group – acting as an *ortho-para* director – presumably facilitates the backward reaction by increasing the nucleophilicity in guaiacol and so stabilising the transesterification of guaiacol with DMC.

During hydrolysis, unlike for alcoholysis, only one transesterification-like reaction takes. DACs are hydrolytically cleaved to a hydrogen aryl carbonate and a phenolic compound. Afterwards, the hydrogen aryl carbonate decomposes into CO_2 and a second phenolic compound. The hydrolytic cleavage of DPC and DGC is significantly different in terms of thermodynamics. The hydrolytic cleavage of DPC is thermodynamically favoured with a K_{eq} of 26, while the cleavage of DGC is rather unfavourable with a K_{eq} of 0.02. The hydrogen aryl carbonate was thermodynamically unstable, resulting in respective K_{eq}values of $5\ 10^{20}$ and $4\ 10^{17}$ for DPC and

DGC. Therefore, the overall DPC and DGC hydrolyse were found to be thermodynamically spontaneous, resulting mainly from the instability of the hydrogen aryl carbonate, and the rapid release of stable gaseous CO_2.

After the initial theoretical validation, the reactivity of the DACs was verified in experimental practice. Not only was methanolysis chosen to favour product formation, as instigated by the thermodynamics, but also because it yielded DMC, which could serve as an industrially important non-phosgene alternative. Initially, the methanolysis of DACs was performed without catalyst addition for 4 h at 40 and 60 °C, which led to about 5 mol% conversion, indicating that the methanolysis of DACs is obstructed by a high activation energy (E_a).

Catalysis was employed to counter this energetic barrier and accelerate the reaction rate. A preliminary catalyst screening – using alkali hydroxides and organocatalysts – was executed to determine the most active catalyst(s). The screening concluded that NaOH and TBD (1,5,7-triazabicyclo[4.4.0]-dec-5-ene) were the most active catalysts for methanolysis of DACs. In addition, this experiment confirmed that DPC is indeed more reactive than DGC.

Next, a kinetic study was performed to investigate the difference in reactivity between DPC and DGC. In these kinetic experiments, NaOH was used as the catalyst (1 and 2 mol% for DPC and DGC, respectively). The difference in reactivity was quantified by determining the (apparent) overall reaction rate constants (k) and E_a's for DAC methanolysis. Based on k, the methanolysis of DPC proceeded five to six times faster than DGC at the respective catalyst concentrations. Furthermore, it was found that the second transesterification is the rate determining step (RDS); k_1 was 15 to 20 times higher than k_2. These observations were confirmed by the differences in activation energy between the first ($E_{a,1}$) and second ($E_{a,2}$) methanolysis step. Namely, $E_{a,1}$ amounted to 4.4 and 23.6 kJ mol^{-1} and $E_{a,2}$ to 17.5 and 36.6 kJ mol^{-1} for DPC and DGC, respectively. This reactivity difference between DPC and DGC was explained by an electronic and steric effect. Regarding electronics, the more electrophilic phenolate anion presumably is a better leaving group in transesterification than guaiacolate anions, and hence the reactivity of DPC towards methanolysis is higher. In terms of stericity, the nucleophilic attack of the methoxide anion on the tetrahedral carbonate carbon might be more sterically hindered due to the *o*-methoxy substituents in DGC and hence leads to a lower reactivity of DGC towards methanolysis.

Despite the lower reactivity of DGC than DPC, full conversion of DGC into DMC and guaiacol was achieved – as predicted by the thermodynamics – under more severe reaction conditions with either NaOH and/or TBD. To compare the activity of both catalysts, first, the kinetics (*i.e.* k and E_a values) of the TBD-catalysed methanolysis of DGC were determined. A significant difference was observed between $k_{2,NaOH}$ and $k_{2,TBD}$. Compared to NaOH, the second transesterification proceeded 17 to 23 times faster when catalysed by TBD. The second (TBD-catalysed) transesterification remained the RDS, here, the difference in reaction rate and activation energy is far less pronounced than for the NaOH-catalysed reaction. Namely, $E_{a,1}$ amounted to 10.8 and 19.3 kJ mol^{-1}, and $E_{a,2}$ to 23.6 and 36.6 kJ mol^{-1} for TBD- and NaOH-catalysed methanolysis of DGC, respectively. In contrast to NaOH, the intermediate – methyl guaiacyl carbonate (MGC) – was only formed in low concentrations with TBD, which makes TBD a desirable chemical recycling catalyst. Unfortunately, whereas NaOH-catalysed methanolysis of DGC achieved full conversion, TBD-catalysed methanolysis stagnated, after being initially faster, resulting in 77 mol% conversion after 8 h at 60 °C with a catalyst loading of 2 mol%. This typical reaction progress (*i.e.* initial fast conversion followed by stagnation) was explained by TBD's mechanism of action. Upon transesterification, TBD's guanidine functionality acts both as an electron donor and electron acceptor, thereby increasing the reagents' nucleophilicity and/or electrophilicity, and stabilising the intermediates, which leads to an increased initial reaction rate. However, at higher conversion, and hence higher DMC yields, the probability that TBD associates with DMC rather than with DGC increases, leading to a stagnation of the conversion due to catalyst deactivation (by the product).

To further corroborate this hypothesis, as a final experiment, the TBD-catalysed methanolysis of DGC was performed at higher catalyst loading to circumvent catalyst deactivation. Indeed, at 60 °C and 5 mol% instead of 2 mol% TBD, full DGC conversion was obtained after 30 min, and quantitative DMC yield was reached after 4 h.

In Summary, methanolysis of DGC, as a model component for bisguaiacol-PCs, is thermodynamically favoured and can be executed at mild reaction conditions using the organocatalyst TBD and NaOH. These findings highlight the ability of bisguaiacol-PCs to undergo chemical recycling.

8. Future perspectives

To put the research of this MSc thesis in perspective, Figure 8.1 illustrates the bigger picture of a bio-based circular PC economy. As an initial entry, the methanolysis of DGC (Fig. 8.1B) was studied as a model reaction for the chemical recycling of bisguaiacol-PCs – this master thesis. DGC, as component of interest, was benchmarked against DPC throughout the research. In theory, the thermodynamics indicated that the methanolysis of DGC is exergonic (spontaneous), exothermic and favourable in the forward direction, which favours the depolymerisation of DGC into DMC. In practice, this was confirmed by the quantitative NaOH- and TBD-catalysed methanolysis of DGC into DMC at 60 °C after 4 and 8 h, respectively. Due to the principle of microscopic reversibility, the thermodynamics of the reverse transesterification of DMC with guaiacol into DGC and MeOH are also know (Fig. 8.1A).

By extension, Figure 8.1 also clearly demonstrates the possible course of the research in the near future and long term. In the short term, a next alluring step might be to apply the optimal conditions of this MSc thesis on actual polymeric bisguaiacol-PCs (Fig. 8.1D). Furthermore, research could aim at the optimisation of the process set-up, for instance, by replacing the co-solvent – 2-MeTHF – with DMC, thereby reducing the complexity and cost of the post-recycling process. Finally, in order to close the circular PC economy, future research might investigate the melt-transesterification reaction of DMC with guaiacol to directly DGC and subsequently bisguaiacol-PCs (Fig 7.1A and C). In the long term, in a similar fashion, the substrate scope could be expanded from bisguaiacols to bissyringols.

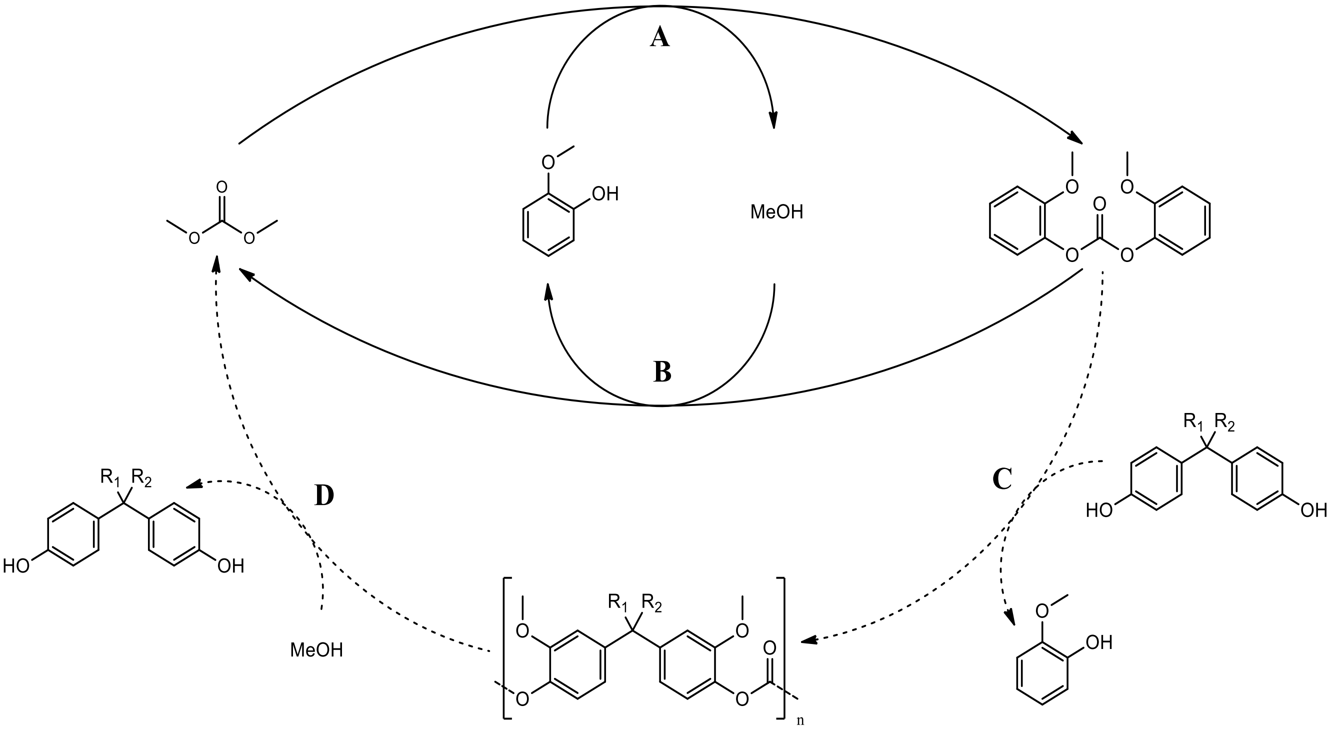

Figure 8.1 General overview of the envisioned bio-based circular PC economy with indication of current and future research stages; (**A**) Transesterification of DMC) with guaiacol into DGC and MeOH; (**B**) Methanolysis of DGC into DMC and guaiacol; (**C**) Melt-transesterification of DGC and bisguaiacol towards bisguaiacol-PC; (**D**) Methanolysis of bisguaiacol-PC into DMC and bisguaiacol. Full arrows: reactions research of current MSc thesis. Dashed arrows: possible future research.

References

1. Elias, H.-G. & Mülhaupt, R. Plastics, General Survey, 1. Definition, Molecular Structure and Properties. in *Ullmann's Encyclopedia of Industrial Chemistry* 1–70 (2015).
2. PlasticsEurope. *Plastics - the fact 2017: An analysis of European plastics production, demand and waste data*. *PlasticsEurope* (2017).
3. Ellen MacArthur Foundation. *The new plastics economy - Rethinking the future of plastics and catalysing action*. (2017).
4. Wittcoff, H. A., Reuben, B. G. & Plotkin, J. S. Chemicals and Polymers from Benzene. in *Industrial Organic Chemicals* 267–311 (John Wiley & Sons, Inc., 2004).
5. Industry Experts. Bisphenol-A – A Global Market Overview. Available at: http://industry-experts.com/verticals/chemicals-and-materials/bisphenol-a-a-global-market-overview. (Accessed: 6th October 2018)
6. PlasticsEurope. *Production and demand volumes*. (2017).
7. Markit, I. Bisphenol A. *Chemical economics handbook* (2016). Available at: https://ihsmarkit.com/products/bisphenol-chemical-economics-handbook.html. (Accessed: 6th October 2018)
8. ICIS. Chemical profile: Bisphenol A. (2008). Available at: https://www.icis.com/resources/news/2008/10/13/9162868/chemical-profile-bisphenol-a/. (Accessed: 10th October 2018)
9. Bisphenol A Europe. Bisphenol sustainability. (2017). Available at: http://bisphenol-a-europe.org/sustainability/. (Accessed: 10th October 2018)
10. PlasticsEurope. Eco-profiles flowchart. (2018). Available at: https://www.plasticseurope.org/en/resources/eco-profiles.
11. Zakoshansky, V. M. The Cumene Process for Phenol—Acetone Production. *Pet. Chem.* **47**, 307–307 (2007).
12. Coker, A. *Phenol, Acetone, Cumene*. (2012).
13. Weissermel, K. & Arpe, H.-J. *Industrial Organic Chemistry*. (VCH Publishers, Inc., 1993).

14. Harmer, M. A. & Sun, Q. Solid acid catalysis using ion-exchange resins. *Appl. Catal. A Gen.* 45–62 (2001).

15. Pressman, E. J., Johnson, B. F. & Shafer, S. J. Monomers for Polycarbonate Manufacture : Synthesis of BPA and DPC. in *Advances in Polycarbonates* (eds. Brunelle, D. J. & Korn, M. R.) 22–38 (American Chemical Society, 2005).

16. Sabu, T. & Visakh, P. M. *Handbook of Engineering and Speciality Thermoplastics*. (John Wiley & Sons, Inc., 2011).

17. Van De Vyver, S. *et al.* Mechanistic insights into the kinetic and regiochemical control of the thiol-promoted catalytic synthesis of diphenolic acid. *ACS Catal.* **2**, 2700–2704 (2012).

18. Zeidan, R. K., Dufaud, V. & Davis, M. E. Enhanced cooperative, catalytic behavior of organic functional groups by immobilization. *J. Catal.* **239**, 299–306 (2006).

19. Database, H. M. Showing metabocard for Bisphenol A (HMDB0032133). (2015).

20. Cousins, I. T., Staples, C. A., Klečka, G. M. & Mackay, D. A multimedia assessment of the environmental fate of bisphenol A. *Hum. Ecol. Risk Assess.* **8**, 1107–1135 (2002).

21. Corrales, J. *et al.* Global Assessment of Bisphenol A in the Environment: Review and Analysis of Its Occurrence and Bioaccumulation. *Dose-respons An Int. J.* (2015).

22. Agency, U. S. E. P. Estimation Programs Interface Suite. (2018).

23. vom Saal, F. S. *et al.* Chapel Hill bisphenol A expert panel consensus statement: Integration of mechanisms, effects in animals and potential to impact human health at current levels of exposure. *Reproductive Toxicology* **24**, 131–138 (2007).

24. Schug, T. T. *et al.* Designing endocrine disruption out of the next generation of chemicals. *Green Chem.* **15**, 181–198 (2013).

25. Dodds, E. C. & Lawson, W. Synthetic Oestrogenic Agents without the Phenanthrene Nucleus. *Nature* (1936).

26. Colborn, T, Clement, C. Chemically-Induced Alterations in Sexual and Functional Development: The Wildlife/Human Connection. *Adv. Mod. Environemental Toxicol.* **21**, 403 (1992).

27. Kitamura, S. *et al.* Comparative study of the endocrine-disrupting activity of bisphenol

A and 19 related compounds. *Toxicol. Sci.* **84**, 249–259 (2005).

28. Vandenberg, L. N., Maffini, M. V, Sonnenschein, C., Rubin, B. S. & Soto, A. M. Bisphenol-A and the Great Divide: A Review of Controversies in the Field of Endocrine Disruption. *Endocr. Rev.* **30**, 75–95 (2009).

29. Rochester, J. R. Bisphenol A and human health: A review of the literature. *Reprod. Toxicol.* **42**, 132–155 (2013).

30. American Chemistry Council. *About BPA*. (2016).

31. Program, N. T. *The CLARITY-BPA Core Study: A Perinatal and Chronic Extended-Dose-Range Study of Bisphenol A in Rats*. *NTP RR 9* (2018).

32. Meeting, F. E. *Toxicological and Health Aspects of Bisphenol A*. (2010).

33. FDA. Questions & Answers on Bisphenol A (BPA) Use in Food Contact Applications. (2018).

34. Vandenberg, L. N., Hauser, R., Marcus, M., Olea, N. & Welshons, W. V. Human exposure to bisphenol A (BPA). *Reprod. Toxicol.* **24**, 139–177 (2007).

35. European Chemicals Agency. MSC unanimously agrees that Bisphenol A is an endocrine disruptor - All news - ECHA. (2017). Available at: https://echa.europa.eu/-/msc-unanimously-agrees-that-bisphenol-a-is-an-endocrine-disruptor. (Accessed: 21st November 2018)

36. Metz, C. M. Bisphenol A: Understanding the Controversy. *Work. Heal. Saf.* **64**, 28–36 (2016).

37. Vandenberg, L. N. Non-monotonic dose responses in studies of endocrine disrupting chemicals: Bisphenol a as a case study. *Dose-Response* **12**, 259–276 (2014).

38. Government of Canada. Bisphenol A. (2018). Available at: https://www.canada.ca/en/health-canada/services/food-nutrition/food-safety/packaging-materials/bisphenol.html. (Accessed: 21st November 2018)

39. European Parliamentary Research Service. *At a glance New rules on bisphenol A in food contact materials*. (2018).

40. Chen, D. *et al.* Bisphenol Analogues Other Than BPA: Environmental Occurrence, Human Exposure, and Toxicity-A Review. *Environ. Sci. Technol.* **50**, 5438–5453 (2016).

41. Usman, A. & Ahmad, M. From BPA to its analogues: Is it a safe journey? *Chemosphere* **158**, 131–142 (2016).

42. Wittcoff, H. A., Reuben, B. G. & Plotkin, J. S. *Industrial Organic Chemicals*. (John Wiley & Sons, Inc., 2004).

43. Kyriacos, D. Polycarbonates. in *Brydson's Plastics Materials: Eighth Edition* 457–485 (Elsevier Ltd, 2016).

44. Fukuoka, S., Tojo, M., Hachiya, H., Aminaka, M. & Hasegawa, K. Green and Sustainable Chemistry in Practice: Development and Industrialization of a Novel Process for Polycarbonate Production from CO2 without Using Phosgene. *Polym. J.* **39**, 91–114 (2007).

45. Harracksingh, R. *Polycarbonate*. (2012).

46. Pacheco, M. A. & Marshall, C. L. Review of dimethyl carbonate (DMC) manufacture and its characteristics as a fuel additive. *Energy and Fuels* **11**, 2–29 (1997).

47. Abts, G., Eckel, T. & Wehrmann, R. Polycarbonates. in *Ullmann's Encyclopedia of Industrial Chemistry* (2016).

48. Ashby, M. F. *Materials and the Environment*. (Elsevier, 2013).

49. Pham, H. Q. & Marks, M. J. Epoxy Resins. in *Ullmann's Encyclopedia of Industrial Chemistry* 155–244 (Wiley-VCH, 2012).

50. Paluvai, N. R., Mohanty, S. & Nayak, S. K. Synthesis and Modifications of Epoxy Resins and Their Composites: A Review. *Polymer - Plastics Technology and Engineering* **53**, 1723–1758 (2014).

51. Staples, C. a, Dom, P. B., Klecka, G. M., Sandra, T. O. & Harris, L. R. A review of the environmental fate, effects, and exposures of Bisphenol A. *Chemosphere* **36**, 2149–2173 (1998).

52. Sajiki, J. & Yonekubo, J. Leaching of bisphenol A (BPA) to seawater from polycarbonate plastic and its degradation by reactive oxygen species. *Chemosphere* **51**, 55–62 (2003).

53. Geens, T. *et al.* A review of dietary and non-dietary exposure to bisphenol-A. *Food an Chem. Toxicol.* **50**, 3725–3740 (2012).

54. Hoekstra, E. J. & Simoneau, C. Release of Bisphenol A from Polycarbonate-A Review. *Crit. Rev. Food Sci. Nutr.* **53**, 386–402 (2011).

55. Van Landuyt, K. L. *et al.* How much do resin-based dental materials release? A meta-analytical approach. *Dent. Mater.* 723–747 (2011).

56. Stahel, W. R. Circular economy. *Nature* **531**, 435–438 (2016).

57. PlasticsEurope. *Plastics - the Facts 2018; An analysis of European plastics production, demand and waste data*. (2018).

58. Geyer, R., Jambeck, J. R. & Law, K. L. Production, uses, and fate of all plastics ever made. *Sci. Adv.* **3**, 5 (2017).

59. World Bank. What a Waste 2.0. (2018).

60. US EPA. Plastics: Material-Specific Data. Available at: https://www.epa.gov/facts-and-figures-about-materials-waste-and-recycling/plastics-material-specific-data. (Accessed: 2nd November 2018)

61. Singh, N. *et al.* Recycling of plastic solid waste: A state of art review and future applications. *Compos. Part B Eng.* **115**, 409–422 (2017).

62. Ritchie, H. & Roser, M. Plastic Pollution. *Ourworldindata.org* (2018). Available at: https://ourworldindata.org/plastic-pollution#empirical-view.

63. Ilyas, M. *et al.* Plastic waste as a significant threat to environment - A systematic literature review. *Reviews on Environmental Health* (2018).

64. Goel Editor, S. *Advances in Solid and Hazardous Waste Management*. (2017).

65. Zhu, Y., Romain, C. & Williams, C. K. Sustainable polymers from renewable resources. *Nature* **540**, 354–362 (2016).

66. Ellen MacArthur Foundation. *The New Plastics Economy: Rethinking the future of plastics*. *Ellen MacArthur Foundation* (2016).

67. North, E. J. & Halden, R. U. Plastics and environmental health: The road ahead. *Rev. Environ. Health* **28**, 1–8 (2013).

68. Goodship, V. *Introduction to plastics recycling*. **40**, (Smithers Rapra, 2007).

69. Hopewell, J., Dvorak, R. & Kosior, E. Plastics recycling: challenges and opportunities.

Philos. Trans. R. Soc. B Biol. Sci. **364**, 2115–2126 (2009).

70. Shen, L. & Worrell, E. Plastic recycling. in *Handbook of Recycling: State-of-the-art for Practitioners, Analysts, and Scientists* 179–190 (Elsevier, 2014).

71. Ignatyev, I. A., Thielemans, W. & Vander Beke, B. Recycling of Polymers: A Review. *ChemSusChem* **7**, 1579–1593 (2014).

72. Ragaert, K., Delva, L. & Van Geem, K. Mechanical and chemical recycling of solid plastic waste. *Waste Management* **69**, 24–58 (2017).

73. Aguado, J. & Serrano, D. P. *Feedstock recycling of plastic waste*. (Royal Society of Chemistry, 1999).

74. Antonakou, E. V & Achilias, • D S. Recent Advances in Polycarbonate Recycling: A Review of Degradation Methods and Their Mechanisms. *Waste and Biomass Valorization* **4**, 9–21 (2013).

75. Lange, J. P. Sustainable development: Efficiency and recycling in chemicals manufacturing. *Green Chem.* **4**, 546–550 (2002).

76. Lange, J. P. Resource Efficiency of Chemical Manufacturing Chains: Present and Future. in *Sustainable Development in the Process Industries: Cases and Impact* 23–37 (Wiley, 2010).

77. Leonard, J. Heats and Entropies of Polymerization, Ceiling Temperatures, Equilibrium Monomer Concentrations and Polymerizability of Heterocyclic Compounds. in *Polymer Handbook* (eds. Brandrup, J., Immergut, E. H. & Grulke, E. A.) 365–403 (John Wiley & Sons, Inc., 1999).

78. Welle, F. *The Facts about PET The interaction of PET with food and water*.

79. Karmenu Vella. Plastics in a circular economy: the European approach. *Government of Europa* (2019). Available at: https://www.governmenteuropa.eu/plastics-in-a-circular-economy/91767/. (Accessed: 27th March 2019)

80. Jim Curtis, T. C.-C. C. Chemical Recycling: Could This Breakthrough Technology Curb Plastic Waste?: The Coca-Cola Company. (2019). Available at: https://www.coca-colacompany.com/stories/chemical-recycling-could-this-breakthrough-technology-curb-plastic-waste. (Accessed: 27th March 2019)

81. De Tijd. Indaver’s solution for 1 million tonnes of end-of-life plastics. *De Tijd* (2018). Available at: https://www.indaver.com/uk-en/media-and-downloads/news-detail/indavers-solution-for-1-million-tonnes-of-end-of-life-plastics/. (Accessed: 27th March 2019)

82. Laermann, M. Chemical recycling of plastic: Waste no more? – EURACTIV.com. *www.euractiv.com* (2019). Available at: https://www.euractiv.com/section/energy-environment/opinion/chemical-recycling-of-plastic-waste-no-more/. (Accessed: 27th March 2019)

83. European Bioplastics. *European Bioplastics Fact Sheet*. (2016).

84. European Bioplastics. *Biobased plastics – Fostering a resource efficient circular economy*. (2012).

85. Hillmyer, M. A. The promise of plastics from plants. *Science* **358**, 868–870 (2017).

86. Nova Institut GmhB *et al. Market study on Bio-based Polymers in the World Capacities , Production and Applications : Status Quo and Trends towards 2020*. (2013).

87. Tagaya, H., Katoh, K., Kadokawa, J. I. & Chiba, K. Decomposition of polycarbonate in subcritical and supercritical water. *Polym. Degrad. Stab.* **64**, 289–292 (1999).

88. Watanabe, M. *et al.* Chemical recycling of polycarbonate in high pressure high temperature steam at 573 K. *Polym. Degrad. Stab.* **94**, 2157–2162 (2009).

89. Piñero, R., García, J. & Cocero, M. J. Chemical recycling of polycarbonate in a semi-continuous lab-plant. A green route with methanol and methanol-water mixtures. in *Green Chemistry* **7**, 380–387 (2005).

90. Liu, F., Li, Z., Yu, S., Cui, X. & Ge, X. Environmentally benign methanolysis of polycarbonate to recover bisphenol A and dimethyl carbonate in ionic liquids. *J. Hazard. Mater.* **174**, 872–875 (2010).

91. Liu, M., Guo, J., Gu, Y., Gao, J. & Liu, F. Versatile Imidazole-Anion-Derived Ionic Liquids with Unparalleled Activity for Alcoholysis of Polyester Wastes under Mild and Green Conditions. *ACS Sustain. Chem. Eng.* **6**, 15127–15134 (2018).

92. Hu, L. C., Oku, A. & Yamada, E. Alkali-catalyzed methanolysis of polycarbonate. A study on recycling of bisphenol A and dimethyl carbonate. *Polymer (Guildf).* **39**, 3841–

3845 (1998).

93. Liu, F.-S. *et al.* Methanolysis and Hydrolysis of Polycarbonate Under Moderate Conditions. (2009). doi:10.1007/s10924-009-0140-0

94. Jehanno, C., Pérez-Madrigal, M. M., Demarteau, J., Sardon, H. & Dove, A. P. Organocatalysis for depolymerisation. *Polym. Chem.* **10**, 172–186 (2019).

95. Quaranta, E., Sgherza, D. & Tartaro, G. Depolymerization of poly(bisphenol A carbonate) under mild conditions by solvent-free alcoholysis catalyzed by 1,8-diazabicyclo[5.4.0]undec-7-ene as a recyclable organocatalyst: a route to chemical recycling of waste polycarbonate. *Green Chem.* **19**, 5422 (2017).

96. Do, T., Baral, E. R. & Kim, J. G. Chemical recycling of poly(bisphenol A carbonate): 1,5,7-Triazabicyclo[4.4.0]-dec-5-ene catalyzed alcoholysis for highly efficient bisphenol A and organic carbonate recovery. *Polymer (Guildf).* **143**, 106–114 (2018).

97. Do, T., Baral, E. R. & Kim, J. G. Chemical recycling of poly(bisphenol A carbonate): 1,5,7-Triazabicyclo[4.4.0]-dec-5-ene catalyzed alcoholysis for highly efficient bisphenol A and organic carbonate recovery. *Polymer (Guildf).* **143**, 106–114 (2018).

98. Calvo-Flores, F. G. & Dobado, J. A. Lignin as renewable raw material. *ChemSusChem* **3**, 1227–1235 (2010).

99. Schutyser, W. *et al.* Chemicals from lignin: An interplay of lignocellulose fractionation, depolymerisation, and upgrading. *Chem. Soc. Rev.* **47**, 852–908 (2018).

100. Cheng, H. *et al.* Theoretical study of bond dissociation energies for lignin model compounds. *J. Fuel Chem. Technol.* **43**, 429–436 (2015).

101. Zakzeski, J., Bruijnincx, P. C. A., Jongerius, A. L. & Weckhuysen, B. M. The catalytic valorization of lignin for the production of renewable chemicals. *Chem. Rev.* **110**, 3552–3599 (2010).

102. Renders, T., Van Den Bosch, S., Koelewijn, S. F., Schutyser, W. & Sels, B. F. Lignin-first biomass fractionation: The advent of active stabilisation strategies. *Energy and Environmental Science* **10**, 1551–1557 (2017).

103. Harvey, B. G. *et al.* A high-performance renewable thermosetting resin derived from eugenol. *ChemSusChem* **7**, 1964–1969 (2014).

104. Meylemans, H. A., Groshens, T. J. & Harvey, B. G. Synthesis of renewable bisphenols from creosol. *ChemSusChem* **5**, 206–210 (2012).

105. Koelewijn, S.-F. *et al.* Sustainable bisphenols from renewable softwood lignin feedstock for polycarbonates and cyanate ester resins. *Green Chem.* **19**, 2561 (2017).

106. Koelewijn, S.-F. *et al.* Promising bulk production of a potentially benign bisphenol A replacement from a hardwood lignin platform †. *Green Chem.* **20**, (2018).

107. Periyasamy, T., Asrafali, S. P., Muthusamy, S. & Kim, S.-C. Replacing bisphenol-A with bisguaiacol-F to synthesize polybenzoxazines for a pollution-free environment †. *New J. Chem* **40**, 9313 (2016).

108. Hernandez, E. D., Bassett, A. W., Sadler, J. M., La Scala, J. J. & Stanzione, J. F. Synthesis and Characterization of Bio-based Epoxy Resins Derived from Vanillyl Alcohol. *ACS Sustain. Chem. Eng.* **4**, 4328–4339 (2016).

109. Hong, H. *et al.* Experimental data extraction and in silico prediction of the estrogenic activity of renewable replacements for bisphenol A. *Int. J. Environ. Res. Public Health* **13**, 705 (2016).

110. Alexander, K. A., Paulhus, E. A., Lazarus, G. M. L. & Leadbeater, N. E. Exploring the reactivity of a ruthenium complex in the metathesis of biorenewable feedstocks to generate value-added chemicals. *J. Organomet. Chem.* **812**, 74–80 (2015).

111. Joback, K. G. & Reid, R. C. Estimation of Pure-Component Properties from Group-Contributions. *Chem. Eng. Commun.* **57**, 233–243 (1987).

112. Otera, J. Transesterification. *Chem. Rev.* **93**, 1449–1470 (1993).

113. Poling, B. E., Prausnitz, J. M. & O’Connell, J. P. *The Properties of Gases and Liquids*. (2001).

114. Marrero, J. & Gani, R. Group-contribution based estimation of pure component properties. *Fluid Phase Equilib.* **183–184**, 183–208 (2001).

115. Zhu, D.-J., Xie, Y.-H., Mei, F.-M., Wang, H.-W. & Li, G.-X. Measurement of standard molar combustion enthalpy of methyl phenyl carbonate. *Huaxue Gongcheng/Chemical Eng.* **35**, (2007).

116. Shen, C., Li, W. & Zhou, C. Investigation on molar heat capacity , standard molar

enthalpy of combustion for guaiacol and acetyl guaiacol ester. *Chinese J. Chem. Eng.* **24**, 1772–1778 (2016).

117. Rivetti, F. The role of dimethylcarbonate in the replacement of hazardous chemicals. *Comptes Rendus l'Academie des Sci. - Ser. IIc Chem.* **3**, 497–503 (2000).

118. Haubrock, J. *et al.* Reaction from Dimethyl Carbonate to Diphenyl Carvonate. 1. Experimental Determination of the Chemical Equilibria. *Ind. Eng. Chem. Res.* **47**, 9854–9861 (2008).

119. Sun, W., Shao, J., Xi, Z. & Zhao, L. Thermodynamics and kinetics of transesterification reactions to produce diphenyl carbonate from dimethyl carbonate catalyzed by tetrabutyl titanate and dibutyltin oxide. *Can. J. Chem. Eng.* **95**, 353–358 (2017).

120. Eastman, H. E., Jamieson, C. & Watson, A. J. *Greener Solvent Alternatives*. *Sigma-Aldrich* **48**, (2015).

121. Rocha, J. G. *et al.* Biodiesel synthesis: Influence of alkaline catalysts in methanol-oil dispersion. *J. Braz. Chem. Soc.* **30**, 342–349 (2019).

122. Ragnar, M. & Lindgren, C. T. pKa -Values of Guaiacyl and Syringyl Phenols Related to Lignin. *J. Wood Chem. Technol.* **20**, 277–305 (2000).

123. Vallance, C. *An Introduction to Chemical Kinetics*. (Morgan & Claypool Publishers, 2017).

124. Horn, H. W. *et al.* Mechanisms of organocatalytic amidation and trans-esterification of aromatic esters as a model for the depolymerization of poly(ethylene) terephthalate. *J. Phys. Chem. A* **116**, 12389–12398 (2012).

Appendix A: List of chemicals

Chemical	**CAS-number**	**Vendor**	**Purity**
1,4-diazabicyclo[2.2.2]octane	280-57-9	Sigma Aldrich	98%
1,5,7-triazabicyclo[4.4.0]dec-5-ene	5807-14-7	Fluka Chemika	>= 98%
1,8-diazabicyclo[5.4.0]undec-7-ene	6674-22-2	Sigma Aldrich	98%
1-methylimidazole	616-47-7	Sigma Aldrich	99%
2-methyl-tetrahydrofuran	96-47-9	Sigma Aldrich	>= 99%
4-dimethylaminopyridine	1122-58-3	Sigma Aldrich	98%
Acetonitrile	75-05-8	Fisher scientific	99,99%
Diethyl carbonate	105-58-8	Acros Organics	99%
Diguaiacyl carbonate	553-17-3	Tokyo Chemical Industry	>98,0%
Dimethyl carbonate	616-38-6	Acros Organics	99+%
Diphenyl carbonate	102-09-0	Sigma Aldrich	99%
Ethanol	64-17-5	Fisher scientific	Absolute
Guaiacol	90-05-1	Acros Organics	99+%
Methanol	67-56-1	Acros Organics	99,9%
Methyl phenyl carbonate	13509-27-8	Alfa Aesar	97%
N,*N*-dimethylaniline	121-69-7	Acros Organics	99%
n-heptane	142-82-5	Acros Organics	99+%
Phenol	108-95-2	Acros Organics	99,5%
Phosphoric acid	7664-38-2	Acros Organics	85 wt%
Potassium hydroxide	1310-58-3	Acros Organics	99,98%
Sodium hydroxide	1310-73-2	Fisher scientific	>= 97%
Tetrahydrofuran	109-99-9	Acros Organics	99,5%
Toluene	108-88-3	Acros Organics	99,5%

Appendix B: Risk Assessment

UNIVERSITY ADMINISTRATION AND CENTRAL SERVICES
UNIVERSITY ADMINISTRATION AND CENTRAL SERVICES POLICY DEPARTMENT
HSE DEPARTMENT
W. DE CROYLAAN 58, BOX 5530
3001 LEUVEN, BELGIUM

RISK ASSESSMENT FOR AN EXPERIMENT WITH CHEMICAL PRODUCTS OF RISK CLASS E3 AND E4 AND NANOPARTICLES

Complete this form electronically, in consultation with your HSE contact for Chemical Safety (CS)[1].

1. Identification of the unit (users)

Requester/contact: Laura Trullemans
Tel: +3216376272
Email address: laura.trullemans@kuleuven.be

Division: M2S-COK-UNIT 2
Stockroom code[2]: 730
Executive[3]: Prof. Bert Sels
Promotor: Prof. Bert Sels

Persons who will be conducting the experiment (only applicable in case of *new* risk assessment):

Last name - First name:	**u-/s-number/...:**	**Staff group:**
Trullemans Laura	**r0118626**	☒ KU ☐ Student KU ☐ UZ ☐ VIB ☐ Externals:
Koelewijn Steven-Friso	**u0091661**	☒ KU ☐ Student KU ☐ UZ ☐ VIB ☐ Externals:
Vermeeren Benjamin	**r0710450**	☐ KU ☒ Student KU ☐ UZ ☐ VIB ☐ Externals:
		☐ KU ☐ Student KU ☐ UZ ☐ VIB ☐ Externals:
		☐ KU ☐ Student KU ☐ UZ ☐ VIB ☐ Externals:
		☐ KU ☐ Student KU ☐ UZ ☐ VIB ☐ Externals:
		☐ KU ☐ Student KU ☐ UZ ☐ VIB ☐ Externals:
		☐ KU ☐ Student KU ☐ UZ ☐ VIB ☐ Externals:

2. Identification of the experiment

2.1. **Title** (name) (max. 40 characters): Solvolytic cleavage of carbonate linkage

2.2. **This risk assessment concerns:**

☒ a new experiment,
☐ an existing experiment without previously submitted notification,
☐ a modification/extension of an existing experiment with previously submitted notification,

- This modification/extension concerns (please indicate and describe further down in this form):
  - ☐ locations where the experiment will be taking place
  - ☐ agents
  - ☐ extension
  - ☐ other risks (brief description):
- File number or reference number of previously submitted notification (if known): ☐

☐ the termination of the experiment with file number ☐

2.3. **Activities for the HSE file** *(in consultation with your HSE network coordinator and Promotor/Executive*[3]*)***:**

☐ *Existing* activity: Enter the number of the activity, as shown in KU Loket*:*
☒ *New* activity for the HSE file: Enter a name for the activity *(max. 40 characters): 492_31-02_176_ZK4#CarboCleave*

2.4. **Desired startup date: 01/09/2018** **Scheduled end date: 07/05/2019**

---

[1] *You can find the members of your local HSE network through KU Loket > HSE & Spaces > My HSE > My HSE network*
[2] *If you don't know the stockroom code, please consult your HSE contact*
[3] *This is the hierarchical responsible according to the official organizational chart.*

3. Identification of the agents:

3.1. Description of all applied (or developed) chemical agents:

Where possible, please replace hazardous agents or processes with less hazardous alternatives.

Product name	CAS-number	Physical state at the start	Nano-material* (< 100 nm)	Applied quantity	Applied concentration	Chemical risk class
1. MeOH	67-56-1	Liquid	No	1 g/ml	99 %	E4
2. Dimethyl carbonate	616-38-6	Liquid	No	0.1 g/ml	99 %	E1
3. 2-methyl-tetrahydrofuran	96-47-9	Liquid	No	1 g/ml	99 %	E3
4. Toluene	108-88-3	Liquid	No	0.05 g/ml	99 %	E2
5. Phenol	108-95-2	Solid	No	0.1 g/ml	99 %	E3
6. Guaiacol	90-05-1	Solid	No	0.1 g/ml	99 %	E1
7. Diphenyl carbonate	102-09-0	Solid	No	0.1 g/ml	99 %	E1
8. Guaiacyl carbonate	553-17-3	Solid	No	0.1 g/ml	98 %	E1
9. NaOH	1310-3-2	Solid	No	0.2-2 g/ml	99 %	E3
10. organic N-bases: TBD, DBU, DMAP, DABCO, NMI, DMA	5807-14-7 6674-22-2 1122-58-3 280-57-9 616-47-7 121-69-7	Solid	No	0.001 g/ml	98-99 %	E3

(*) The nanomaterial is produced for a third party: No

3.2. Hazards associated with the application of chemical agents:

*Indicate the hazards for all products of risk classes **E3** and **E4**.*

Ensure that the H- and R-phrases are known when using chemicals. These can be found in the KU Leuven database of hazardous substances ([via KU Loket > General > Hazardous materials)]() or in the manufacturer's safety data sheets.

	Name of chemical:					
	Phenol	*MeOH*	*2-methyl-THF*	*NaOH*	*TBD, DBU, NMI*	*DMAP and DMA*
Explosion and fire hazard:						
Extremely or highly flammable (**H220**, **H222**, **H224**, H225)	☐	☒	☒	☐	☐	☐
Flammable gas, aerosol, solid (H221, H223**, H228**)	☐	☐	☐	☐	☐	☐
Flammable due to self-heating **(H251, H252)**	☐	☐	☐	☐	☐	☐
Fire, explosive with projection hazard (H204, **H202**, **H203**),	☐	☐	☐	☐	☐	☐

mass explosion in fire (H205)						
Explosive (**EUH001, EUH006, H200, H201**) + Oxidizing substances (H271, H272) / (R9, R16), Heating may cause explosion (H240, H241), Heating under confinement may cause explosion (EUH044)	☐	☒	☐	☐	☐	☐
Flammable vapor-air mixture (EUH018)	☐	☐	☐	☐	☐	☐
Explosive peroxides (EUH019)	☐	☐	☐	☐	☐	☐
Incompatible with water (EUH014, H260)	☐	☐	☐	☐	☐	☐
Catches fire spontaneously if exposed to air **(H250)**	☐	☐	☐	☐	☐	☐
Unstable product (EUH018, EUH019)	☐	☐	☒	☐	☐	☐
Acute health hazard:						
Fatal if swallowed (H300), in contact with skin (H310), if inhaled (H330)	☐	☐	☐	☐	☐	☒
Toxic in contact with skin (H311), if inhaled (H331), by eye contact (EUH070)	☒	☐	☐	☐	☐	☒
Contact with water liberates toxic gas (EUH029)	☐	☐	☐	☐	☐	☐
Contact with acids liberates toxic (EUH031), very toxic (EUH032) gas	☐	☐	☐	☐	☐	☐
Severe skin burns and eye damage (H314)	☒	☐	☐	☒	☒	☐
Longer term health hazards:						
Carcinogenic or possibly carcinogenic (**H350, H350i, H351**)	☐	☐	☐	☐	☐	☒
Teratogenic (H361d, **H360D**) / (**R61**, R63) and harmful to fertility (H361f, **H360F**), both hazards (H361fd, **H360FD, H360Df**, **H360Fd)**	☐	☐	☐	☐	☐	☐
Mutagenic (H341, **H340**)	☐	☐	☐	☐	☐	☐
Damage to certain organs (H371, H372, **H370**) through prolonged or repeated exposure (H373)	☒	☐	☐	☐	☐	☒
List all other relevant intrinsic hazards, per product (incl. E1- & E2-products):						

4. Description of the experiment and the risk assessment

4.1. Description of the operations, applied techniques and location:

Number sub-experiment	**Description of operations and techniques**	**Equipment used**	**Numbers[4] of the applied products**
1	Solvolysis of diphenyl(guaiacyl)carbonate in MeOH as a solvent at temperatures between 30 °C and 60 °C	MAP#492-31_02-176_ZK4#MSH2_00001	1-10
2			
3			
4			
5			

---

[4] Number of product as indicated in section 3.1.

Number sub-experiment	Building	Room	Containment level	Room specifications[5]
1.	492-31	02.176		☒ own unit ☐ allocated to another unit:
2.				☐ own unit ☐ allocated to another unit:
3.				☐ own unit ☐ allocated to another unit:
4.				☐ own unit ☐ allocated to another unit:
5.				☐ own unit ☐ allocated to another unit:
6.				☐ own unit ☐ allocated to another unit:

4.2. **Frequency of execution of the experiment:**

☒ Daily
☐ Weekly
☐ Monthly
☐ Less than monthly

4.3. **Use this space to include any additional information essential to perform the risk assessment (e.g. photo's, descriptions, schematic of the reaction) or to refer to any annexes:**

4.4. **Risks associated with the experiment:**

Risks associated with the use of chemical agents or nanoparticles

☒ Risk of inhaling, transferring, heating ...
☐ Risk of spattering
☐ Risk of evaporation and diffusion through heating
☒ Risk of cutting from use of needles/ sharp objects
☐ Risk of pressure build up due to reactions
☐ Transport of chemicals or nanoparticles

---

[5] If manipulations are conducted within a room allocated to another unit, then a copy of this risk assessment must be sent to the concerned manager (in cc.).

☐ within the building or compound: Describe measures
☐ between KU Leuven facilities (not on public road): Describe measures :
☐ external transport (on public road)
☐ Other:

Other risks associated with the experiment
☒ Burning, freezing (☒ high or low temperatures, ☐ cryogenic substances ...)
☐ Implosion, explosion (☐ high pressure, ☐ low pressure, ☐ underpressure ...)
☒ Fire (☐ ovens, ☐ heating spirals, ☐ bunsen burners, ☒ oil baths ...)
☐ Non-ionizing radiation (☐ NMR, ☐ lasers, ☐ UV lamps ...)
☐ Electrocution (☐ unprotected outlets, ☐ humid environment, ☐ high voltage ...)
☐ Isolated employment remote location.
Describe the conditions (e.g. second person present, dead-man switch ...):
☐ Risk of falling (☐ set-ups at height, ☐ aloft, ☐ difficult to reach ...)
☐ Biological risk: specify in table below:

Biological agent / host				**Genetically modified organisms**					
No. + name	**Hazard class**			**Vector(s)**	**Insert(s)**	**Donor-organism (insert)**	**Hazard class**		
	Human	**Animal**	**Plant**				**Human**	**Animal**	**Plant**
	Select class	Select class	Select class				Select class	Select class	Select class
	Select class	Select class	Select class				Select class	Select class	Select class
	Select class	Select class	Select class				Select class	Select class	Select class
	Select class	Select class	Select class				Select class	Select class	Select class

☐ Gasses:
☐ Ionizing radiation (X-rays, radio-isotopes ...). Specify:
☐There is a risk that in case of a grave incident, one is **NOT** able to autonomously raise the alarm (e.g.when using highly toxic fumes or gases, risk of explosion, presence of asphyxiating gas ...)
☐ Other:

5. Precautionary measures

If not all precautionary measures can be applied, the HSE Department advises against starting up the activities.

5.1. Collective protective equipment:

Number sub-experiment[6]:	**1**	**2**	**3**	**4**	**5**
Closed system (specify type, f.ex. glove box):	☒	☐	☐	☐	☐
Fume cabinet (extraction hood)	☒	☐	☐	☐	☐
Ventilated casing / Reactor cabinet	☐	☐	☐	☐	☐
Weighing cabinet	☐	☐	☐	☐	☐
Flexible extraction arm	☐	☐	☐	☐	☐

---

[6] Number of the sub-experiment as indicated in section 4.1.

Local extraction hood	☐	☐	☐	☐	☐
Biosafety cabinet with extraction to extraction channel	☐	☐	☐	☐	☐
Biosafety cabinet without extraction to extraction channel	☐	☐	☐	☐	☐
Spillage collectors underneath the setup	☐	☐	☐	☐	☐
Gas detection (type) flammable or toxic gases:					
- Portable	☐	☐	☐	☐	☐
- In the room/lab	☒	☐	☐	☐	☐
- Fire detection (general)	☒	☐	☐	☐	☐
- Other:	☐	☐	☐	☐	☐
Other:	☐	☐	☐	☐	☐

5.2. **Personal protective equipment[7]:**

Number of sub-experiment[6]:	**1**	**2**	**3**	**4**	**5**
General protection:					
- Lab coat/workwear	☒	☐	☐	☐	☐
- Disposable overshoes	☐	☐	☐	☐	☐
- Disposable hygienic hairnet	☐	☐	☐	☐	☐
- Disposable overalls	☐	☐	☐	☐	☐
- Disposable lab coat	☐	☐	☐	☐	☐
- Other:	☐	☐	☐	☐	☐
Facial protection:					
- Safety glasses	☒	☐	☐	☐	☐
- Safety visor	☐	☐	☐	☐	☐
- Face shield	☐	☐	☐	☐	☐
- Other:	☐	☐	☐	☐	☐
Respiratory protection:					
- Disposable dust mask P1	☐	☐	☐	☐	☐
- Disposable dust mask P3	☐	☐	☐	☐	☐
- Disposable hygienic mask/surgical mask	☐	☐	☐	☐	☐
- Other:	☐	☐	☐	☐	☐
Gloves:					
- Disposable nitrile EN 374	☒	☐	☐	☐	☐
- Disposable vinyl EN 374	☐	☐	☐	☐	☐
- Nitrile EN 374	☐	☐	☐	☐	☐
- Cryogenic gloves	☐	☐	☐	☐	☐
- Other:	☐	☐	☐	☐	☐
Hearing protection:					
- Disposable earplugs	☐	☐	☐	☐	☐
- Hearing bracket	☐	☐	☐	☐	☐
- Earmuffs	☐	☐	☐	☐	☐
- Other:	☐	☐	☐	☐	☐

5.3. **Specific precautionary measures:**

☒ Check functioning of fume hood
☒ Check glassware for cracks
☐ Attach hose clamps to cooling ducts
☐ Foresee automatic shutdown of heating system in case of cooling flaw
☐ Overpressure safeguard system
☐ Fire extinguisher for metal fires (D-extinguisher) present
☐ Oxygen kit present (mandatory when working with cyanides)
☐ Gas mask with specific filters present (intervention)
☐ Calcium gluconate ointment present (when handling ~~hydrogen acid~~ hydrofluoric acid)
☒ Check presence of intervention kit

---

[7] For guidelines on how to acquire Personal protective equipment (PPE), please consult your HSE contacts or visit the HSE Department website.

☐ Specific neutralization product present, i.e.
☐ Presence of a second person in the vicinity required
☐ Automatic alarm system (e.g. dead-man alarm)
☐ Other:

5.4. Work practices

☒ Apply the Code of Good Laboratory Practice
☒ Foresee internal training and guidance
☒ Selective waste collection - chemical waste
☐ Other:

6. Waste management - Chemical waste

6.1. Indicate which waste fractions you expect and mark the category of chemical waste for each fraction:

Waste fraction	**Waste category**
Pure substances:	
n.a.	☐1 - ☐2 - ☐ 3 - ☐ 4 - ☐5 - ☐ 6 - ☐ Other
	☐1 - ☐2 - ☐ 3 - ☐ 4 - ☐5 - ☐ 6 - ☐ Other
	☐1 - ☐2 - ☐ 3 - ☐ 4 - ☐5 - ☐ 6 - ☐ Other
	☐1 - ☐2 - ☐ 3 - ☐ 4 - ☐5 - ☐ 6 - ☐ Other
	☐1 - ☐2 - ☐ 3 - ☐ 4 - ☐5 - ☐ 6 - ☐ Other
	☐1 - ☐2 - ☐ 3 - ☐ 4 - ☐5 - ☐ 6 - ☐ Other
Mixtures:	
Main component: diphenyl/guaiacyl carbonate with phenol/guaiacol components	☐1 - ☐2 - ☒ 3 - ☐ 4 - ☐5 - ☐ 6 - ☐ Other
Main component: MeOH with 1-4 <3%	☒1 - ☒2 - ☐ 3 - ☐ 4 - ☒5 - ☐ 6 - ☐ Other
Main component: with	☐1 - ☐2 - ☐ 3 - ☐ 4 - ☐5 - ☐ 6 - ☐ Other
Main component: with	☐1 - ☐2 - ☐ 3 - ☐ 4 - ☐5 - ☐ 6 - ☐ Other
Main component: with	☐1 - ☐2 - ☐ 3 - ☐ 4 - ☐5 - ☐ 6 - ☐ Other
Main component: with	☐1 - ☐2 - ☐ 3 - ☐ 4 - ☐5 - ☐ 6 - ☐ Other
Other:	
	☐1 - ☐2 - ☐ 3 - ☐ 4 - ☐5 - ☐ 6 - ☐ Other
	☐1 - ☐2 - ☐ 3 - ☐ 4 - ☐5 - ☐ 6 - ☐ Other

7. Measures for particular situations

7.1. In case of failure and reactivation of utilities (incl. deviation from the specifications):

Utilities:	Consequence(s) in case of failure/malfunction:	Is this an HSE issue, yes/no?	If yes, please describe the measures:
Electricity	No hazards. Reaction will stop automatically	no	
Ventilation	If no ventilation is present, the reaction will be stopped or not carried out. Reaction products will be stored in ventilated cupboards or fumehoods	no	
Gas-supply		no	
(Cooling) water		no	
Compressed air			
Inert atmosphere	No hazard, oxygen in the reaction vail will not cause any additional reaction/risks	no	
Vacuum			
Other:			

Nutsvoorziening:	Consequence(s) in case of reactivation:	Is this an HSE issue, yes/no?	If yes, please describe the measures:
Electricity	Reactivation of the electricity might start the heating plate/reaction again. This will not cause any additional risks.	no	
Other:			

7.2. **Can the experiment take place when the setup is left unattended (= continuous experiments)?**

☐ Not applicable: the setup will never be left unattended.

☒ Yes.

Apply the procedure "Continuous activities - unattended".

☐ No, additional measures are required.

Describe the additional measures:

In addition, apply the procedure "Continuous activities - unattended".

7.3. **Is working outside normal working hours permitted?**

☐ No

☒ Yes. Describe which additional measures have been put in place (e.g. ventilation, second person present, dead-man switch ...): Yes. It is permitted for this reaction. Ventilation should be checked and Vmax activated. A second person should be present

7.4. **Describe your procedure for rapid shutdown, or the measures to be taken in case of evacuation of the premises:**

No specific measures should be taken in case of evacuation. If electricity stops, the reaction vail will cool down and reaction will stop. In evacuation, the experiment can continue as an unattended reaction.

7.5. **Describe the guidelines for a spilling incident:**

In case of a spilling incident, the spilling kit will be used to remove the spilled chemicals and the spill incident will be reported to the VGM antenne.

8. Conclusion / Comments / Questions

Use this space to note down any additional comments or questions you may have:

Deliver the completed risk assessment form to
your HSE network coordinator and your supervisor.

If acute dangerous class E4-products are involved, the HSE network coordinator will forward this risk assessment to the HSE Department.

9. Advice by HSE Department

This space is reserved for the HSE Department:

Summary in layman's terms

Plastic materials are ubiquitous in all facets of life. Plastics have a wide range of beneficial properties and are used in a variety of different applications. Nevertheless, public concerns have recently arisen about plastics because they are not sustainable. Almost all plastics are produced from non-renewable fossil fuels, which are strongly linked to greenhouse gas emissions such as CO_2. Moreover, plastic waste pollution poses a huge threat to the environment because it takes decades to break down. Plastic waste accumulates in the environment due to underdeveloped waste management systems. 60% of all plastics ever produced ends up in the environment. To make plastics sustainable, these two problems need to be tackled by the plastic industry.

A specific example of such a plastic industry is the polycarbonate (PC) industry. PC is a transparent and impact-resistant plastic used in, for example, safety glasses, car parts, water bottles and microwave resistant cookware. PCs are usually made from the high-volume chemical bisphenol A (BPA). However, besides the fact that BPA is produced out of fossil fuels, it is a controversial chemical because it might cause harmful, toxic effects in the environment. The quest for a renewable and safer alternative led to the production of 'so-called' bisguaiacols from wood feedstock. Such bisguaiacols can potentially replace common BPA-based PCs.

This MSc thesis aimed to develop of a proper waste management system for these bisguaiacol-based PCs. This research concluded that chemical recycling might be a very promising end-of-life purpose for such polycarbonates. In chemical recycling, the plastic waste is degraded – under controlled conditions – into the original building units. Afterwards, these building units can be used to produce new PCs which will be again recycled after use. Consequently, a cycle is created between the building units and the plastic connected by production and recycling phases. This way, plastic 'waste' becomes valuable feedstock, and hence harmful environmental effects will strongly reduce as far less material ends up in the environment.